NASA Contractor Report 3606

Integrated Airframe Propulsion Control

Robert E. Fennell and Stephen B. Black

GRANT NAG1-81
AUGUST 1982

NASA

NASA Contractor Report 3606

Integrated Airframe Propulsion Control

Robert E. Fennell and Stephen B. Black
Clemson University
Clemson, South Carolina

Prepared for
Langley Research Center
under Grant NAG1-81

NASA

National Aeronautics
and Space Administration

Scientific and Technical
Information Branch

1982

SUMMARY

The objective of this research is to develop models and methods to analyze the interaction between flight and propulsion systems. In this report, perturbation equations which describe flight dynamics and engine operation about a given operating point are combined to form an integrated aircraft/propulsion system model. The equations used to describe aircraft dynamics include dependence of aerodynamic coefficients upon atmospheric variables and, as a result, altitude is used as a state variable. The engine equations are derived from a low order engine model. In order to describe the interface between flight and engine variables, an off-design engine performance model is used to develop perturbation equations which describe the effect of flight condition and inlet performance upon propulsion system variables. These perturbation equations are used to identify interaction parameters in the integrated system model.

Linear quadratic regulator methods and numerical linear algebra techniques have provided a flexible means to analyze interaction effects upon the stability and control of the integrated system model. The inclusion of interaction effects in the model changes the overall system behavior. To analyze interaction effects on control, consideration is first given to control requirements for the airframe and engine models separately. For the separate airframe model, feedback control provides substantial improvement in the short period damping. For the integrated airframe/propulsion system model, feedback control compensates for coupling present in the model and provides good overall system stability. Analysis of suboptimal control strategies indicates that performance of the closed loop integrated system can be maintained with a feedback matrix in which the number of non-zero gains is small, relative to the total number of components in the feedback matrix. A method based on eigenvalue sensitivity analysis has proved to be an effective means for determining which gains in the integrated system feedback matrix can be set to zero while, at the same time, maintaining system performance.

INTRODUCTION

In present and future aircraft designs consideration will be given to problems associated with thrust management, fuel efficiency, improved maneuverability and pilot workload . Concepts such as variable geometry inlets and engines along with thrust vectoring and reversing provide a degree of interaction between propulsive and aerodynamic forces that requires a more complete integration of airframe and propulsion control systems. Improved performance is also predicted through further integration of flight controls with guidance, fire control, weapon delivery, and structual control systems . This trend toward integration of subsystem controls has motivated the development of models and methods to analyze the behavior of dynamically coupled subsystems and to design control laws for the improvement of subsystem cooperation and the enhancement of overall system performance.

Flight propulsion interface. Airframe/propulsion interactions are a major concern in aircraft design and many complex problems are associated with the description of this interface. Major problems are associated with the description of external airflow effects on the airframe, inlets, engines, and nozzles. Problems also occur in the development of aerodynamic accounting systems and in the verification of performance criteria. Many aspects of these problems have been previously considered, and references [1, 2, 3] indicate the scope of past activities. Two NASA programs which have dealt with interaction problems are the Cooperative Control Program (YF12) and the Integrated Propulsion Control Program (IPCS). The interaction between flight and propulsion system is broadly described by the effect of flight condition variables upon propulsion system mass flow, pressures and temperatures and by the effect of propulsion system forces and moments upon the aircraft. Examples of severe engine/inlet/airframe subsystem interactions have been observed in NASA flight research programs. An indication of the types of interactions observed is given in table 1.

TABLE 1. Airframe/Propulsion interactions.

Aircraft	Interaction	Result	Ref.
F-104	airframe/inlet	divergent lateral oscillations	4
F-111	engine/inlet	distortion factor exceeds limits	4
YF-12	airframe/inlet/engine	unstable dutch roll and phugoid	4
F-15	airframe/inlet	improved static stability	5

Both open and closed loop interactions have been observed between airframe, inlet, and engine. These interactions are a consequence of airflow variations between engine and inlet, airframe forces and moments induced by the propulsion system, and variations of inlet/engine operation with flight condition. Subsystem interactions have had a direct effect on aircraft stability, control, and performance. Further aspects of interaction effects are discussed by Schweikhard and Berry [4] and by Hunt, Surber and Grant [6].

Control configured aircraft with variable geometry engines and inlets will utilize interaction effects by design. In this application, consideration must be given to the physical interaction between flight and propulsion state variables and the cross-coupling effect of subsystem controls.

Models and control. The development of models of subsystem interactions for a given control requirement is complicated by the complexity of the system under consideration. In a simulation of the YF-12 aircraft [7], six degree of freedom aircraft motions were represented along with a three axis stability augmentation system. The effect of mixed compression, variable geometry inlets on aircraft forces and moments was simulated along with effects of aircraft motions on the behavior of inlets in the started mode. Further effects of changes in flight condition upon engine operating conditions were also considered in the simulation. Other simulations and models of the flight/propulsion interface are discussed by Tinling and Cole [8] and by Cole, Sellers and Tinling [9].

A low order model of a variable geometry inlet and a turbofan engine were interfaced in the work of Michael and Farrar [10]. Optimal control methods were used to design a closed loop controller for the integrated system. The control of an integrated airframe/propulsion system by state regulation was previously considered by W. R. Seitz [11].

For interacting systems, problems arise in deciding which interactions to include in a model and in the development of appropriate models of the interface between subsystems. The necessity of considering an integrated model which incorporates a full set of propulsion system control parameters along with the airframe control parameters has been discussed by Sevich and Beattie [12]. Sevich and Beattie indicate that a manageable design approach is to first optimize propulsion system control based upon overall system requirements. Then add to the aircraft control parameters those engine control parameters which effect the given control requirements. Control of the integrated system model should then be considered. The decomposition of a control problem for an interacting system into problems for lower dimensional subsystems is a common approach. The subsequent solution of control problems for each subsystem and their combination into a solution for the overall system has been called the decomposition principle. Further examples and background on the decomposition principle appear in the work of D. D. Siljak [13].

The objective of this research is to develop models and methods to analyze the interaction between flight and propulsion systems. In this report, perturbation equations are obtained which describe flight dynamics and engine operation about a given operating point. A model of the standard atmosphere [14] is used to describe changes in ambient temperature, pressure, air density and speed of sound with altitude. The equations used to describe aircraft dynamics include dependence of aerodynamic coefficients upon atmospheric variables and, as a result, altitude is used as a state variable. The engine equations are derived from a low order engine model, which was used in control design studies by DeHoff, Hall, Adams and Gupta [15]. In order to describe the interface between flight and engine variables, an off-design engine performance model is used to develop perturbation equations which describe the effect of flight condition and inlet performance upon propulsion system variables. These equations are used to develop an operating point model of an airframe/propulsion system at a given flight condition. Although a single integrated airframe/propulsion system model is analyzed in this report, the methods used to obtain this model apply at other flight conditions.

Linear quadratic regulator methods and multivariable system analysis techniques are used to analyze subsystem interaction effects on stability and control. For the given operating point, feedback controllers are designed for the separate flight and engine models. These results are used to aid in the design of a feedback controller for the integrated airframe/propulsion model. Feedback controllers for the integrated system designed by linear quadratic regulator methods involve a large number of nonzero gains and consequently, result in a complex control system with many active controls. In this report, various stategies to obtain less complex control laws are compared. The analysis indicates that the inclusion of subsystem interactions can change the overall stability and control of the system. Analysis of suboptimal control strategies indicates that control system performance can be maintained using feedback matrices with a small number of nonzero gains.

Acknowledgement. The principal investigator, Dr. Robert E. Fennell, spent a sabbatical leave from Clemson University at NASA Langley Research Center in 1979-80. During this period the principal investigator worked in close cooperation with Mr. F. J. Lallman of NASA Langley Research Center in the development of the problem and methods of analysis discussed in this report.

SYMBOLS

Air. Ctr. Aircraft with feedback control.

Aircraft

perturbation variables

	v	velocity (m/sec)
	α	angle of attack (rad)
	q	pitch rate (rad/sec)
	θ	pitch attitude (rad)
	h	altitude (km)
	γ	glide path angle (rad)
	δe	horizontal stabilator (rad)
	M	Mach number

nominal variables

	v_0	velocity (m/sec)
	M_0	Mach number
	h_0	altitude (km)

c1, c2, c3 weighting coefficients

D /Dt differentiation with respect to time

E( ) expected value

Eng. Ctr. engine with feedback control

Engine

perturbation variables

	N1	fan speed (rpm)
	N2	compressor speed (rpm)
	P5	augmentor pressure (kPa)
	Wf	main burner fuel flow (N/sec)
	P2	compressor discharge pressure (kPa)
	Wfc	command fuel flow (N/sec)
	A	nozzle area (sq.m)
	CIVV	inlet guide vane (deg)
	RCVV	rear compressor variable vane (deg)
	BLC	compressor bleed (%)
	Th	net thrust per engine (N)
	Wa	fan airflow (kg/sec)
	T4	turbine inlet temperature (K)
	SMAF	fan stall margin
	SMHF	compressor stall margin
	DP/P	relative fan exit pressure change
	Pr	inlet pressure recovery ratio

SYMBOLS

nominal variables

- TH thrust (N)
- WA fan airflow (kg/sec)
- WF/WA fuel to air ratio
- ST specfic thrust (thrust per unit mass flow)
- $r_{1,0}$ inlet pressure recovery ratio

GSM(g) gain significance matrix

Im. imaginary part of complex number

Int. open loop integrated system

Int. Ctr. integrated system with feedback control

J, JA, JE, JI performance indices

K feedback gain matrix

Re. real part of complex number

Sen(λ,ε) relative sensitivity of λ with respect to ε

St1, St2, St3, St4 suboptimal control strategies

T modal matrix

th time to half amplitude

tp time of period of oscillation

ua, ue, u aircraft, engine and integrated system control vectors

xa, xe, x aircraft, engine and integrated system state vectors

x0 initial vector

Xi fundamental mode

ya, ye, y aircraft, engine and integrated system response vectors

GREEK SYMBOLS

δ_i pressure at engine location i relative to sea level standard (101.4 kPa)

ε system parameter

θ_i temperature at engine location i relative to sea level standard (288.2 K)

SYMBOLS

Λ	real Jordan canonical form
λ	eigenvalue
ξ	damping coefficient
ωn	natural frequency (rad/sec)

SUBSCRIPTS

i	engine location
s	static

SUPERSCRIPTS

1	first row of a matrix
'	matrix transpose

INTEGRATED SYSTEMS

Control system design problems arise in the analysis of large scale systems composed of many interconnected subsystems. Use of an integrated system model allows the investigation of interaction effects in the control design process. In this manner, physical interactions between subsystem state variables and control variable cross-coupling effects can be considered from the outset in the design process.

Design methods frequently focus upon operating point conditions, which provide a simplified system model. Linearization procedures and model reduction techniques provide further simplifications. The interaction between a given subsystem and other subsystems at a given operating point may be described by the linear system of equations

$$D(XI)/Dt = AI \bullet XI + BI \bullet UI + \Sigma_{J \neq I}\ CIJ \bullet YJ + DI \bullet VI$$

$$YI \quad = FI \bullet XI + GI \bullet UI + \Sigma_{J \neq I}\ HIJ \bullet YJ + EI \bullet ZI$$

where XI, UI, VI, ZI denote the state, control, and noise variables for the I-th subsystem and the YJ denote interaction variables between the subsystems. Here AI, BI, CIJ, DI, FI, GI, HIJ, and EI denote appropriate system matrices. The matrices CIJ and HIJ are referred to as interconnection matrices in this report and describe the interaction between subsystems at a given operating point.

In order to introduce the coordination of subsystem controls into the design process an adequate model of subsystem interactions is necessary. Frequently these interactions are difficult to describe and the determination of adequate models of interaction effects requires detailed analysis of subsystem properties. The problem of determining parameters in an interaction matrix from given system properties and data is commonly referred to as a parameter identification problem. A method to determine subsystem interaction matrices for an airframe/propulsion system model will be presented in this report. Details of this method are presented in appendix A. In this example, interaction matrices are determined in a mannner so that the steady state responses of the system to changes in interconnection variables agree with previously developed steady state design point models.

In this report, linear quadratic regulator methods and multivariable system analysis techniques are used to analyze the effect of subsystem interactions upon overall system stability and control. Combination of subsystem models into an integrated system model results in a system in the standard form

$$Dx/Dt = A \bullet x + B \bullet u + D \bullet v$$

$$y \quad = F \bullet x + G \bullet u + E \bullet z.$$

Control systems of this form have received extensive study. The stability and response of the unperturbed system is determined by the eigen-structure (eigenvalues and eigenvectors) of the system matrix A. The representation of solutions of this system is described in most system analysis texts [16], [17]. The following approach is used in this report. The real Jordan canonical form of A is denoted by Λ. The matrix T denotes the modal matrix such that

$$A \bullet T = T \bullet \Lambda. \tag{1}$$

Solutions of the initial value problem

$$Dx/Dt = A \bullet x \qquad x(0) = x0$$

may be written as

$$\begin{aligned} x(t) &= e^{At} \bullet x0 \\ &= T \bullet e^{\Lambda t} \bullet T^{-1} \bullet x0 \\ &= c1 \bullet X1(t) + c2 \bullet X2(t) + \ldots + cn \bullet Xn(t) \end{aligned}$$

where

$$T(c1,\ c2,\ \ldots\ ,cn)' = x0$$

and

$$T \bullet e^{\Lambda t} = (X1(t),\ X2(t),\ \ldots\ ,Xn(t)).$$

The functions Xi(t), i=1,..., n, are the fundamental modes of the system and the structure of the modal matrix T determines the interdependence between system components and the fundamental modes, and consequently the interdependence between system components. Coupling between subsystems caused by the inclusion of subsystem interactions will be illustrated in the airframe/propulsion system model which follows.

Frequently subsystem interactions have been treated as small perturbations and neglected in control design studies. The sensitivity of system eigenvalues and eigenvectors to small perturbations has been extensively studied, an introduction to this analysis is given in the text by G. W. Stewart [18]. Small perturbations can drastically change the system eigen-structure. Equation (1) may be used to analyze the sensitivity of the eigen-structure to changes in system parameters. If ε denotes a system parameter then

$$(DA/D\varepsilon)T + A(DT/D\varepsilon) = (DT/D\varepsilon)\Lambda + T(D\Lambda/D\varepsilon)$$

whenever these derivatives exist. These equations may be solved to determine eigenvalue and eigenvector senitivities, details are presented in references [19], [20].

For the case of distinct eigenvalues the canonical form Λ, the modal matrix T, and the fundamental modes Xi, i = 1,...,n, have a particularly simple structure. In this case changes in the system eigen-structure caused by the inclusion of interaction matrices may be readily calculated and the determination of $D\Lambda/D\varepsilon$ is straightforward. For completeness these details are summarized in appendix B and an identity is presented which avoids complex arithmetic in the calculation of the sensitivity of complex eigenvalues.

Sensitivity analysis techniques may be used to study interaction effects upon open and closed loop stability and control. In this report the effect of a system parameter upon stability will be described by the relative changes in system eigenvalues due to changes in the system parameter. Thus, if λ and ε denote a system eigenvalue and parameter respectively then the sensitivity of λ with respect to ε is measured by

$$\mathrm{Sen}(\lambda,\varepsilon) = (D\lambda/D\varepsilon)\bullet|\varepsilon/\lambda|.$$

To a first approximation, one obtains

$$\Delta\lambda = (D\lambda/D\varepsilon)\Delta\varepsilon$$

and consequently

$$\Delta\lambda/|\lambda| = \mathrm{Sen}(\lambda,\varepsilon)[\Delta\varepsilon/|\varepsilon|].$$

Thus $\mathrm{Sen}(\lambda,\varepsilon)$ is a measure of the relative change in λ due to a change in ε.

Linear quadratic regulator methods [16], [17] will be used to determine stable regulators for interacting systems. Systems will be written in the standard form

$$Dx/Dt = A\bullet x + B\bullet u$$

$$y \quad = F\bullet x + G\bullet u$$

with a performance index of the form

$$J = \int_{[o,\infty)} y'\bullet W_1\bullet y + u'\bullet U_1\bullet u \; dt.$$

The control which minimizes this performance index is

$$u = -U^{-1}(B'\bullet Q + R')x$$

where Q satisfies the matrix Riccati equation

$$A'\bullet Q + Q\bullet A + W - (Q\bullet B+R)U^{-1}(B'\bullet Q+R') = 0$$

or equivalently

$$(A-B\bullet U^{-1}\bullet R')'Q + Q(A-B\bullet U^{-1}\bullet R') + F'(W_1-W_1\bullet G\bullet U^{-1}\bullet G'\bullet W_1)F - Q\bullet B\bullet U^{-1}\bullet B'\bullet Q = 0$$

where

$$W = F' \bullet W_1 \bullet F$$

$$R = F' \bullet W_1 \bullet G$$

$$U = U_1 + G' \bullet W_1 \bullet G.$$

In this case if $x(0) = x0$ then $J = x0' \bullet Q \bullet x0$. In general if $u = K \bullet x$ is a stabilizing feedback control then $J = x0' \bullet Q \bullet x0$ where Q satisfies the Liapounov equation

$$(A+B \bullet K)'Q + Q(A+B \bullet K) + (F+G \bullet K)'W_1(F+G \bullet K) + K' \bullet U_1 \bullet K = 0$$

In either case if x0 is considered as a random initial condition with covariance matrix $cov(x0,x0) = I$ then the expected value of J, denoted E(J), may be used as a scalar performance index [17,p.371] and

$$E(J) = Trace(Q).$$

A numerical package of Fortran coded subroutines, ORACLS [20], was used to perform the numerical linear algebra required in this report and to solve linear quadratic regulator problems. The solution of the regulator problem uses principally one of two routines from the ORACLS package, RICTNWT and ASYMREG. RICTNWT uses the Newton-Kleinman algorithm to solve the continuous steady-state Riccati equation. Some numerical problems arose when RICTNWT was used to solve the regulator problem for the airframe/propulsion example of this report. The algorithm did not converge. As a result the routine ASYMREG was used to solve the associated Riccati equation and with this procedure satisfactory results were obtained.

INTEGRATED AIRFRAME/PROPULSION MODEL

A description of an integrated airframe/propulsion system operating point model is presented in this section. All equations represent variations about the given operating point and all variables should be interpreted as perturbations about the given operating point. Longitudinal flight conditions are considered.

Airframe. The linearized aircraft longitudinal equations of motion are of the form

$$Dxa/Dt = AA \bullet xa + BA \bullet ua + CAE \bullet ye$$

$$ya = FA \bullet xa$$

The state, control, and response variables and typical equilibrium values for this model are as follows:

xa_1	v, velocity (265.6 m/sec)
xa_2	α, angle of attack (0.0761 rad)
xa_3	q, pitch rate (0. rad/sec)
xa_4	θ, pitch attitude (0.0761 rad)
xa_5	h, altitude (13.72 km)
ua_1	δe, horizontal stabilator (-0.0346 rad)
ya_1	M, Mach number (0.9)
ya_2	h, altitude (13.72 km)
ye_1	Th, net thrust per engine(12 833 N).

The interaction matrix CAE describes the effect of thrust upon the longitudinal state variables. Data in this report is derived from a twin-engine, advanced fighter aircraft model in which it is assumed that thrust acts parallel to the aircraft centerline and the engines are located a short distance below the center of gravity. In the derivation of these equations a model of the standard atmosphere [14] was used to describe changes in ambient temperature, pressure, air density and speed of sound with altitude. The dependence of aerodynamic coefficients upon these variables resulted in the inclusion of altitude as a state variable. It will be noted later in this report that the resulting model is unstable.

System matrices for the given operating point are listed in table 11 of appendix C. This data was supplied by NASA.

Engine. Multivariable control design methods have been used extensively in the design of control laws for turbofan engines. The report [15] contains a discussion of current control design methods. In large scale problems, model reduction techniques may be used to provide simplified system models. The model studied in the present report is derived from a low order engine model which was obtained through model reduction techniques [15] and has the form

$$Dxe/Dt = AE \bullet xe + BE \bullet ue + CEA \bullet ya + CEI \bullet yi$$

$$ye = FE \bullet xe + GE \bullet ue + HEA \bullet ya + HEI \bullet yi.$$

The state, control, and response variables and typical equilibrium values for this model are as follows:

xe_1 N1, fan speed (9 785 rpm)
xe_2 N2, compressor speed (12 401 rpm)
xe_3 P5, augmentor pressure (74.89 kPa)
xe_4 Wf, main burner fuel flow (3.31 N/sec)
xe_5 P2, compressor discharge pressure (673.8 kPa)

ue_1 Wfc,command fuel flow (3.31 N/sec)
ue_2 A, nozzle area (0.259 m^2)
ue_3 CIVV, inlet guide vane (0.997 deg)
ue_4 RCVV, rear compressor variable vane (3.99 deg)
ue_5 BLC, compressor bleed (0.997%)

ye_1 Th, net thrust (12 833 N)
ye_2 Wa, fan airflow (27.58 kg/sec)
ye_3 T4, turbine inlet temperature (1 590 K)
ye_4 SMAF, fan stall margin(0.14164)
ye_5 SMHC, compressor stall margin(0.1445)
ye_6 DP/P, relative fan exit pressure change (0.9973).

Corresponding system matrices are listed in table 12 of appendix C.

Inlet. In this example the aircraft inlet is characterized by a single parameter, Pr, inlet pressure recovery ratio. The presure recovery ratio is defined as the ratio of total pressure at the engine face to the total freestream pressure. Optimal engine performance requires high pressure recovery. The main requirement of an aircraft inlet is to provide mass-flow of sufficient uniformity to the engine to preclude stalls and to operate at high pressure recovery. In general, the subsonic inlet must supply air at the engine face at a specified Mach number and without separation of the flow. The supersonic inlet must decelerate the flow. Variable geometry inlets are currently designed to match variations in airflow demanded at the engine face with variations in flight condition and engine operating condition. Changes in inlet geometry affect not only engine performance but also aerodynamic forces and moments. Variable geometry inlet effects are not included in the model presented in this report.

Integrated model. A simplified off-design performance model of a dry turbofan cycle developed by F. J. Lallman [21] is used to analyze the effect of flight condition and inlet pressure recovery upon engine state and response variables. This off-design performance model expresses the engine specific thrust, fuel to air ratio, along with total temperatures and pressures throughout the engine, as a function of Mach number, ambient temperature, inlet pressure recovery ratio, fan pressure ratio, compressor pressure ratio, and burner temperature. Specification of fan pressure ratio, compressor pressure ratio, and burner temperature yields a design point model from which engine performance and state variables are determined as functions of Mach number, altitude, and pressure recovery ratio. Details of this analysis are contained in appendix A.

For a turbofan engine with a fan pressure ratio of 2.9, a compressor pressure ratio of 7.93 and a burner temperature of 1559 K at a flight condition with a Mach number of 0.9 and altitude of 13.72 km, the design point model yields the following perturbation equations:

$$
\begin{array}{lclclcl}
P5 & = & 42.020\ M & - & 15.938\ h & + & 101.016\ Pr \\
Wf & = & 2.717\ M & - & 0.5905\ h & + & 3.749\ Pr \\
P2 & = & 635.55\ M & - & 90.631\ h & + & 574.812\ Pr \\
Th & = & 8\ 267\ M & - & 2\ 121\ h & + & 17\ 826\ Pr \\
Wa & = & 25.678\ M & - & 4.35\ h & + & 27.586\ Pr
\end{array}
$$

The interaction matrices CEA, CEI, HEA, and HEI in the engine model are determined so that the steady state response of the variables augmentor pressure, P5, compressor pressure, P2, thrust per engine, Th, and fan airflow, Wa, to step changes in Mach number, M, altitude, h, and pressure recovery ratio, Pr, agrees with the above relationships. Details of this procedure are presented in appendix A and values for the interaction matrices for the given operating point are contained in table 12 of appendix C. It should be noted that the dependence of fuel flow, wf, upon flight condition has been removed in the determination of interaction matrices and consequently changes in the overall system behavior should be expected.

Combination of the airframe and engine models leads to the following operating point model for the integrated system:

$$Dx/Dt = AAAE \bullet x + BABE \bullet u$$

$$y = FAFE \bullet x + GAGE \bullet u$$

where

$$AAAE = \begin{bmatrix} AA + CAE \bullet HEA \bullet FA & CAE \bullet FE \\ CEA \bullet FA & AE \end{bmatrix} \qquad BABE = \begin{bmatrix} BA & CAE \bullet GE \\ 0 & BE \end{bmatrix}$$

and

$$FAFE = \begin{bmatrix} FA & 0 \\ HEA & FE \end{bmatrix} \qquad GAGE = \begin{bmatrix} 0 & 0 & 0 \\ 0 & GE & HEI \end{bmatrix}.$$

For the given operating point values of the matrices appear in table 13 of appendix C. In this model the term CAE•HEA•FA is due to the dependence of thrust upon Mach number and altitude, the term CAE•FE results from the dependence of thrust on engine states, and the term CEA•FA results from the dependence of engine temperatures and pressures on Mach number and altitude. The term CAE•GE represents changes in thrust due to engine controls.

Interaction effects. The inclusion of subsystem interactions in the airframe/propulsion system model has changed the overall system behavior. This change in the system behavior is due to changes in the eigen-structure of the open loop system. Separate and integrated system eigenvalues are listed in table 2, below, whereas the separate and integrated system modal matrices are listed in table 14 of appendix C. Eigenvectors corresponding to the engine in the separate and integrated system models are essentially unchanged whereas eigenvectors corresponding to the airframe have changed significantly. The magnitude of the difference between corresponding eigenvectors of separate and integrated systems along with the angle between these vectors is listed in table 2. It should be noted that corresponding normalized eigenvectors are being compared, i.e. eigenvectors of unit length.

TABLE 2. Interaction effects on stability.

System eigenvalues.					
		Airframe			
Separate	-2.76E-3	3.74E-4 ± j3.25E-2		-6.78E-1 ± j2.20E+0	
Integrated	1.91E-3	-3.65E-4 ± j3.65E-2		-6.78E-1 ± j2.20E+0	
		Engine			
Separate	-5.81E-1	-1.88E+0	-6.59E+0	-1.00E+1	-1.72E+2
Integrated	-5.63E-1	-1.88E+0	-6.59E+0	-1.00E+1	-1.72E+2
System eigenvectors.					
		Airframe			
Distance	1.37	1.37	1.37	1.28	1.28
Angle (deg)	86.4	86.2	86.2	79.6	79.6
		Engine			
Distance	0.00	0.00	0.00	0.00	0.00
Angle (deg)	0.00	0.00	0.00	0.00	0.00

The significance of these changes in the system eigen-structure is evidenced by a comparision of the transient response of the separate and integrated models. The separate models do not include coupling between airframe and engine state variables and, consequently, changes in the states of one system do not effect the states of the other system. Also, the response of the open loop, integrated system to small offsets in engine state variables indicates weak coupling in the system. In this case, the open loop engine states respond almost exactly as in the separate model and small oscillations, relative to the given operating point values, are induced in the airframe states. This behavior is expected due to the structure of the system eigenvectors. Typical responses of the separate and integrated system models to an offset in fan speed, N1, are depicted in figure 1. The response of the model to small changes in airframe states illustrates the effect of coupling present in the integrated system model. Within a small time period, offsets in the values of velocity, v, and altitude, h, can lead to significant changes in engine state and output variables. Also the airframe response, in this case, differs slightly from that of separate model because thrust variation with altitude has been included in the model. Offsets in the values of angle of attack, α, pitch rate, q, and pitch attitude, Θ, have little effect upon engine variables. The response of the separate and integrated models to offsets in values of angle of attack and altitude are depicted in figures 2 and 3. Here a one per cent offset in the value of altitude leads to equivalent changes in the values of augmentor pressure, P5, compressor pressure, P2, thrust, Th, and inlet airflow, Wa. It should, also, be noted that within the given time period some variables have not attained their maximum displacement.

In general, sensitivity analysis may be used to study the effect of subsystem interconnections upon system stability. If ε denotes a parameter in the system matrix $A(\varepsilon)$, then the sensitivity of an eigenvalue λi to the parameter ε can be measured as

$$\mathrm{Sen}(\lambda i,\varepsilon) = D\lambda i/D\varepsilon \bullet |\varepsilon/\lambda i| .$$

The parameter ε may be a parameter in an interconnection matrix or some other interconnection parameter. For example, consider the system matrix

$$A(\varepsilon) = \begin{bmatrix} AA + \varepsilon^2 CAE \bullet HEA \bullet FA & \varepsilon \bullet CAE \bullet FE \\ \varepsilon \bullet CEA \bullet FA & AE \end{bmatrix}$$

which is obtained by replacing CAE, CEA, and HEA by $\varepsilon\bullet$CAE, $\varepsilon\bullet$CEA, and $\varepsilon\bullet$HEA in the integrated system model. Here $\varepsilon = 0$ corresponds to the separated models while $\varepsilon = 1$ corresponds to the integrated model. Calculations for the example model indicate that $\mathrm{Sen}(\lambda 1)$, $\mathrm{Sen}(\lambda 2)$, and $\mathrm{Sen}(\lambda 3)$ are large in comparision to $\mathrm{Sen}(\lambda i)$, $i=4,\ldots,10$. Consequently, the first three modes are most sensitive to this interconnection parameter. These are the modes associated with the phugoid motion and the mode introduced by consideration of altitude as a state variable. Values of $D\lambda i/D\varepsilon$ and $\mathrm{Sen}(\lambda i,\varepsilon)$ for $\varepsilon = 1$ are listed in table 3.

TABLE 3. Sensitivity to subsystem interactions.

λi	Dλi/Dε	Sen(λi,1)
1.912E-3	7.411E-3	3.875E+0
-3.654E-4 + j3.647E-2	-5.175E-4 + j7.554E-3	-1.416E+0 + j2.071E-1
-3.654E-4 - j3.647E-2	-5.175E-3 - j7.554E-3	-1.416E-0 - j2.071E-1
-5.628E-1	-2.137E-3	-3.797E-3
-1.883E+0	3.771E-4	2.002E-4
-6.781E-1 + j2.200E+0	9.565E-5 - j2.252E-4	1.411E-4 - j1.024E-4
-6.781E-1 - j2.200E+0	9.565E-5 + j2.252E-4	1.411E-4 + j1.024E-4
-6.587E+0	-3.896E-3	-5.915E-4
-1.000E+1	5.543E-19	5.543E-20
-1.722E+2	-5.524E-3	-3.208E-5

SYSTEM CONTROL

Linear quadratic regulator methods are used to design a feedback control law for the integrated airframe/propulsion system and subsystem interaction effects upon the resulting feedback control law are analyzed. Consideration is first given to the control requirements for each subsystem at compatible operating conditions. Feedback control laws are determined for each subsystem and these results are used to aid in the design of a feedback control of the integrated system. To allow full consideration of all interactions full state feedback is considered for the integrated system. Control of the integrated system involves several active controls which are determined by a feedback control law with many non-zero gains. Suboptimal control strategies are compared to determine if performance can be maintained with simplified feedback control laws. In particular, a method which uses sensitivity analysis is found to provide an effective means for determining simplified feedback control laws.

Flight control. The objective of the flight control problem is to improve longitudinal performance through coordinated utilization of interacting aerodynamic and propulsive forces and moments. For the operating point of this example the short period damping is marginal. The performance index used is of the form

$$JA = \int_{[0,\infty)} ya'\bullet WA\bullet ya + ua'\bullet UA\bullet ua \, dt$$

where the response vector ya = FFA•xa + GGA•ua has components

ya_1 = v, velocity
ya_2 = γ, glide path angle
ya_3 = q, pitch rate

and the control vector has components

ua_1 = δe, horizontal stabilator
ua_2 = Th, thrust per engine.

Weighting matrices WA and UA were chosen with a small penalty on the use of thrust, in order to allow thrust control in the longitudinal model. The particular weighting matrices and other system matrices are listed in table 11 of appendix C.

Solution of the optimization problem provides the feedback control relation ua = -K•xa with

$$K = \begin{bmatrix} 8.11E-5 & 3.15E-1 & -3.89E-1 & -2.48E-1 & -3.72E-4 \\ 8.25E+0 & -5.02E+3 & 5.40E+3 & 4.46E+3 & 3.14E+2 \end{bmatrix}.$$

and $xa = (v, \alpha, q, \theta, h)'$. The large gains in this feedback matrix are due to the choice of units for thrust. If thrust were measured in kilo-Newtons then each entry in the second row of K would be scaled by 0.001.

The improvement in performance obtained through the use of this feedback control may be illustrated by comparing the stability, performance, and transient response of the system

$$Dxa/Dt = (AA - \varepsilon \bullet BA \bullet K)xa$$

where ε is a parameter which ranges between zero and one. The value $\varepsilon = 0$ corresponds to the open loop system while $\varepsilon = 1$ corresponds to the closed loop system with feedback relation $ua = -K \bullet xa$. The transition in eigenvalues and short period performance may be observed by varying ε between zero and one. The eigenvalues of $AA - \varepsilon \bullet BA \bullet K$ with ε = 0.0, 0.2, 0.4, 0.8, and 1.0 are listed in table 4.

TABLE 4. Longitudinal eigenvalues $AA - \varepsilon \bullet BA \bullet K$.

ε	Eigenvalues		
0.0	-2.76E-3	3.74E-4 ± j3.25E-2	-6.78E-1 ± j2.20E+0
0.2	-2.90E-3	-1.88E-2 ± j2.65E-2	-1.00E-1 ± j2.14E+0
0.4	-3.03E-3	-1.95E-2 , -5.50E-2	-1.22E+0 ± j2.02E+0
0.6	-3.13E-3	-1.11E-2 , -9.95E-2	-1,49E+0 ± j1.85E+0
0.8	-3.21E-3	-8.34E-3 , -1.38E-1	-1.76E+0 ± j1.61E+0
1.0	-3.24E-3	-6.97E-3 , -1.77E-1	-2.03E+0 ± j1.26E+0

Calculation of the short period natural frequency, damping coefficient, period, and time to half amplitude illustrates the effect of the feedback control on longitudinal performance. Changes in short period performance are listed in table 5. The substantial improvement in short period damping should be noted.

TABLE 5. Short period variables.

ωn - natural frequency (rad/sec) ξ - damping coefficient
tp - period (sec) th - time to half amplitude(sec) .

ε	ωn	ξ	tp	th
0.0	2.303	0.2945	2.729	1.022
0.2	2.336	0.4054	2.690	0.732
0.4	2.360	0.5154	2.662	0.570
0.6	2.377	0.6254	2.644	0.466
0.8	2.385	0.7364	2.634	0.395
1.0	2.385	0.8496	2.635	0.342

The improved damping and stability obtained from the feedback control is further illustrated by a comparison of the transient response of the closed loop system with that of the open loop system. The transient response of the open and closed loop models to an offset in each state variable is depicted in figures 4 through 8. Several properties of the closed loop system are apparent in these figures. The improved short period damping due to the weight on pitch rate, q, in the performance index is evidenced by the absence of oscillations in the closed loop system response. In each case, it appears that altitude, h, is being traded off for improvements in velocity, v, and glide path angle, γ. Also, it appears that a small amount of thrust control, Th, is being used. Although it is not apparent from the figures, it should be noted that the closed loop system is stable and all variables will return to equilibrium.

To determine the significance of thrust control in this example, a second regulator problem was posed with only the horizontal stabilator, δe, as a control. Use of a performance index with WA as previously defined and UA = 4 resulted in a feedback control law δe = -K1•xa with

$$K1 = [\ 7.69E-5 \quad 3.17E-1 \quad -3.89E-1 \quad -2.49E-1 \quad -5.42E-4\ ]$$

The gains in this feedback control are very similar to those of the first row of the previously determined feedback matrix, K. The eigenvalues for the closed loop system AA -BA•K1 are -2.24E-3, -6.97E-3, -1.77E-1 and -2.03±j1.26. These eigenvalues should be compared with those of the closed loop system AA - BA•K (see table 4). The only difference in eigenvalues is in the stability of the mode associated with the introduction of altitude as a state variable. This mode is most closely associated with the phugoid motion. It should also be noted that the improvement in short period damping previously obtained is also obtained by use of the control δe = -K1•xa. Comparisons of the transient response of the two closed loop systems indicates that the two systems respond in a similar manner to offsets in state variables. The main difference between the two systems is that velocity responds faster in the system with thrust control, i.e. AA - BA•K, than in the system with the horizontal stabilator as the only control, AA - BA•K1. Typical responses of the two closed loop systems are compared in figure 9.

Engine control. Detailed analysis of the regulator design for the engine is contained in reference [16]. At this operating point the engine is in a region of fan stability sensitivity to augmentor ignition. The performance index adapted from reference [16] is

$$JE = \int_{[0,\infty)} xe'\bullet WE\bullet xe + ue'\bullet UE\bullet ue \; dt$$

where xe and ue represent the state and control variables of the engine model (see p. 13). Table 14 of appendix C contains values for the matrices WE and UE. The resulting gain matrix is

$$K = \begin{bmatrix} 9.02E-4 & 1.40E-3 & 6.58E-4 & 3.48E-1 & -7.93E-4 \\ 3.72E-5 & 2.03E-6 & -8.58E-4 & -1.36E-3 & -1.78E-5 \\ -8.99E-3 & 3.33E-3 & 1.03E-1 & -6.31E-1 & -8.38E-3 \\ 6.78E-4 & -7.98E-3 & 2.21E-2 & 3.96E-1 & 2.30E-2 \\ -4.02E-5 & -5.86E-5 & -1.32E-3 & -3.17E-2 & -6.58E-4 \end{bmatrix}.$$

Integrated system control. In order to pose a regulator problem for the integrated system a weighted performance index of the form

$$J = c1 \bullet JA + c2 \bullet JE + c3 \bullet JI$$

is used where JA, JE are as before and

$$JI = \int_{[o,\infty)} YI' \bullet YI \, dt$$

denote performance indices for the airframe, engine and inlet respectively and c1, c2 and c3 denote the weights. In the model example, YI denotes the single parameter Pr, inlet pressure recovery ratio. This performance index may be written in the standard form

$$J = \int_{[o,\infty)} y' \bullet W \bullet y + u' \bullet U \bullet u \, dt$$

where $y = FF \bullet x + GG \bullet u$ with $y = (v, \gamma, q, Th, N1, N2, P5, Wf, P2)'$, $x = (v, \alpha, q, \theta, h, N1, N2, P5, Wf, P2)'$, $u = (\delta e, Wfc, A, CIVV, RCVV, BLC, Pr)'$ and

$$FF = \begin{bmatrix} FA & 0 \\ (HEA \bullet FA)^1 & (FE)^1 \\ 0 & I \end{bmatrix} \qquad GG = \begin{bmatrix} 0 & 0 & 0 \\ 0 & (GE)^1 & (HEI)^1 \\ 0 & 0 & 0 \end{bmatrix}$$

and

$$W = \begin{bmatrix} c1 \bullet WA & 0 & 0 \\ 0 & c1 \bullet UA_{22} & 0 \\ 0 & 0 & c2 \bullet WE \end{bmatrix} \qquad U = \begin{bmatrix} c1 \bullet UA_{11} & 0 & 0 \\ 0 & c2 \bullet UE & 0 \\ 0 & 0 & c3 \bullet I \end{bmatrix}.$$

The superscript 1 in the above equations is used to denote the first row of the indicated matrices. In this model thrust is no longer a control variable. For each choice of weights a feedback control

$$u = -K(c1, c2, c3) \bullet x$$

is determined. The feedback obtained by normalizing JA and JE about their previously obtained optimal values and by placing a large weight on JI (c1 = .318, c2 = .338, c3 = 10E6) is

$$
K = \begin{bmatrix}
4.587D-02 & 1.722D+00 & -6.485D-01 & -2.730D+00 & -5.480D+00 & 7.025D-05 & 1.200D-03 & -1.233D-03 & 4.144D-02 & 5.781D-05 \\
1.364D-02 & -9.822D-02 & -6.178D-03 & 5.680D-02 & 5.118D-02 & 9.010D-04 & 1.386D-03 & 6.823D-04 & 3.474D-01 & -7.938D-04 \\
-1.114D-04 & -1.166D-03 & 2.404D-05 & 1.445D-03 & 2.529D-02 & 3.714D-05 & 1.943D-06 & -8.578D-04 & -1.368D-03 & -1.779D-05 \\
2.085D-02 & -9.874D-03 & -2.022D-02 & -1.181D-01 & -3.324D+00 & -8.988D-03 & 3.303D-03 & 1.026D-01 & -6.317D-01 & -8.383D-03 \\
-2.746D-02 & 1.151D-02 & 3.746D-02 & 2.115D-01 & 1.110D+00 & 6.865D-04 & -7.898D-03 & 2.197D-02 & 3.992D-01 & 2.300D-02 \\
-6.721D-04 & 4.447D-03 & 1.102D-04 & -3.712D-03 & 1.537D-03 & -4.019D-05 & -5.847D-05 & -1.321D-03 & -3.173D-02 & -6.575D-04 \\
2.029D-06 & -2.379D-05 & -8.380D-07 & 1.870D-05 & -3.436D-06 & 4.987D-08 & 2.355D-07 & 1.829D-06 & 4.577D-05 & 7.266D-07
\end{bmatrix}
$$

In this example c1 = 1/E(JA) and c2 = 1/E(JE), where E(JA) and E(JE) denote the expected value of the performance indices for the separate flight and engine control problems when the previously derived feedback controls are used. It should be noted, for this choice of weights, that the gain matrix developed for the engine separately is essentially the same as the corresponding components of the integrated system feedback matrix. Also, it should be noted that each control variable will be active since the gain matrix K has all non-zero entries. This structure of the feedback matrix will change as the weights in the performance index are varied. The use of a large weight on JI negates use of pressure recovery as a control. Variation of the parameter c3 would allow one to study the effect of pressure recovery ratio upon the integrated system control.

The introduction of this feedback control improves the stability of the overall system and maintains the improvement in short period damping ratio which was obtained in the separate airframe control problem. Eigenvalues for the open loop integrated system (Int.), for the separate systems with the previously derived feedback controls (Air. Ctr., Eng. Ctr.) and for the integrated system with feedback control (Int. Ctr.) are listed in table 6. Corresponding short period variables are listed in table 7.

TABLE 6. Feedback control effects on stability.
Eigenvalues.

Airframe			
Int.	-2.762E-3	3.743E-4 ± j3.253E-2	-6.782E-1 ± j2.201E+0
Air. Ctr.	-3.242E-3	-6.973E-3 , -1.767E-1	-2.026E+0 + j1.258E+0
Int. Ctr.	-4.729E-3	-1.464E+0 ± j1.117E+0	-1.865E+0 ± j1.031E+0

Engine				
Int.	-5.617E-1	-1.883E+0	-6.585E+0 , -1.000E+1	-1.722E+2
Eng. Ctr.	-1.484E+0	-3.374E+0	-1.007E+1 ± j1.984E+0	-2.624E+2
Int. Ctr.	-7.721E-1	-3.374E+0	-1.007E+1 ± j1.983E+0	-2.624E+2

TABLE 7. Short period variables.

ωn - natural frequency (rad/sec)	ξ - damping coefficient
tp - period (sec)	th - time to half amplitude(sec)

	ωn	ξ	tp	th
Int.	2.303	0.2945	2.729	1.022
Air. Ctr.	2.385	0.8496	2.635	.3422
Int. Ctr.	2.130	0.8752	2.948	.3716

The transient response of the integrated system to offsets in state variables from trim indicates the significance of the above determined feedback control. Several general observations can be made concerning the integrated system with this feedback control.

For initial offsets in values of airframe states the following, observations can be made.

1.) The integrated control system compensates for the coupling between airframe and engine variables present in the open loop integrated system model and provides good engine control. Recall that small perturbations in airframe states can lead to significant changes in engine variables.

2.) The closed loop integrated system and the separate closed loop airframe model, which was previously analyzed, respond in a similar manner. Responses of angle of attack, pitch rate and pitch attitude are similar and there appears to be a trade-off between velocity and altitude in the two control problems.

3.) The dependence of engine states on altitude introduces an implicit penalty on deviations of altitude from its trim value. This penalty was not present in the separate airframe control problem and is most evident in the response of the integrated system to an initial offset in altitude.

4.) All control variables are active to some extent.

For initial offsets in values of engine states the following observations can be made.

1.) Small oscillations in angle of attack, pitch rate and pitch attitude, which were present in the open loop system model, are amplified. These oscillations are still small relative to the given operating point values.

2.) The integrated control system provides good engine control.

3.) Again all controls are active.

The possibility of achieving similar responses with less complex control laws will be considered in the next section of this report.

Transient responses of the open and closed loop integrated model to small offsets in the trim values of angle of attack, altitude, compressor speed and augmentor pressure are depicted in figures 10 through 13. For an initial offset in angle of attack, the system responds with good damping in angle of attack, pitch rate and pitch attitude (see figure 10). If this figure is compared with figure 5, one observes the similar behavior of angle of attack, pitch rate, pitch attitude, glide path angle and thrust. Also, slightly better response in velocity is observed for the integrated system. Here the horizontal stabilator, δe, is pulsed for control and it is difficult to see if all engine controls are necessary. For an initial offset in altitude, figure 11, one should notice the increased oscillations of angle of attack, pitch rate and pitch attitude and that these disturbances are damped out faster in the integrated system than in the separate airframe model (see figure 8). Figure 11 shows a rapid altitude change not apparent in figure 8. One should note the high h to δe gain of -5.48 in the integrated system, this gain was -0.0037 previously. Other δe gains are higher, also. The performance index for the integrated system has no explicit weight on altitude but altitude effects on engine variables are included in the integrated system model. In this case the aircraft seems to be reacting to minimize engine perturbations. The response of the integrated system to an offset in compressor speed (figure 12) illustrates coupling present in the integrated sytem with feedback control. Similar responses will occur for an offset in fan speed. For initial offsets in the trim values of augmentor pressure, fuel flow and compressor discharge pressure, very little coupling is apparent in the integrated system transient response. This behavior is depicted in figure 13.

Suboptimal control. Because of the large number of gains present in the integrated system feedback matrix, studies were made to determine if performance could be maintained using a feedback matrix with a smaller number of non-zero gains. Four strategies for determining suboptimal feedback matrices were used. The first strategy, St1, uses a feedback gain matrix obtained from the feedback matrices determined in the separate flight and engine control problems. In this case the dependence of thrust upon airframe states is neglected. In the second strategy, St2, the gain matrix is obtained by zeroing gains in the integrated system feedback matrix which correspond to control system cross-coupling. In suboptimal strategy three, St3(ε), all state and control variables, except pitch rate, are normalized relative to their given trim value. Gains in the normalized system feedback matrix, whose magnitudes are less than some preassigned tolerance ε, are set to zero. The corresponding gains in the integrated system feedbackmatrix are set to zero. In the final strategy, St4(ε), sensitivity analysis is used to determine which gains should be set to zero. In this method a gain sensitivity matrix

$$GSM(g) = (Sen(\lambda 1,g), \ldots, Sen(\lambda 10,g))$$

is calculated, where λi, i =1, ..., 10 denote the eigenvalues of AAAE - BABE•K and g denotes a gain in the feedback matrix K. In this strategy a gain is set to zero whenever all entries in the corresponding gain sensitivity matrix are less than some preassigned tolerance ε. That is, gain g = 0 if

$$\max\{ |Sen(\lambda i,g)| : i = 1,\ldots, 10 \} < \varepsilon$$

were ε denotes a preassigned tolerance.

These strategies determine various feedback matrices to be compared with the full integrated system feedback matrix previously determined. The expected value of the performance index may be used for such a comparison. Values of the expected value of performance corresponding to use of different feedback matrices are listed in table 8.

TABLE 8. Suboptimal control.
Expected performance.

Strategy	E(J)	Strategy	E(J)	Strategy	E(J)
Int.Ctr.	1 367	St3(.1)	1 371	St4(.1)	1 759
St1	23 349	St3(.01)	1 368	ST4(.01)	1 376
St2	3 330	St3(.001)	1 367	St4(.001)	1 368

Feedback matrices used in these control strategies are listed in table 9. It shoud be noted that gains are being elimated in different orders by strategies St3 and St4.

The performance of the closed loop systems determined by strategies St1 and St2 is not as good as that of the system with full feedback control. In each case the feedback controls do not compensate, as well as the controls determined by the full feedback matrix, for coupling between airframe and engine variables. In particular for an offset in the value of an airframe state variable, neither of these suboptimal strategies control the engine as well as the control determined by the full feedback matrix. A typical illustration of this type of behavior is depicted in figure 14, where the response of the system with feedback determined by strategy St1 is compared with that of the system with full feedback control.

The number of gains set to zero using strategy St3(ε) with ε = .1 is 27, with ε = .01 is 13 and with ε = .001 is 10. In strategy St3 larger values of the tolerance lead to unstable feedback systems. The number of gains set to zero using strategy St4(ε) with ε = .1 is 55 , with ε = .01 is 39 and with ε = .001 is 14. For the feedback control laws determined by strategies St4(.1) and St4(.01) the eigenvalues for the closed loop system AAAE - BABE•K compare favorably with those of the integrated system with full feedback, these eigenvalues are listed in table 10. The corresponding modal matrices for these two strategies are listed in table 15 of appendix C. For strategy St4 larger values of the tolerance yielded eigenvalues which did not compare favorably with those of the integrated system with full feedback.

Since strategy St4(.1) resulted in 55 gains set to zero leaving only 15 non-zero gains (see table 9), the integrated system with corresponding feedback control was analyzed further. In this case, rear compressor variable

TABLE 9. Suboptimal control feedback matrices.

Strategy St1

	v	α	q	θ	h	N1	N2	P5	Wf	P2
δe	8.113D-05	3.153D-01	-3.887D-01	-2.478D-01	-3.718D-04	0.0	0.0	0.0	0.0	0.0
Wfc	0.0	0.0	0.0	0.0	0.0	9.019D-04	1.395D-03	6.577D-04	3.477D-01	-7.935D-04
A	0.0	0.0	0.0	0.0	0.0	3.715D-05	2.032D-06	-8.580D-04	-1.365D-03	-1.779D-05
CIVV	0.0	0.0	0.0	0.0	0.0	-8.985D-03	3.329D-03	1.025D-01	-6.313D-01	-8.383D-03
RCVV	0.0	0.0	0.0	0.0	0.0	6.784D-04	-7.977D-03	2.213D-02	3.964D-01	2.300D-02
BLC	0.0	0.0	0.0	0.0	0.0	-4.020D-05	-5.862D-05	-1.321D-03	-3.174D-02	-6.575D-04
PR	0.0	0.0	0.0	0.0	0.0	0.0	0.0	0.0	0.0	0.0

Strategy St2

	v	α	q	θ	h	N1	N2	P5	Wf	P2
δe	4.587D-02	1.722D+00	-6.485D-01	-2.730D+00	-5.480D+00	0.0	0.0	0.0	0.0	0.0
Wfc	0.0	0.0	0.0	0.0	0.0	9.010D-04	1.386D-03	6.823D-04	3.474D-01	-7.938D-04
A	0.0	0.0	0.0	0.0	0.0	3.714D-05	1.943D-06	-8.578D-04	-1.368D-03	-1.779D-05
CIVV	0.0	0.0	0.0	0.0	0.0	-8.988D-03	3.303D-03	1.026D-01	-6.317D-01	-8.383D-03
RCVV	0.0	0.0	0.0	0.0	0.0	6.865D-04	-7.898D-03	2.197D-02	3.992D-01	2.300D-02
BLC	0.0	0.0	0.0	0.0	0.0	-4.019D-05	-5.847D-05	-1.321D-03	-3.173D-02	-6.575D-04
PR	0.0	0.0	0.0	0.0	0.0	0.0	0.0	0.0	0.0	0.0

Strategy St3(.1)

	v	α	q	θ	h	N1	N2	P5	Wf	P2
δe	4.587D-02	1.722D+00	-6.485D-01	-2.730D+00	-5.480D+00	7.025D-05	1.200D-03	0.0	0.0	0.0
Wfc	1.364D-02	-9.822D-02	0.0	0.0	5.118D-02	9.010D-04	1.386D-03	0.0	3.474D-01	-7.938D-04
A	-1.114D-04	0.0	0.0	0.0	2.529D-02	3.714D-05	0.0	-8.578D-04	0.0	0.0
CIVV	2.085D-02	0.0	0.0	-1.181D-01	-3.324D+00	-8.988D-03	3.303D-03	1.026D-01	-6.317D-01	-8.383D-03
RCVV	-2.746D-02	0.0	0.0	2.115D-01	1.110D+00	6.865D-04	-7.898D-03	2.197D-02	3.992D-01	2.300D-02
BLC	-6.721D-04	4.447D-03	0.0	-3.712D-03	1.537D-03	-4.019D-05	-5.847D-05	-1.321D-03	-3.173D-02	-6.575D-04
PR	0.0	0.0	0.0	0.0	0.0	0.0	0.0	0.0	0.0	0.0

TABLE 9 concluded.

Strategy St3(.01)

v	α	q	θ	h	N1	N2	P5	Wf	P2
4.587D-02	1.722D+00	-6.485D-01	-2.730D+00	-5.480D+00	7.025D-05	1.200D-03	-1.233D-03	4.144D-02	5.781D-05
1.364D-02	-9.822D-02	0.0	5.680D-02	5.118D-02	9.010D-04	1.386D-03	6.823D-04	3.474D-01	-7.938D-04
-1.114D-04	-1.166D-03	0.0	1.445D-03	2.529D-02	3.714D-05	1.943D-06	-8.578D-04	-1.368D-03	-1.779D-05
2.085D-02	-9.874D-03	-2.022D-02	-1.181D-01	-3.324D+00	-8.988D-03	3.303D-03	1.026D-01	-6.317D-01	-8.383D-03
-2.746D-02	1.151D-02	0.0	2.115D-01	1.110D+00	6.865D-04	-7.898D-03	2.197D-02	3.992D-01	2.300D-02
-6.721D-04	4.447D-03	1.102D-04	-3.712D-03	1.537D-03	-4.019D-05	-5.847D-05	-1.321D-03	-3.173D-02	-6.575D-04
0.0	0.0	0.0	0.0	0.0	0.0	0.0	0.0	0.0	0.0

Strategy St4(.1)

v	α	q	θ	h	N1	N2	P5	Wf	P2
4.587D-02	1.722D+00	-6.485D-01	-2.730D+00	-5.480D+00	0.0	1.200D-03	0.0	0.0	0.0
1.364D-02	-9.822D-02	0.0	5.680D-02	0.0	9.010D-04	1.386D-03	0.0	3.474D-01	0.0
0.0	0.0	0.0	0.0	0.0	3.714D-05	0.0	0.0	0.0	0.0
0.0	0.0	0.0	0.0	0.0	-8.988D-03	0.0	0.0	0.0	0.0
0.0	0.0	0.0	0.0	0.0	0.0	0.0	0.0	0.0	0.0
0.0	0.0	0.0	0.0	0.0	0.0	0.0	0.0	0.0	-6.575D-04
0.0	0.0	0.0	0.0	0.0	0.0	0.0	0.0	0.0	0.0

Strategy St4(.01)

	v	α	q	θ	h	N1	N2	P5	Wf	P2
δe	4.587D-02	1.722D+00	-6.485D-01	-2.730D+00	-5.480D+00	0.0	1.200D-03	0.0	4.144D-02	0.0
Wfc	1.364D-02	-9.822D-02	-6.178D-03	5.680D-02	0.0	9.010D-04	1.386D-03	0.0	3.474D-01	0.0
A	-1.114D-04	-1.166D-03	0.0	1.445D-03	2.529D-02	3.714D-05	0.0	-8.578D-04	0.0	0.0
CIVV	0.0	0.0	0.0	0.0	0.0	-8.988D-03	0.0	0.0	0.0	0.0
RCVV	-2.746D-02	0.0	0.0	0.0	0.0	0.0	-7.898D-03	0.0	0.0	0.0
BLC	-6.721D-04	4.447D-03	0.0	-3.712D-03	0.0	-4.019D-05	-5.847D-05	-1.321D-03	-3.173D-02	-6.575D-04
PR	0.0	0.0	0.0	0.0	0.0	0.0	0.0	0.0	0.0	0.0

vane position, RCVV, and pressure recovery ratio, Pr, are not used as controls and there is only one gain associated with nozzle area, a, inlet guidevane, CIVV, and compressor bleed, BLC. Also changes in compressor speed are fed back to control δe, whereas, changes in velocity, angle of attack and pitch attitude are fed back to control fuel flow. Transient responses of the integrated system using suboptimal feedback matrices determined by strategy St4(.1) and the full feedback matrix previously determined are nearly the same for offsets in any state variable. Typical responses for the integrated system using the control determined by strategy St4(.1) and the full feedback matrix previously determined are depicted in figures 15 and 16. In each case, it should be observed that the integrated system with suboptimal feedback behaves in a manner very similar to the system with full feedback control.

TABLE 10. Suboptimal control effects on stabilty.
System eigenvalues.

Airframe				
Int. Ctr.	-4.729E-3	-1.464E+0 ± j1.117E+0	-1.865E+0 ± j1.031E+0	
ST4(.1)	-4.800E-3	-1.395E+0 ± j1.105E+0	-1.893E+0 ± j1.083E+0	
ST4(.01)	-4.735E-3	-1.450E+0 ± j1.100E+0	-1.863E+0 ± j1.052E+0	
Engine				
Int. Ctr.	-7.721E-1	-3.374E+0	-1.007E+1 ± j1.983E+0	-2.624E+2
ST4(.1)	-7.105E-1	-3.519E+0	-0.902E+1 ± j0.803E+0	-2.590E+2
ST4(.01)	-7.689E-1	-3.352E+0	-1.015E+1 ± j1.982E+0	-2.577E+2

CONCLUDING REMARKS

In this report numerical and analytical techniques are used to develop models of aircraft subsystem interactions and to analyze the effect of subsystem interactions upon system stability and control.

The inclusion of subsystem interactions in the airframe/propulsion system model changed the overall system behavior. Also, the approach used to develop the flight/propulsion system model in this report is general since standard flight and propulsion system models are combined to form the integrated system model.

Methods presented in this report provide a means to identify interaction parameters in an operating point model of a flight/propulsion model.

The model, developed in this report, provides a means for further parameter studies. For example, the effect of changing the location of the engine below the center of gravity or the effect of using inlet pressure recovery ratio as a control parameter could be readily analyzed using this model.

The problem of developing adequate models of subsystem interactions remains difficult. For example, the effect of variable geometry inlets upon aerodynamic forces and moments have not been included in the model . Also angle of attack and sideslip angle effects upon engine airflow have not been considered.

Linear quadratic regulator methods and numerical linear algebra techniques have provided flexible means to analyze the control of integrated systems.

For the separate airframe model, feedback control provides substantial improvement in short period damping.

For the integrated flight/propulsion model, feedback control conpensates for coupling present in the model and provides good overall system stability. In the model example, the aircraft appears to be reacting to minimize engine perturbations. This behavior results from the dependence of engine variables upon Mach number and altitude. In the performance index used for this example, the engine was referenced to a fixed trim point. Perhaps the engine should have been referenced to trim values which change with Mach number and altitude.

Analysis of suboptimal control strategies, indicates that performance of the closed loop integrated system can be maintained with a feedback matrix in which the number of nonzero gains is small relative to the number of components in the feedback matrix.

A method based on senitivity analysis, proved to be an effective means for determining which gains in the integrated system feedback matrix can be set to zero while, at the same time, maintaining system performance.

APPENDIX A

AIRCRAFT EFFECTS ON ENGINE

The off-design performance model for a turbofan engine developed by F. J. Lallman [21] expresses total temperatures and pressures throughout the engine along with specific thrust and fuel to air ratio as functions of flight condition (Mach number and ambient temperature), inlet performance (pressure recovery ratio), fan pressure ratio, compressor pressure ratio and burner temperature. This model may be used to obtain engine perturbation equations which describe the effect of varying flight condition and inlet performance upon propulsion system operation.

Notation consistent with that of reference [21] will be used in this appendix. For a given operating point, perturbation equations will be presented which express the effect of changes in Mach number, altitude amd pressure recovery ratio upon engine temperatures, pressures and performance variables.

The engine characteristics are as listed in Table I of [21]. A full power engine operating point is assumed, this condition corresponds to a fan pressure ratio of 2.9, a compressor pressure ratio of 7.93 and a burner temperature of 1559 K. The engine design point model is as follows:

$$\delta_{0_S} = \begin{cases} \Theta_{0_S}^{\;5.256} & 0 \le h_0 \le 11 \\ 0.2233\, e^{-0.157(h_0-11)} & 11 \le h_0 \le 20 \end{cases}$$

$$\delta_0 = (\Theta_0/\Theta_{0_S})^{3.518}\, \delta_{0_S}$$

$$\delta_1 = r_{1,0}\, \delta_0$$

$$\delta_{1'} = 2.9\, \delta_1$$

$$\delta_2 = 7.93\, \delta_{1'}$$

$$\delta_3 = 0.95\, \delta_2$$

$$\delta_4 = (1.016 - 0.3908\, \Theta_1)^{4.290}\, \delta_3$$

$$\delta_5 = \delta_4$$

and

$$\Theta_{0_S} = \begin{cases} 1 - 0.02256 h_0 & 0 \le h_0 \le 11 \\ 0.7519 & 11 \le h_0 \le 20 \end{cases}$$

$$\Theta_0 = (1 + 0.199M_0^{2})\Theta_{0_S}$$

$$\Theta_1 = \Theta_0$$

$$\Theta_{1'} = 1.387\Theta_1$$

$$\Theta_2 = 1.864\Theta_{1'}$$

$$\Theta_3 = 5.41$$

$$\Theta_4 = 5.488 - 1.903\Theta_1$$

$$\Theta_5 = 4.677 - 1.234\Theta_1$$

also

$$v_0 = 340.4(\Theta_{0_S})^{1/2}M_0$$

$$WA = 79.887\delta_1/(\Theta_1)^{1/2}$$

$$WF/WA = 0.02332 - 0.01086\Theta_1$$

$$WF = (WF/WA)WA$$

$$ST = ST1 + ST2 - v_0$$

$$ST1 = 482.9(1-(\delta_5/\delta_{0_S})^{-0.2698})^{1/2}(\Theta_5)^{1/2}$$

$$ST2 = 273.9(1-(\delta_{1'}/\delta_{0_S})^{-0.266})^{1/2}(\Theta_{1'})^{1/2}$$

$$TH = ST \bullet WA$$

where the δ's represent engine pressures relative to sea level standard (101.4 kPa), the Θ's represent engine temperatures relative to sea level standard (288.2 K), WA fan airflow, WF/WA fuel to air ratio, v^0 aircraft velocity, ST specific thrust (thrust per unit mass flow), and TH denotes thrust.

Using the notation

$$\Delta h_0 = h, \quad \Delta r_{1',0} = Pr, \quad \Delta M_0 = M, \quad \Delta WF = Wf \quad \Delta TH = Th$$

the perturbation equations for this design point are as follows:

$$\Delta\delta_{0_S} = \begin{cases} 5.256\theta_{0_S}{}^{4.256}\Delta\theta_{0_S} & 0 \le h_0 \le 11 \\ -0.1577\delta_{0_S}h & 11 \le h_0 \le 20 \end{cases}$$

$$\Delta\delta_0 = (\theta_0/\theta_{0_S})^{3.518}\Delta\delta_{0_S} + 3.518\delta_{0_S}(\theta_0/\theta_{0_S})^{2.518}\Delta(\theta_0/\theta_{0_S})$$

$$\Delta\delta_1 = r_{1,0}\Delta\delta_0 + \delta_0 Pr$$

$$\Delta\delta_{1'} = 2.9\Delta\delta_1$$

$$\Delta\delta_2 = 7.93\Delta\delta_{1'}$$

$$\Delta\delta_3 = 0.95\Delta\delta_2$$

$$\Delta\delta_4 = -1.6765\delta_3(1.016-0.3908\theta_1)^{3.29}\Delta\theta_1 + 0.95(1.016-0.3908\theta_1)^{4.29}\Delta\delta_2$$

$$\Delta\delta_5 = \Delta\delta_4$$

and

$$\Delta\theta_{0_S} = \begin{cases} -0.02256h & 0 \le h_0 \le 11 \\ 0 & 11 \le h_0 \le 20 \end{cases}$$

$$\Delta\theta_0 = 0.398\theta_{0_S}M_0 \bullet M + (1 + 0.199M_0^{\,2})\Delta\theta_{0_S}$$

$$\Delta\theta_1 = \Delta\theta_0$$

$$\Delta\theta_{1'} = 1.387\Delta\theta_1$$

$$\Delta\theta_2 = 1.864\Delta\theta_{1'}$$

$$\Delta\theta_3 = 0.0$$

$$\Delta\theta_4 = -1.903\Delta\theta_1$$

$$\Delta\theta_5 = -1.234\Delta\theta_1$$

and

$$\Delta v_0 = 170.2M_0(\theta_{0_S})^{-1/2}\Delta\theta_{0_S} + 340.4(\theta_{0_S})^{1/2}M$$

$$\Delta WA = WA(\Delta\delta_1/\delta_1 - 0.5\Delta\theta_1/\theta_1)$$

$$\Delta(WF/WA) = -0.01086\Delta\theta_1$$

$$Wf = WA\Delta(WF/WA) + (WF/WA)\Delta WA$$

$$\Delta ST = \Delta ST1 + \Delta ST2 - \Delta v_0$$

$$\Delta ST1 = 65.143\Theta_5^{.5}((1-(\delta_5/\delta_{0_S})^{-.2698})^{-.5}\,(\delta_5/\delta_{0_S})^{-1.2698}\Delta(\delta_5/\delta_{0_S})$$

$$+\ 241.45\Theta_5^{-.5}\,(1-(\delta_5/\delta_{0_S})^{-.2698})^{.5}\Delta\Theta_5$$

$$\Delta ST2 = 36.429(\Theta_{1,})^{.5}(1-(\delta_{1,}/\delta_{0_S})^{-.266})^{-.5}\,(\delta_{1,}/\delta_{0_S})^{-1.266}\Delta(\delta_{1,}/\delta_{0_S})$$

$$+\ 136.95\Theta_{1,}^{-.5}(1-(\delta_{1,}/\delta_{0_S})^{-.266})^{.5}\,\Delta\Theta_{1,}.$$

$$Th = (\Delta ST)\bullet WA + (\Delta WA)\bullet ST$$

For the control design example under consideration the nominal values of Mach number, altitude and inlet pressure recovery ratio are

$$M_0 = 0.9 \qquad h_0 = 12.\ \text{km} \qquad r_{1,0} = 1.0$$

The engine variables of interest are P2, P5, Wf, Th and Wa where

$$P2 = 101.4\delta_2 \text{ and } P5 = 101.4\delta_5.$$

For this flight condition and pressure recovery ratio the resulting perturbation equations may be written as

$$P5 = 42.02\ M - 15.938\ h + 101.016\ Pr$$

$$Wf = 2.717\ M - 0.5905\ h + 3.7487\ Pr$$

$$P2 = 635.55\ M - 90.631\ h + 554.812\ Pr$$

$$Th = 8267.0\ M - 2121.0\ h + 17826.0\ Pr$$

$$Wa = 25.678\ M - 4.350\ h + 27.586\ Pr.$$

These equations describe perturbations in P5, Wf, P2, Th, and Wa due to perturbations in Mach number, altitude, and pressure recovery ratio necessary to maintain the operating condition.

The engine dynamics about the operating point are described by the differential equations

$$Dxe/Dt = AE\bullet xe + BE\bullet ue + CEA\bullet ya + CEI\bullet yi$$

$$ye = FE\bullet xe + GE\bullet ue + HEA\bullet ya + HEI\bullet yi.$$

In order to determine the interaction matrices CEA, CEI, HEA, HEI, it is convenient to rewrite the above perturbation equations in matrix form as follows

$$\begin{bmatrix} P5 \\ P2 \end{bmatrix} = E1 \bullet \begin{bmatrix} M \\ h \\ Pr \end{bmatrix} \qquad [Wf] = E2 \bullet \begin{bmatrix} M \\ h \\ Pr \end{bmatrix} \qquad \begin{bmatrix} Th \\ Wa \end{bmatrix} = E3 \bullet \begin{bmatrix} M \\ h \\ Pr \end{bmatrix}$$

where E1, E2, and E3 are appropriate matrices.

At the given operating point it is assumed that ya and yi have no direct effect upon the variables N1, N2, and Wf. Consequently the first, second, and fourth rows of CEA and CEI are zero while the remaining entries of CEA, CEI, HEA, and HEI are chosen so that the steady state response of the dynamic system to changes in ya and yi agrees with the previously derived perturbation equations.

Algebraically, these assumptions determine the following equations for the unknown entries of the matrices CEA, CEI, HEA, and HEI. With no control the steady state response of the engine is given by the equations

$$xe = -(AE)^{-1}[\ CEA \bullet ya + CEI \bullet yi\ ]$$

$$ye = FE \bullet xe + HEA \bullet ya + HEI \bullet yi.$$

In order that these equations agree with the previously determined perturbation equations for P5, P2, Th and Wa it is necessary that

$$E1 = \begin{bmatrix} 0. & 0. & 0. & 1. & 0. & 0. \\ 0. & 0. & 0. & 0. & 0. & 1. \end{bmatrix} \bullet AE^{-1}[CEA,\ CEI]$$

$$[HEA,\ HEI] = E3 + \begin{bmatrix} FE1 \\ FE2 \end{bmatrix} \bullet AE^{-1}[CEA,\ CEI]$$

where [CEA,CEI] and [HEA,HEI] denote the matrices whose columns are the corresponding columns of CEA, CEI, HEA, and HEI. FE1 and FE2 denote the first and second rows, respectively, of the matrix FE. Using the modelling assumption that the first two rows of CEA and CEI are zero, these equations may be inverted to obtain the unknown components of CEA, CEI, HEA, and HEI.

APPENDIX B

EIGENVALUE SENSITIVITY CALCULATIONS

In the case of distinct eigenvalues the real Jordan canonical form Λ of a matrix A is a block diagonal matrix. The i-th diagonal block Λi of Λ is λ, if λ is a real eigenvalue of A or

$$\Lambda i = \begin{bmatrix} a & b \\ -b & a \end{bmatrix}$$

if $\lambda = a + jb$ is a complex eigenvalue. The modal matrix T such that

$$A \bullet T = T \bullet \Lambda \qquad \text{(B.1)}$$

is determined by the eigenvectors of A. If λ is a real eigenvalue with corresponding eigenvector u then the corresponding column of T equals u. Whereas if λ is complex with eigenvector u + jv then the corresponding columns of T equal u and v. In the real case the fundamental mode corresponding to λ is

$$X(t) = u \bullet e^{\lambda t}.$$

In the complex case the fundamental modes corresponding to $\lambda = a + jb$ are

$$X(t) = e^{at}[\ u \bullet \cos(bt) - v \bullet \sin(bt)\ ]$$

$$Y(t) = e^{at}[\ u \bullet \sin(bt) + v \bullet \cos(bt)\ ].$$

If the matrix A depends on a parameter ε then differentiation of equation (B.1) yields

$$T^{-1} \bullet DA/D\varepsilon \bullet T + \Lambda \bullet T^{-1} \bullet DT/D\varepsilon = T^{-1} \bullet DT/D\varepsilon \bullet \Lambda + D\Lambda/D\varepsilon.$$

In this last equation if the i-th diagonal block of Λ corresponds to a real eigenvalue then

$$(\ \Lambda \bullet T^{-1} \bullet DT/D\varepsilon\ )_{i,i} = (\ T^{-1} \bullet DT/D\varepsilon \bullet \Lambda\ )_{i,i}$$

and it follows that

$$D\lambda/D\varepsilon = (\ T^{-1} \bullet DA/D\varepsilon \bullet T\ )_{i,i}.$$

If the i-th diagonal block of Λ corresponds to a complex eigenvalue then

$$(\Lambda \bullet T^{-1} \bullet DT/D\varepsilon)_{i,i} = (a \bullet T^{-1} \bullet DT/D\varepsilon)_{i,i} + (b \bullet T^{-1} \bullet DT/D\varepsilon)_{i+1,i}$$

$$(\Lambda \bullet T^{-1} \bullet DT/D\varepsilon)_{i,i+1} = (a \bullet T^{-1} \bullet DT/D\varepsilon)_{i,i+1} + (b \bullet T^{-1} \bullet DT/D\varepsilon)_{i+1,i+1}$$

$$(\Lambda \bullet T^{-1} \bullet DT/D\varepsilon)_{i+1,i} = (-b \bullet T^{-1} \bullet DT/D\varepsilon)_{i,i} + (a \bullet T^{-1} \bullet DT/D\varepsilon)_{i+1,i}$$

$$(\Lambda \bullet T^{-1} \bullet DT/D\varepsilon)_{i+1,i+1} = (-b \bullet T^{-1} \bullet DT/D\varepsilon)_{i,i+1} + (a \bullet T^{-1} \bullet DT/D\varepsilon)_{i+1,i+1}$$

$$(T^{-1} \bullet DT/D\varepsilon \bullet \Lambda)_{i,i} = (a \bullet T^{-1} \bullet DT/D\varepsilon)_{i,i} - (b \bullet T^{-1} \bullet DT/D\varepsilon)_{i,i+1}$$

$$(T^{-1} \bullet DT/D\varepsilon \bullet \Lambda)_{i,i+1} = (b \bullet T^{-1} \bullet DT/D\varepsilon)_{i,i} + (a \bullet T^{-1} \bullet DT/D\varepsilon)_{i,i+1}$$

$$(T^{-1} \bullet DT/D\varepsilon \bullet \Lambda)_{i+1,i} = (a \bullet T^{-1} \bullet DT/D\varepsilon)_{i+1,i} - (b \bullet T^{-1} \bullet DT/D\varepsilon)_{i+1,i+1}$$

$$(T^{-1} \bullet DT/D\varepsilon \bullet \Lambda)_{i+1,i+1} = (b \bullet T^{-1} \bullet DT/D\varepsilon)_{i+1,i} + (a \bullet T^{-1} \bullet DT/D\varepsilon)_{i+1,i+1}.$$

Since

$$T^{-1} \bullet DA/D\varepsilon \bullet T + \Lambda \bullet T^{-1} \bullet DT/D\varepsilon = T^{-1} \bullet DT/D\varepsilon \bullet \Lambda + D\Lambda/D\varepsilon$$

t follows that

$$(T^{-1} \bullet DA/D\varepsilon \bullet T)_{i,i} + (T^{-1} \bullet DA/D\varepsilon \bullet T)_{i+1,i+1} + (\Lambda \bullet T^{-1} \bullet DT/D\varepsilon)_{i,i}$$
$$+ (\Lambda \bullet T^{-1} \bullet DT/D\varepsilon)_{i+1,i+1}$$
$$= (T^{-1} \bullet DT/D\varepsilon \bullet \Lambda)_{i,i} + (T^{-1} \bullet DT/D\varepsilon \bullet \Lambda)_{i+1,i+1} + 2Da/D\varepsilon$$

and consequently

$$Da/D\varepsilon = ((T^{-1} \bullet DA/D\varepsilon \bullet T)_{i,i} + (T^{-1} \bullet DA/D\varepsilon \bullet T)_{i+1,i+1})/2$$

Similarly

$$Db/D\varepsilon = ((T^{-1} \bullet DA/D\varepsilon \bullet T)_{i,i+1} - (T^{-1} \bullet DA/D\varepsilon \bullet T)_{i+1,i})/2.$$

These identities are used to calculate sensitivity derivatives in this report.

APPENDIX C

SYSTEM MATRICES

System matrices for the models presented in this report are contained in this appendix. In table 11 matrices associated with the separate airframe model are listed. This data was supplied by NASA. In table 12 matrices associated with the separate engine model are listed. This data was derived from data presented in the report [15]. System matrices for the integrated flight/propulsion model are presented in table 13. Modal matrices for the separate flight and engine models and for the integrated model, are listed in table 14. In table 15 the eigenvalues and modal matrices for suboptimal control strategies St1, St2, St3 and St4 are listed. The modal matrices listed in tables 14, 15 have been denoted by the symbol T in the body of this report. The colunms of these matrices consist of eigenvectors corresponding to real eigenvalues and the real and imaginary part of complex eigenvectors corresponding to complex eigenvalues. The order in which real and imaginary parts of eigenvectors appear in these modal matrices is the order in which eigenvalues are listed in tables 14, 15.

TABLE 11. Airframe matrices.

$$
AA = \begin{bmatrix}
-1.5729D-02 & -1.1923D+01 & 0.0 & -9.8065D+00 & 2.0029D-01 \\
-3.6756D-04 & -5.9740D-01 & 1.0000D+00 & 0.0 & 5.8608D-03 \\
-3.1733D-03 & -4.8424D+00 & -7.4522D-01 & 0.0 & 5.0486D-03 \\
0.0 & 0.0 & 1.0000D+00 & 0.0 & 0.0 \\
0.0 & -2.6556D-01 & 0.0 & 2.6556D-01 & 0.0
\end{bmatrix}
\qquad
BA = \begin{bmatrix}
-2.3459D+00 \\
-6.4267D-02 \\
-7.4235D+00 \\
0.0 \\
0.0
\end{bmatrix}
$$

$$
CAE = \begin{bmatrix}
1.2246D-04 & 0.0 & 0.0 & 0.0 & 0.0 & 0.0 \\
-3.5175D-08 & 0.0 & 0.0 & 0.0 & 0.0 & 0.0 \\
2.5561D-06 & 0.0 & 0.0 & 0.0 & 0.0 & 0.0 \\
0.0 & 0.0 & 0.0 & 0.0 & 0.0 & 0.0 \\
0.0 & 0.0 & 0.0 & 0.0 & 0.0 & 0.0
\end{bmatrix}
$$

$$
FA = \begin{bmatrix}
3.3887D-03 & 0.0 & 0.0 & 0.0 & 0.0 \\
0.0 & 0.0 & 0.0 & 0.0 & 1.0000D+00
\end{bmatrix}
$$

$$
FFA = \begin{bmatrix}
1.0000D+00 & 0.0 & 0.0 & 0.0 & 0.0 \\
0.0 & -1.0000D+00 & 0.0 & 1.0000D+00 & 0.0 \\
0.0 & 0.0 & 1.0000D+00 & 0.0 & 0.0
\end{bmatrix}
\qquad
GGA = \begin{bmatrix}
0.0 & 0.0 \\
0.0 & 0.0 \\
0.0 & 0.0
\end{bmatrix}
$$

$$
WA = \begin{bmatrix}
4.0000D-08 & 0.0 & 0.0 \\
0.0 & 2.5000D-01 & 0.0 \\
0.0 & 0.0 & 1.0000D+00
\end{bmatrix}
$$

$$
UA = \begin{bmatrix}
4.0000D+00 & 0.0 \\
0.0 & 2.5000D-11
\end{bmatrix}
$$

TABLE 12. Engine system matrices

AE

-9.606D-01	-5.966D-01	-1.611D+02	1.082D+03	1.881D+01
7.955D-01	-1.644D+00	-3.841D+01	-1.546D+02	9.823D+00
1.786D-02	-3.572D-02	-8.886D+00	4.126D+01	5.756D-01
0.0	0.0	0.0	-1.000D+01	0.0
-5.128D+00	1.252D+01	6.572D+02	9.626D+03	-1.697D+02

BE

-1.936D+02	-3.886D+03	-2.723D+01	-8.001D+00	2.800D+03
3.329D+01	9.136D+02	1.747D+01	-1.417D+01	7.194D+03
-3.654D+00	-1.541D+03	6.288D-01	-5.130D-01	-2.559D+01
1.000D+01	0.0	0.0	0.0	0.0
-1.640D+03	-1.437D+04	-8.543D+01	9.729D+01	-1.327D+05

FE

1.649D+00	-2.028D+00	-2.785D-02	-2.705D+02	2.779D+01
1.962D-03	8.641D-07	-8.671D-04	8.153D-02	2.878D-07
8.306D-02	-5.002D-02	-2.912D+00	1.887D+02	-8.533D-02
2.068D-04	1.862D-06	-8.733D-03	9.428D-03	4.263D-05
-6.204D-05	1.524D-04	6.960D-03	6.722D-02	-1.606D-03
5.705D-05	-3.729D-05	-6.370D-03	-3.538D-02	1.157D-04

GE

1.882D+01	1.141D+04	4.025D+01	-1.378D+01	1.503D+04
2.333D-04	9.960D-01	8.160D-02	1.698D-04	7.013D-01
6.200D+00	3.067D+02	1.357D+00	-2.441D-01	1.072D+03
7.775D-04	2.770D-01	7.355D-04	1.406D-04	5.909D-01
-2.063D-02	-2.143D-01	-1.070D-03	-1.621D-03	-4.019D-01
1.148D-02	3.074D-01	1.901D-03	-2.397D-04	2.633D-01

CEA

0.0	0.0
0.0	0.0
1.066D+02	-9.594D+01
0.0	0.0
4.237D+04	-3.505D+03

CEI

0.0
0.0
1.066D+02
0.0
4.237D+04

HEA

-5.557D+03	-4.607D+02
2.021D+01	-5.878D+00
0.0	0.0
0.0	0.0
0.0	0.0
0.0	0.0

HEI

7.293D+03
3.726D+01
0.0
0.0
0.0
0.0

WE

5.000D-04	0.0	0.0	0.0	0.0
0.0	5.000D-04	0.0	0.0	0.0
0.0	0.0	1.052D-02	0.0	0.0
0.0	0.0	0.0	0.0	0.0
0.0	0.0	0.0	0.0	2.104D-02

UE

6.550D+01	0.0	0.0	0.0	0.0
0.0	4.634D+04	0.0	0.0	0.0
0.0	0.0	5.000D-01	0.0	0.0
0.0	0.0	0.0	2.000D-01	0.0
0.0	0.0	0.0	0.0	1.000D+04

TABLE 13. Integrated system matrices.

AAAE

-1.804D-02	-1.192D+01	0.0	-9.806D+00	1.439D-01	2.019D-04	-2.484D-04	-3.411D-06	-3.313D-02	3.404D-03
-3.669D-04	-5.974D-01	1.000D+00	0.0	5.877D-03	-5.799D-08	7.133D-08	9.797D-10	9.516D-06	-9.776D-07
-3.221D-03	-4.842D+00	-7.452D-01	0.0	3.871D-03	4.214D-06	-5.184D-06	-7.119D-08	-6.915D-04	7.104D-05
0.0	0.0	1.000D+00	0.0	0.0	0.0	0.0	0.0	0.0	0.0
0.0	-2.656D-01	0.0	2.656D-01	0.0	0.0	0.0	0.0	0.0	0.0
0.0	0.0	0.0	0.0	0.0	-9.606D-01	-5.966D-01	-1.611D+02	1.082D+03	1.881D+01
0.0	0.0	0.0	0.0	0.0	7.955D-01	-1.644D+00	-3.841D+01	-1.546D+02	9.823D+00
3.611D-01	0.0	0.0	0.0	-9.594D+01	1.786D-02	-3.572D-02	-8.886D+00	4.126D+01	5.756D-01
0.0	0.0	0.0	0.0	0.0	0.0	0.0	0.0	-1.000D+01	0.0
1.436D+02	0.0	0.0	0.0	-3.505D+03	-5.128D+00	1.252D+01	6.572D+02	9.626D+03	-1.697D+02

BABE

-2.346D+00	2.305D-03	1.397D+00	4.929D-03	-1.687D-03	1.841D+00	8.932D-01
-6.427D-02	-6.621D-07	-4.012D-04	-1.416D-06	4.846D-07	-5.287D-04	-2.565D-04
-7.424D+00	4.812D-05	2.915D-02	1.029D-04	-3.521D-05	3.842D-02	1.864D-02
0.0	0.0	0.0	0.0	0.0	0.0	0.0
0.0	0.0	0.0	0.0	0.0	0.0	0.0
0.0	-1.936D+02	-3.886D+03	-2.723D+01	-8.001D+00	2.800D+03	0.0
0.0	3.329D+01	9.136D+02	1.747D+01	-1.417D+01	7.194D+03	0.0
0.0	-3.654D+00	-1.541D+03	6.288D-01	-5.130D-01	-2.559D+01	1.066D+02
0.0	1.000D+01	0.0	0.0	0.0	0.0	0.0
0.0	-1.640D+03	-1.437D+04	-8.543D+01	9.729D+01	-1.327D+05	4.237D+04

FAFE

3.389D-03	0.0	0.0	0.0	0.0	0.0	0.0	0.0	0.0	0.0
0.0	0.0	0.0	0.0	1.000D+00	0.0	0.0	0.0	0.0	0.0
-1.883D+01	0.0	0.0	0.0	-4.607D+02	1.649D+00	-2.028D+00	-2.785D-02	-2.705D+02	2.779D+01
6.848D-02	0.0	0.0	0.0	-5.878D+00	1.962D-03	8.641D-07	-8.671D-04	8.153D-02	2.878D-07
0.0	0.0	0.0	0.0	0.0	8.306D-02	-5.002D-02	-2.912D+00	1.887D+02	-8.533D-02
0.0	0.0	0.0	0.0	0.0	2.068D-04	1.862D-06	-8.733D-03	9.428D-03	4.263D-05
0.0	0.0	0.0	0.0	0.0	-6.204D-05	1.524D-04	6.960D-03	6.722D-02	-1.606D-03
0.0	0.0	0.0	0.0	0.0	5.705D-05	-3.729D-05	-6.370D-03	-3.538D-02	1.157D-04

GAGE

0.0	0.0	0.0	0.0	0.0	0.0	0.0
0.0	0.0	0.0	0.0	0.0	0.0	0.0
0.0	1.882D+01	1.141D+04	4.025D+01	-1.378D+01	1.503D+04	7.293D+03
0.0	2.333D-04	9.960D-01	8.160D-02	1.698D-04	7.013D-01	3.726D+01
0.0	6.200D+00	3.067D+02	1.357D+00	-2.441D-01	1.072D+03	0.0
0.0	7.775D-04	2.770D-01	7.355D-04	1.406D-04	5.909D-01	0.0
0.0	-2.063D-02	-2.143D-01	-1.070D-03	-1.621D-03	-4.019D-01	0.0
0.0	1.148D-02	3.074D-01	1.901D-03	-2.397D-04	2.633D-01	0.0

TABLE 13. concluded.

FF

1.000D+00	0.0	0.0	0.0	0.0	0.0	0.0	0.0	0.0	0.0
0.0	-1.000D+00	0.0	1.000D+00	0.0	0.0	0.0	0.0	0.0	0.0
0.0	0.0	1.000D+00	0.0	0.0	0.0	0.0	0.0	0.0	0.0
-1.883D+01	0.0	0.0	0.0	-4.606D+02	1.649D+00	-2.028D+00	-2.785D-02	-2.705D+02	2.779D+01
0.0	0.0	0.0	0.0	0.0	1.000D+00	0.0	0.0	0.0	0.0
0.0	0.0	0.0	0.0	0.0	0.0	1.000D+00	0.0	0.0	0.0
0.0	0.0	0.0	0.0	0.0	0.0	0.0	1.000D+00	0.0	0.0
0.0	0.0	0.0	0.0	0.0	0.0	0.0	0.0	1.000D+00	0.0
0.0	0.0	0.0	0.0	0.0	0.0	0.0	0.0	0.0	1.000D+00

GG

0.0	0.0	0.0	0.0	0.0	0.0	0.0
0.0	0.0	0.0	0.0	0.0	0.0	0.0
0.0	0.0	0.0	0.0	0.0	0.0	0.0
0.0	1.882D+01	1.141D+04	4.025D+01	-1.378D+01	1.503D+04	7.293D+03
0.0	0.0	0.0	0.0	0.0	0.0	0.0
0.0	0.0	0.0	0.0	0.0	0.0	0.0
0.0	0.0	0.0	0.0	0.0	0.0	0.0
0.0	0.0	0.0	0.0	0.0	0.0	0.0
0.0	0.0	0.0	0.0	0.0	0.0	0.0

W

1.274D-08	0.0	0.0	0.0	0.0	0.0	0.0	0.0	0.0
0.0	7.962D-02	0.0	0.0	0.0	0.0	0.0	0.0	0.0
0.0	0.0	3.185D-01	0.0	0.0	0.0	0.0	0.0	0.0
0.0	0.0	0.0	7.962D-12	0.0	0.0	0.0	0.0	0.0
0.0	0.0	0.0	0.0	1.689D-04	0.0	0.0	0.0	0.0
0.0	0.0	0.0	0.0	0.0	1.689D-04	0.0	0.0	0.0
0.0	0.0	0.0	0.0	0.0	0.0	3.553D-03	0.0	0.0
0.0	0.0	0.0	0.0	0.0	0.0	0.0	0.0	0.0
0.0	0.0	0.0	0.0	0.0	0.0	0.0	0.0	7.107D-03

U

1.274D+00	0.0	0.0	0.0	0.0	0.0	0.0
0.0	2.213D+01	0.0	0.0	0.0	0.0	0.0
0.0	0.0	1.566D+04	0.0	0.0	0.0	0.0
0.0	0.0	0.0	1.689D-01	0.0	0.0	0.0
0.0	0.0	0.0	0.0	6.757D-02	0.0	0.0
0.0	0.0	0.0	0.0	0.0	3.378D+03	0.0
0.0	0.0	0.0	0.0	0.0	0.0	1.000D+06

TABLE 14. Modal matrices.

		Re.	Im.
Eigenvalues	Airframe	-2.762D-03	0.0
		3.743D-04	3.253D-02
		3.743D-04	-3.253D-02
		-6.782D-01	2.200D+00
		-6.782D-01	-2.200D+00
	Engine	-5.617D-01	0.0
		-1.884D+00	0.0
		-6.585D+00	0.0
		-1.000D+01	0.0
		-1.722D+02	0.0

Separate systems modal matrix.

1.000D+00	-9.996D-01	0.0	8.688D-01	-4.136D-01	0.0	0.0	0.0	0.0	0.0
-6.603D-04	6.991D-04	-1.124D-05	-3.761D-03	-1.045D-01	0.0	0.0	0.0	0.0	0.0
1.693D-06	-1.046D-04	4.457D-05	2.307D-01	0.0	0.0	0.0	0.0	0.0	0.0
-6.128D-04	1.333D-03	3.230D-03	-2.950D-02	-9.573D-02	0.0	0.0	0.0	0.0	0.0
-4.573D-03	2.652D-02	-4.871D-03	1.846D-03	2.538D-03	0.0	0.0	0.0	0.0	0.0
0.0	0.0	0.0	0.0	0.0	5.805D-01	-8.893D-01	9.755D-01	9.977D-01	-1.125D-01
0.0	0.0	0.0	0.0	0.0	8.129D-01	4.529D-01	-9.501D-02	3.756D-02	-5.741D-02
0.0	0.0	0.0	0.0	0.0	9.585D-04	6.389D-04	5.659D-02	4.563D-02	-3.497D-03
0.0	0.0	0.0	0.0	0.0	0.0	0.0	0.0	-2.089D-03	0.0
0.0	0.0	0.0	0.0	0.0	4.630D-02	6.347D-02	1.900D-01	3.279D-02	9.920D-01

		Re.	Im.
Eigenvalues	Airframe	1.912D-03	0.0
		-3.654D-04	3.647D-02
		-3.654D-04	-3.647D-02
		-6.781D-01	2.200D+00
		-6.781D-01	-2.200D+00
	Engine	-5.628D-01	0.0
		-1.883D+00	0.0
		-6.587D+00	0.0
		-1.000D+01	0.0
		-1.722D+02	0.0

Integrated system modal matrix.

6.311D-02	-6.567D-02	6.543D-03	1.578D-01	-7.433D-02	-1.237D-04	3.794D-05	-1.304D-04	-3.715D-05	-1.956D-05
-4.040D-05	4.330D-05	-4.337D-06	-5.929D-04	-1.898D-02	3.945D-07	-2.717D-07	4.942D-07	9.540D-08	7.988D-09
-7.929D-08	-8.824D-06	1.399D-06	4.186D-02	1.971D-04	-1.201D-08	3.416D-07	-2.759D-06	-8.036D-07	-4.102D-07
-4.146D-05	4.079D-05	2.416D-04	-5.273D-03	-1.740D-02	2.134D-08	-1.814D-07	4.189D-07	8.036D-08	2.383D-09
-1.475D-04	1.791D-03	2.924D-07	3.329D-04	4.622D-04	1.761D-07	-1.273D-08	3.038D-09	3.995D-10	8.646D-12
4.844D-01	7.614D-01	3.697D-02	2.417D-01	-5.362D-01	5.808D-01	-8.894D-01	9.756D-01	9.977D-01	-1.125D-01
8.596D-01	-5.572D-01	1.015D-01	-3.801D-01	-6.515D-01	8.128D-01	4.527D-01	-9.479D-02	3.758D-02	-5.741D-02
1.133D-02	-3.788D-02	1.147D-03	7.452D-03	-2.262D-02	9.381D-04	6.457D-04	5.659D-02	4.563D-02	-3.497D-03
0.0	0.0	0.0	0.0	0.0	0.0	0.0	0.0	-2.088D-03	0.0
1.491D-01	-3.034D-01	1.641D-02	1.181D-01	-1.942D-01	4.609D-02	6.352D-02	1.899D-01	3.279D-02	9.920D-01

TABLE 15. Suboptimal control eigen-structure.

St1 eigenvalues

	Re.	Im.
Airframe	-3.076D-03	0.0
	-7.380D-03	0.0
	-1.744D-01	0.0
	-2.019D+00	1.268D+00
	-2.019D+00	-1.268D+00
Engine	-1.483D+00	0.0
	-3.374D+00	0.0
	-1.007D+01	1.984D+00
	-1.007D+01	-1.984D+00
	-2.624D+02	0.0

St1 modal matrix

1.612D-01	-1.279D-02	-2.953D-02	-5.528D-02	-1.053D-01	1.639D-04	1.349D-05	1.785D-05	3.771D-05	-1.783D-05
-9.425D-05	3.826D-05	5.603D-04	-1.328D-02	-7.892D-03	-4.108D-06	-3.318D-07	-2.489D-08	-1.362D-07	6.515D-09
3.044D-07	2.832D-07	1.878D-04	2.970D-02	-5.713D-03	3.746D-06	9.373D-07	4.508D-07	1.186D-06	-3.775D-07
-9.898D-05	-3.838D-05	-1.077D-03	-1.182D-02	-4.594D-03	-2.526D-06	-2.778D-07	-2.076D-08	-1.218D-07	1.439D-09
4.085D-04	2.758D-03	2.493D-03	5.754D-05	-3.975D-04	-2.833D-07	-4.252D-09	-3.289D-11	-3.852D-10	5.137D-12
2.104D-01	9.690D-01	9.390D-01	-2.349D-01	-5.019D-01	-1.340D-01	-9.901D-01	-9.649D-01	-2.439D-01	-7.868D-02
9.608D-01	-1.966D-01	-3.082D-01	-4.882D-01	6.599D-01	9.909D-01	1.316D-01	-5.821D-02	4.900D-02	-5.734D-02
3.421D-04	-2.743D-02	-2.540D-02	-3.905D-03	-1.302D-02	-1.045D-02	-4.464D-03	-4.056D-02	-1.517D-02	-2.129D-03
-1.088D-03	-5.180D-04	-3.889D-04	7.044D-04	-5.135D-04	-1.051D-03	7.431D-04	2.328D-03	-9.779D-04	-3.784D-05
8.161D-02	-1.462D-01	-1.478D-01	-2.973D-02	-4.972D-02	-7.100D-03	4.842D-02	1.082D-02	-4.113D-02	9.952D-01

St2 eigenvalues

	Re.	Im.
Airframe	-3.674D-03	0.0
	-1.551D+00	9.138D-02
	-1.551D+00	-9.138D-02
	-1.672D+00	1.450D+00
	-1.672D+00	-1.450D+00
Engine	-9.833D-01	0.0
	-3.374D+00	0.0
	-1.007D+01	1.985D+00
	-1.007D+01	-1.985D+00
	-2.624D+02	0.0

St2 modal matrix

1.482D-01	-8.583D-03	8.560D-03	1.003D-01	8.178D-02	5.324D-02	-2.521D-05	-2.629D-05	-3.202D-05	-1.783D-05
-7.714D-05	-7.801D-04	8.367D-04	1.520D-02	1.377D-04	3.517D-03	-2.089D-06	2.637D-08	-6.850D-08	6.614D-09
3.475D-07	7.012D-04	-9.081D-04	-1.699D-02	2.230D-02	-1.493D-03	6.041D-06	5.044D-08	8.922D-07	-3.570D-07
-9.459D-05	-4.851D-04	5.571D-04	1.240D-02	-2.583D-03	1.518D-03	-1.790D-06	1.198D-08	-8.621D-08	1.360D-09
1.261D-03	-5.317D-05	4.476D-05	3.967D-05	4.666D-04	5.398D-04	-2.349D-08	2.766D-10	5.214D-10	5.317D-12
5.072D-01	-1.790D-01	3.274D-02	3.520D-01	3.961D-01	2.424D-01	9.901D-01	9.952D-01	0.0	-7.868D-02
8.484D-01	9.761D-01	1.174D-01	4.013D-01	-7.322D-01	9.686D-01	-1.314D-01	4.446D-02	-6.178D-02	-5.734D-02
-8.375D-03	-1.060D-02	-7.769D-04	7.554D-03	8.893D-03	-1.061D-02	4.455D-03	4.304D-02	4.768D-03	-2.129D-03
-1.190D-03	-1.001D-03	-1.519D-04	-6.275D-04	6.513D-04	-1.246D-03	-7.442D-04	-2.018D-03	1.519D-03	-3.784D-05
3.081D-02	-9.240D-03	1.765D-03	5.474D-02	3.264D-02	-3.925D-03	-4.846D-02	-4.284D-04	4.255D-02	9.952D-01

TABLE 15. concluded.

St4(.1) eigenvalues

	Re.	Im.
Airframe	-4.800D-03	0.0
	-1.395D+00	1.105D+00
	-1.395D+00	-1.105D+00
	-1.892D+00	1.083D+00
	-1.892D+00	-1.083D+00
Engine	-7.105D-01	0.0
	-3.519D+00	0.0
	-9.021D+00	8.033D-01
	-9.021D+00	-8.033D-01
	-2.590D+02	0.0

St4(.1) modal matrix

2.823D-01	1.523D-01	-7.052D-02	1.457D-01	1.048D-01	8.338D-02	-2.384D-03	-2.703D-05	-4.240D-06	-1.710D-05
-1.444D-04	8.493D-03	-1.402D-02	2.145D-02	2.750D-03	4.626D-03	-5.105D-04	6.056D-06	-2.942D-06	1.606D-08
9.177D-07	8.655D-03	2.117D-02	-3.174D-02	2.008D-02	-6.966D-04	1.549D-03	-5.232D-05	3.249D-05	1.625D-06
-1.912D-04	3.571D-03	-1.235D-02	1.721D-02	-7.652D-04	9.805D-04	-4.402D-04	6.072D-06	-3.061D-06	-6.276D-09
2.591D-03	7.312D-04	2.597D-04	2.361D-04	6.283D-04	1.363D-03	-5.299D-06	-7.919D-10	3.414D-09	2.291D-11
4.660D-01	3.953D-01	1.766D-01	1.068D-01	4.028D-01	6.021D-01	9.914D-01	9.965D-01	-6.517D-02	-8.105D-02
8.351D-01	-4.595D-01	-7.546D-01	7.380D-02	-8.844D-01	7.912D-01	-1.256D-01	2.626D-02	-2.162D-02	-5.634D-02
-3.687D-02	1.731D-03	2.632D-04	6.084D-03	4.925D-03	-2.276D-02	6.886D-03	3.541D-02	-1.989D-03	-2.202D-03
-4.032D-03	-8.687D-04	1.050D-03	-9.241D-04	-1.320D-04	-1.863D-03	-7.151D-04	-1.996D-03	5.590D-04	-6.165D-06
-6.627D-02	2.180D-02	-4.891D-02	6.571D-02	7.234D-03	-6.314D-02	-3.477D-02	-2.225D-03	1.745D-02	9.951D-01

St4(.01) eigenvalues

	Re.	Im.
Airframe	-4.735D-03	0.0
	-1.450D+00	1.099D+00
	-1.450D+00	-1.099D+00
	-1.863D+00	1.052D+00
	-1.863D+00	-1.052D+00
Engine	-7.689D-01	0.0
	-3.352D+00	0.0
	-1.015D+01	1.982D+00
	-1.015D+01	-1.982D+00
	-2.577D+02	0.0

St4(.01) modal matrix

4.223D-01	1.238D-01	1.364D-01	1.463D-01	1.148D-01	1.344D-01	3.884D-03	-2.074D-05	-2.969D-05	-1.710D-05
-2.173D-04	1.782D-02	4.646D-03	2.169D-02	3.906D-03	7.733D-03	7.861D-04	-3.529D-06	-3.256D-06	1.612D-08
1.346D-06	-2.098D-02	1.577D-02	-3.258D-02	1.823D-02	-1.617D-03	-2.248D-03	4.453D-05	2.567D-05	1.643D-06
-2.843D-04	1.442D-02	6.055D-05	1.745D-02	6.992D-05	2.103D-03	6.706D-04	-3.751D-06	-3.262D-06	-6.378D-09
3.758D-03	-9.666D-06	8.326D-04	2.247D-04	6.736D-04	1.945D-03	9.152D-06	5.555D-09	1.240D-09	2.318D-11
7.281D-02	-2.408D-02	3.697D-01	1.276D-01	3.591D-01	4.400D-01	-9.890D-01	9.961D-01	-3.012D-04	-8.140D-02
8.979D-01	6.180D-01	-6.672D-01	2.048D-01	-8.807D-01	8.858D-01	1.395D-01	3.477D-02	-5.647D-02	-5.637D-02
-4.132D-02	-5.539D-03	1.188D-03	-2.139D-03	4.732D-03	-2.250D-02	-4.649D-03	4.219D-02	3.934D-03	-2.227D-03
-5.253D-03	-1.475D-03	-4.623D-04	-1.257D-03	-3.843D-05	-2.225D-03	6.619D-04	-1.993D-03	1.425D-03	-6.212D-06
-9.114D-02	2.106D-02	-4.357D-03	2.056D-02	4.067D-05	-5.569D-02	4.870D-02	-3.841D-03	4.030D-02	9.951D-01

TABLE 15. continued

St3(.1) eigenvalues

		Re.	Im.
Airframe		-4.756D-03	0.0
		-1.322D+00	1.052D+00
		-1.322D+00	-1.052D+00
		-2.002D+00	1.197D+00
		-2.002D+00	-1.197D+00
Engine		-7.592D-01	0.0
		-3.331D+00	0.0
		-1.008D+01	1.976D+00
		-1.008D+01	-1.976D+00
		-2.622D+02	0.0

St3(.1) modal matrix

4.471D-01	1.407D-01	-7.945D-02	1.215D-01	1.008D-01	1.418D-01	-1.708D-03	-4.699D-05	-6.643D-06	-1.707D-05
-2.297D-04	6.857D-03	-1.343D-02	1.991D-02	3.325D-03	8.115D-03	-3.422D-04	1.598D-05	-2.632D-06	1.697D-08
1.434D-06	9.109D-03	1.748D-02	-3.290D-02	1.962D-02	-1.617D-03	9.713D-04	-1.586D-04	6.468D-05	1.794D-06
-3.015D-04	2.220D-03	-1.145D-02	1.642D-02	2.080D-05	2.131D-03	-2.915D-04	1.636D-05	-3.210D-06	-6.843D-09
4.008D-03	7.633D-04	2.111D-04	1.483D-04	5.270D-04	2.093D-03	-4.041D-06	-1.246D-08	1.278D-08	2.411D-11
3.354D-02	1.721D-01	-9.282D-02	3.455D-01	-2.435D-02	4.021D-01	9.906D-01	9.865D-01	-1.340D-01	-7.907D-02
8.875D-01	-6.464D-01	-7.185D-01	-1.206D-01	-9.146D-01	9.027D-01	-1.270D-01	3.216D-02	-6.527D-02	-5.733D-02
-4.437D-02	1.458D-03	8.206D-04	9.677D-03	3.126D-03	-2.256D-02	3.815D-03	4.421D-02	-1.685D-03	-2.240D-03
-5.689D-03	-3.815D-04	7.008D-04	1.747D-04	1.766D-04	-2.281D-03	-7.559D-04	-1.724D-03	1.720D-03	-3.783D-05
-9.622D-02	8.076D-03	-2.777D-02	4.097D-02	1.174D-02	-5.280D-02	-5.033D-02	8.245D-03	3.995D-02	9.952D-01

St3(.01) eigenvalues

Airframe		-4.727D-03	0.0
		-1.447D+00	1.080D+00
		-1.447D+00	-1.080D+00
		-1.881D+00	1.089D+00
		-1.881D+00	-1.089D+00
Engine		-7.713D-01	0.0
		-3.377D+00	0.0
		-1.007D+01	1.984D+00
		-1.007D+01	-1.984D+00
		-2.624D+02	0.0

St3(.01) modal matrix

4.494D-01	1.682D-01	-8.241D-02	1.527D-01	1.147D-01	1.472D-01	-2.266D-03	-2.729D-05	-2.663D-05	-1.768D-05
-2.313D-04	9.653D-03	-1.592D-02	2.268D-02	3.289D-03	8.487D-03	-4.624D-04	-7.952D-07	-2.243D-06	8.815D-09
1.429D-06	8.924D-03	2.466D-02	-3.372D-02	2.090D-02	-1.795D-03	1.334D-03	1.365D-05	2.136D-05	9.839D-08
-3.024D-04	4.206D-03	-1.390D-02	1.825D-02	-5.466D-04	2.327D-03	-3.951D-04	-9.025D-07	-2.298D-06	-3.749D-10
3.992D-03	8.202D-04	2.408D-04	2.338D-04	6.769D-04	2.121D-03	-5.290D-06	2.448D-09	1.928D-09	9.300D-12
-1.993D-02	2.760D-01	6.960D-02	1.563D-01	2.428D-01	3.876D-01	9.911D-01	9.855D-01	-1.388D-01	-7.868D-02
8.877D-01	-5.219D-01	-7.809D-01	1.170D-01	-9.292D-01	9.080D-01	-1.234D-01	3.536D-02	-6.736D-02	-5.734D-02
-4.243D-02	-7.361D-04	4.322D-03	1.378D-04	3.474D-03	-2.346D-02	4.311D-03	4.328D-02	-1.284D-03	-2.129D-03
-5.637D-03	-8.486D-04	1.187D-03	-1.029D-03	-5.634D-05	-2.401D-03	-7.485D-04	-1.786D-03	1.785D-03	-3.784D-05
-8.840D-02	3.578D-03	-2.240D-02	2.436D-02	1.099D-03	-5.440D-02	-4.927D-02	5.540D-03	4.217D-02	9.952D-01

REFERENCES

1. Proceedings of the Air Force Airframe-Propulsion Compatibility Symposium. AFAPL-TR-69-103, U.S. Air Force, June 1970. (Available from DTIC as AD876 608.)

2. Airframe/Engine Integration. AGARD Lecture Series No.53, 1972.

3. Airframe/Propulsion Interface. AGARD Conference Proceedings, No. 150, 1975.

4. Schweikhard, W. G. and Berry, D. T.: Cooperative Airframe/Propulsion Control for Supersonic Cruise Aircraft. SAE Paper-740478, 1974.

5. Imfield, W. F.: The Development Program for the F-15 Inlet. AIAA Paper 74-1061, 1974.

6. Hunt, B. L., Surber, L. E. and Grant, G. K.: Propulsion System Integration for Tactical Aircraft. Astronautics and Aeronautics, Vol. 18, no.6, June 1980, pp 62-67.

7. Brown,S. C.: Computer Simulation of Aircraft Motions and Propulsion System Dynamics for the YF-12 Aircraft at Supersonic Cruise Conditions. NASA TM X-62,245,1973.

8. Tinling, B. E. and Cole, G. L.: Simulation Study of the Interaction Between the Propulsion and Flight Control Systems of a Subsonic Lift Fan VTOL. NASA TM-81239, 1980.

9. Cole, G. L., Sellers, J. F. and Tinling, B. E.: Propulsion System Mathematical Model for a Lift/Cruise Fan V/STOL Aircraft. NASA TM-81663, 1980.

10. Michael, G. J. and Farrar, F. A.: Development of Optimal Control Modes for Advanced Technology Propulsion Systems. N911620-2, United Technology Research Laboratories, 1974.

11. Seitz, W. R.: Integrated Flight/Propulsion Control by State Regulation. AIAA Paper No. 75-1075, 1975.

12. Sevich, G. J. and Beattie, E. C.: Integrated Flight/Propulsion Control Design Techniques Starting with the Engine. SAE Paper-740481, 1974.

13. Siljak, D. D.: Large-Scale Dynamic Systems - Stability and Control. North Holland, New York, 1978.

14. Anon.: U.S. Standard Atmosphere, 1962. NASA, U.S. Air Force, and U.S. Weather Bur., December 1962.

15. DeHoff, R. L., Hall, W. E. Adams, R. J. and Gupta , N. K.: F-100 Multivariable Control Synthesis Program, Vol. 1, 2. AFAPL TR-77-35, 1977.

16. Kwakernaak, H. and Sivan, R.: Linear Optimal Control Systems. Wiley-Interscience, 1972.

17. Russell, D. L.: Mathematics of Finite Dimensional Control Systems - Theory and Design. Marcel Dekker Inc., 1979.

18. Stewart, G. W.: Introduction to Matrix Computations. Academic Press, 1973.

19. Porter, B. and Crossley, R.: Modal Control - Theory and Applications. Barnes and Noble Book Co., 1972.

20. Armstrong, E. S.: ORACLS - A System for Linear-Quadratic-Gaussian Control Law Design. NASA TP-1106, 1978.

21. Lallman, F. J.: Simplified Off-Design Performance Model of a Dry Turbofan Engine Cycle. NASA TM-83204, 1981.

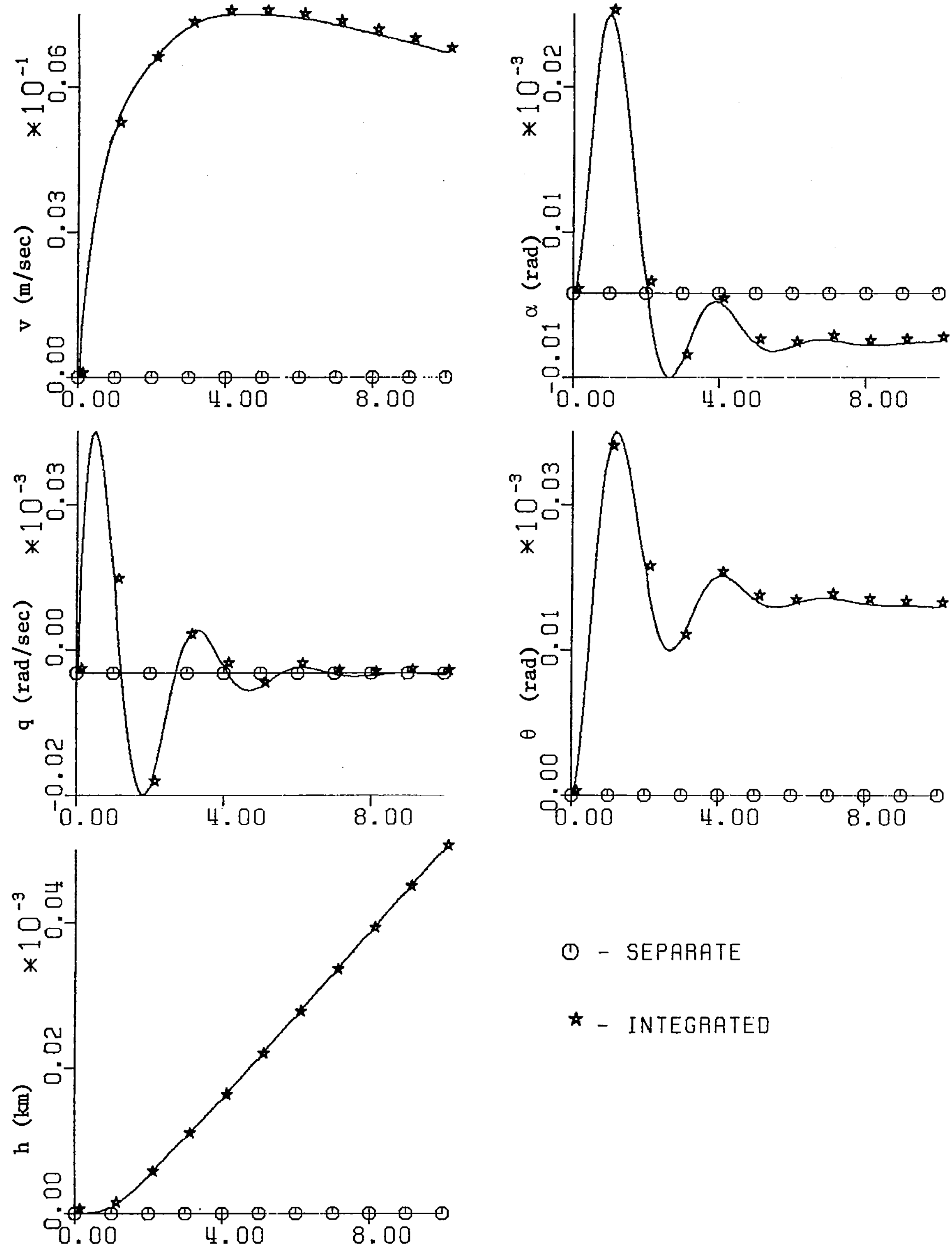

FIGURE 1. Separate and integrated system transinet response. Offset in fan speed of 97.9 rpm.

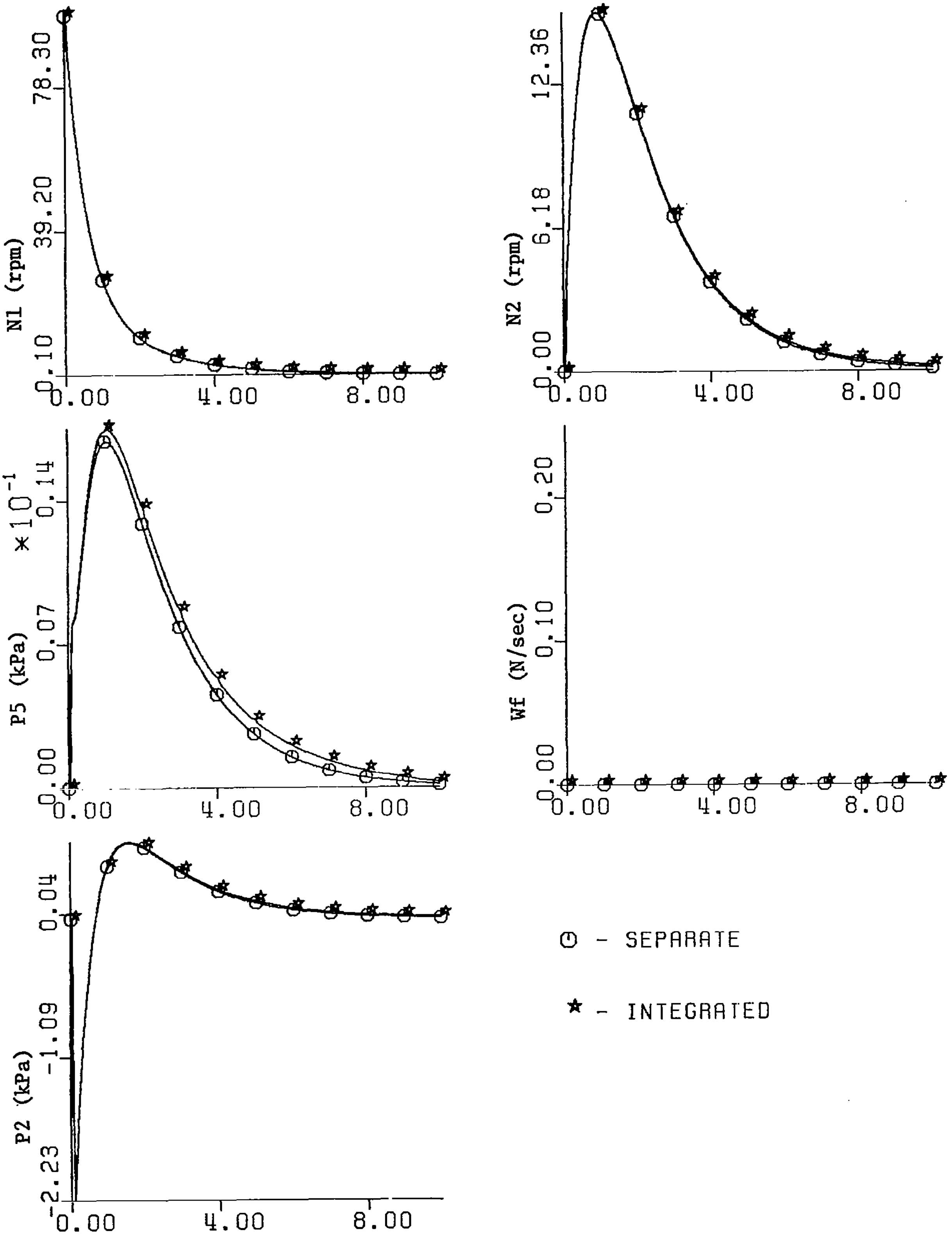

FIGURE 1. continued

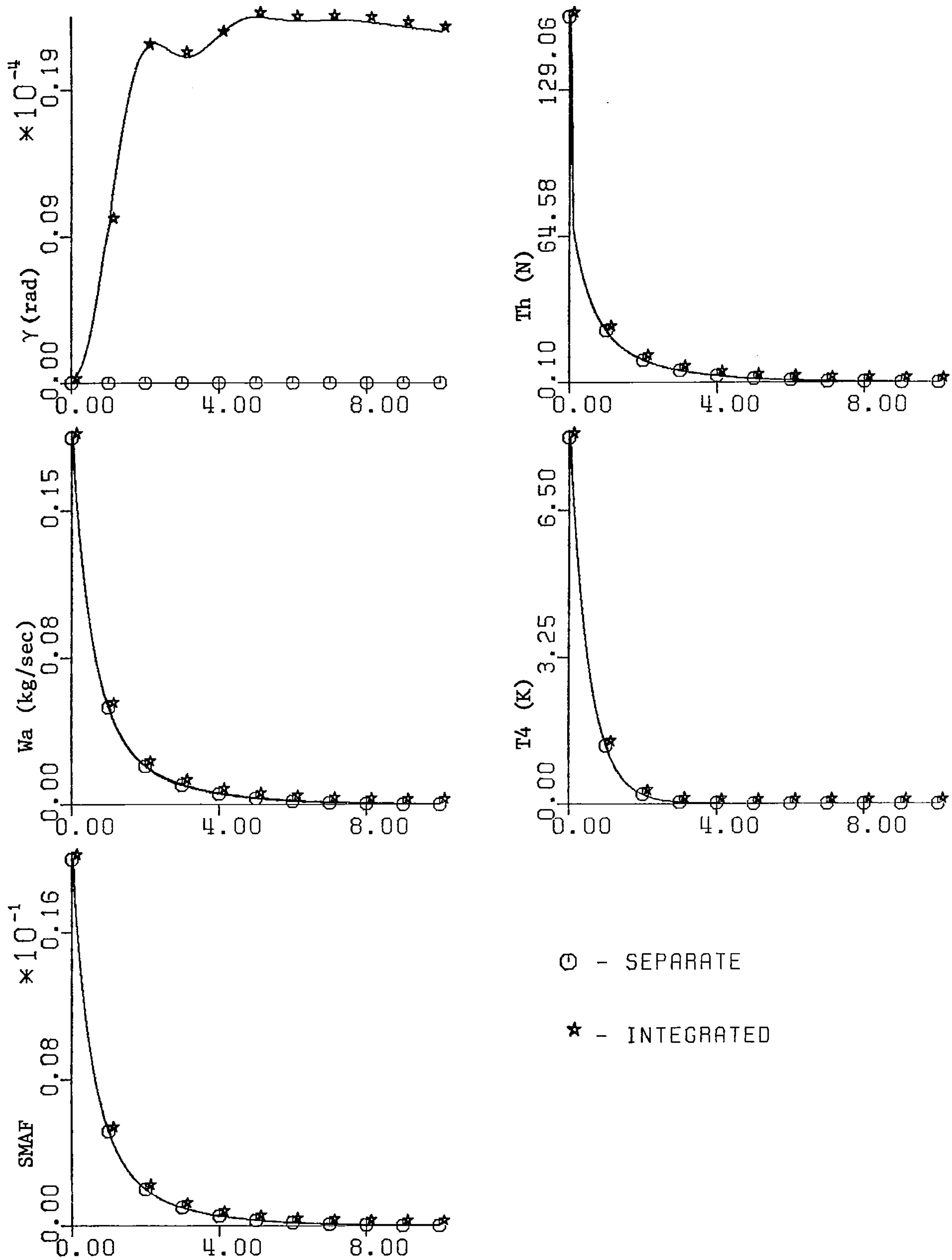

FIGURE 1. Continued

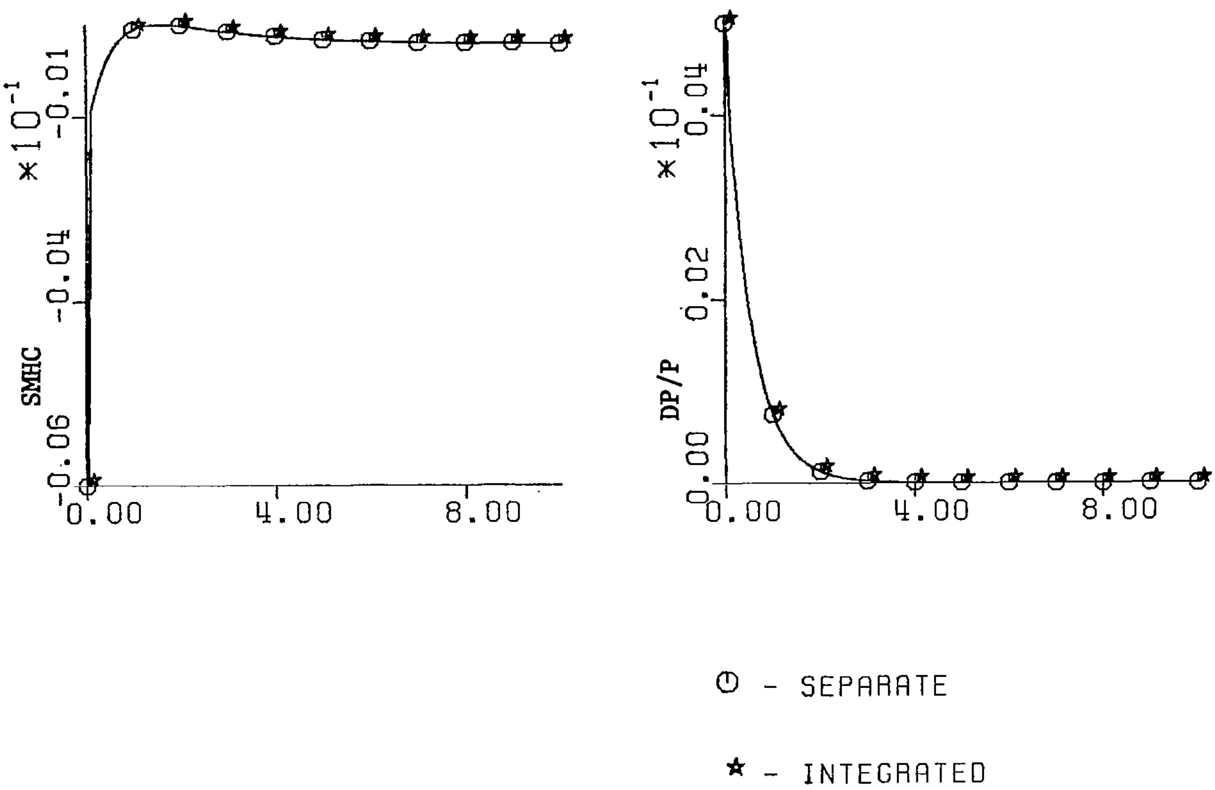

FIGURE 1. concluded.

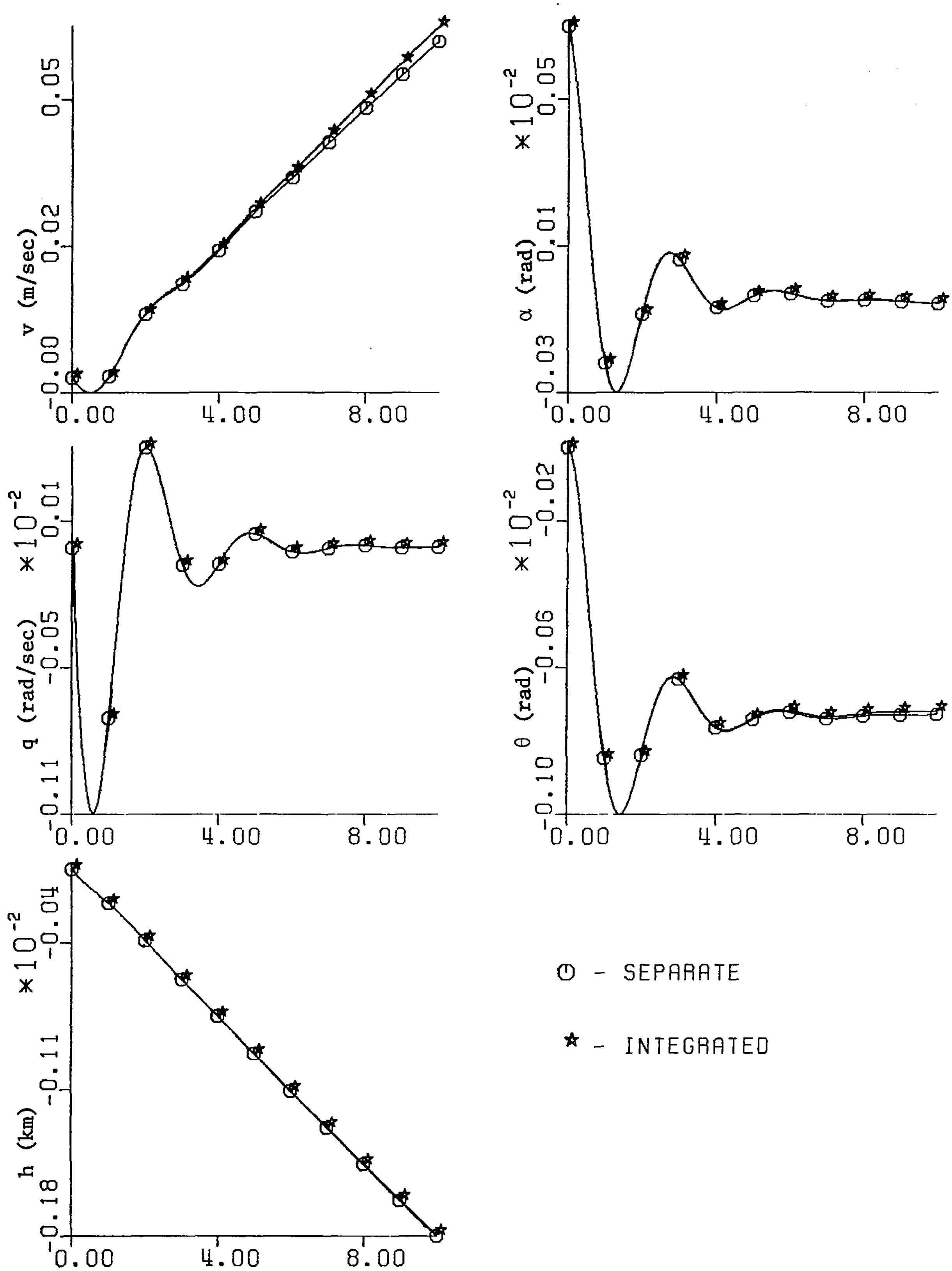

FIGURE 2. Separate and integrated system transient response. Offset in angle of attack of 0.0008 rad.

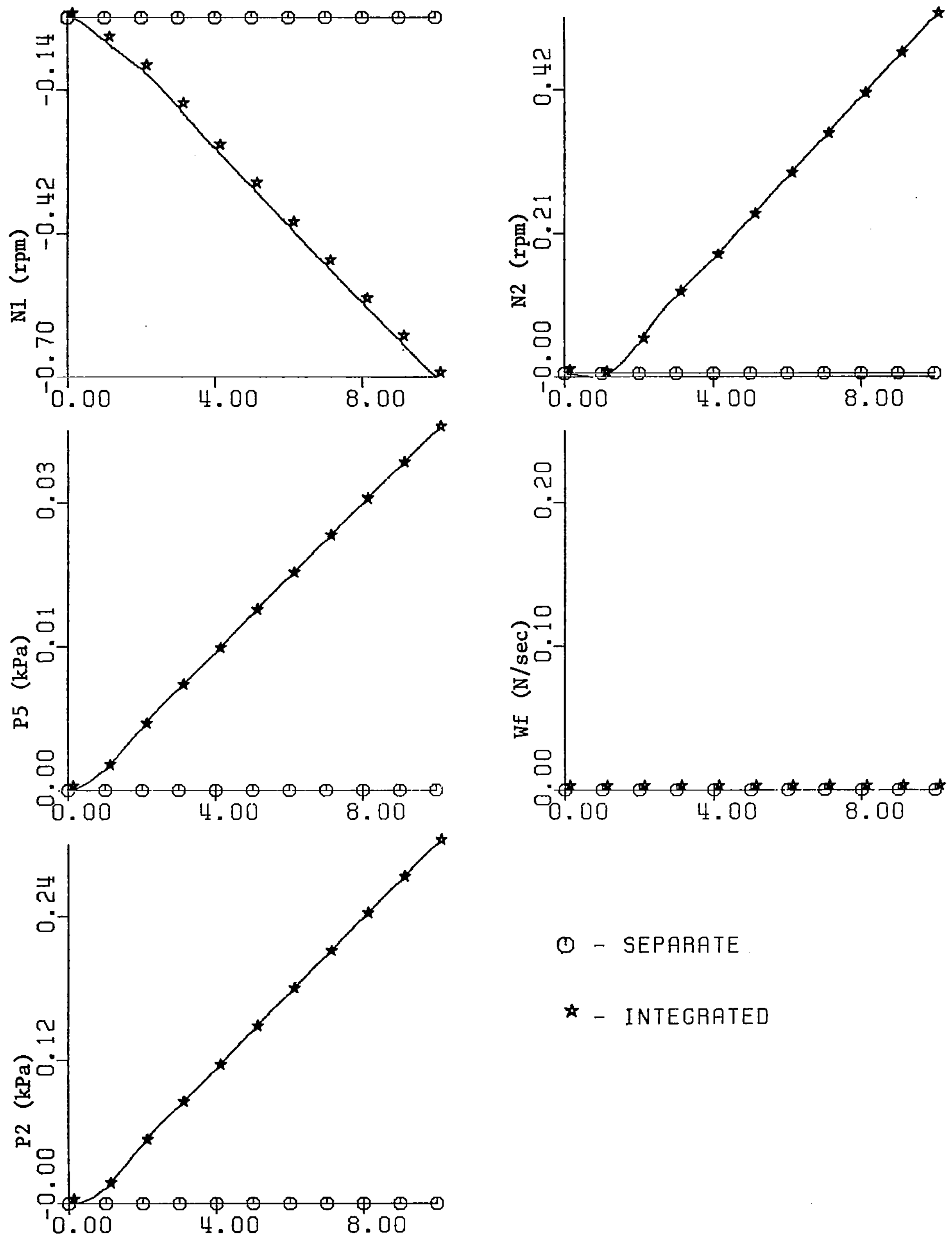

FIGURE 2. continued

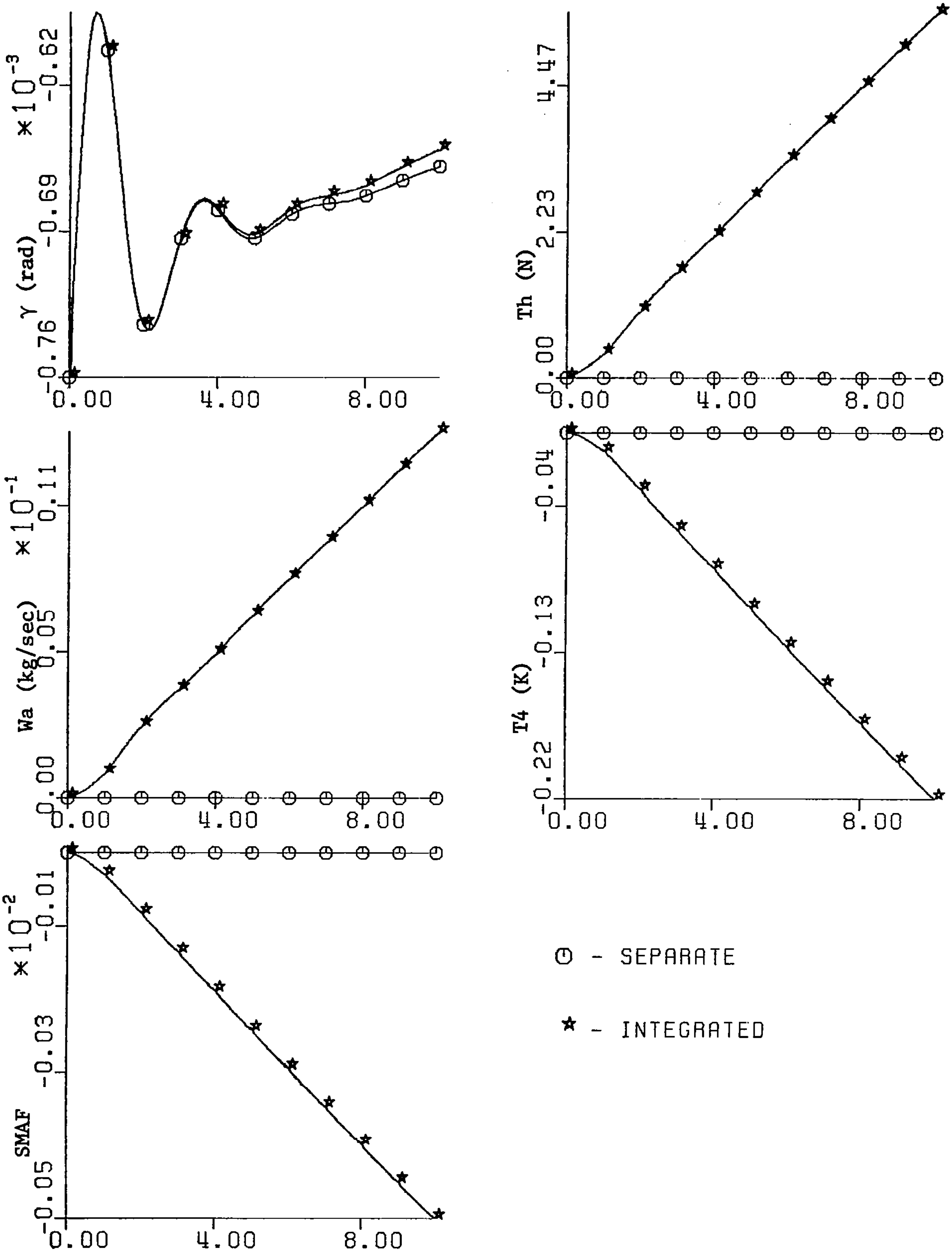

FIGURE 2. continued

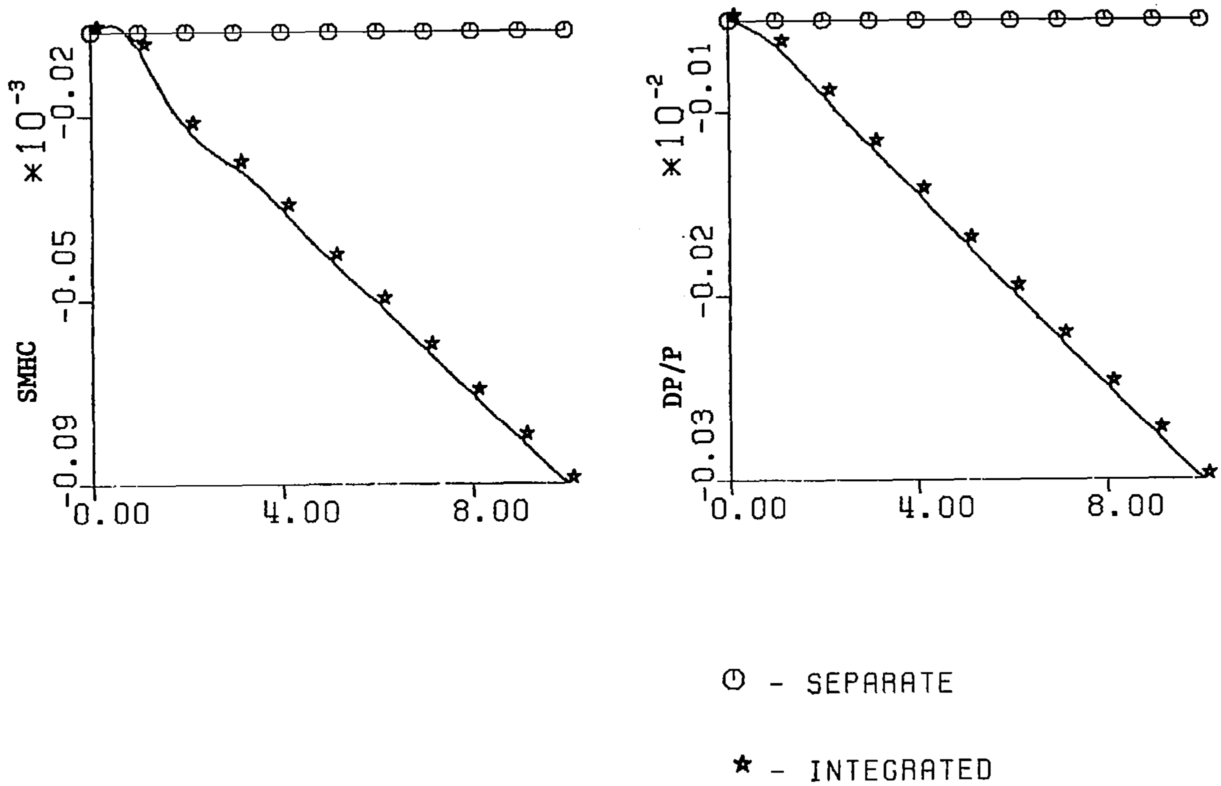

FIGURE 2. concluded.

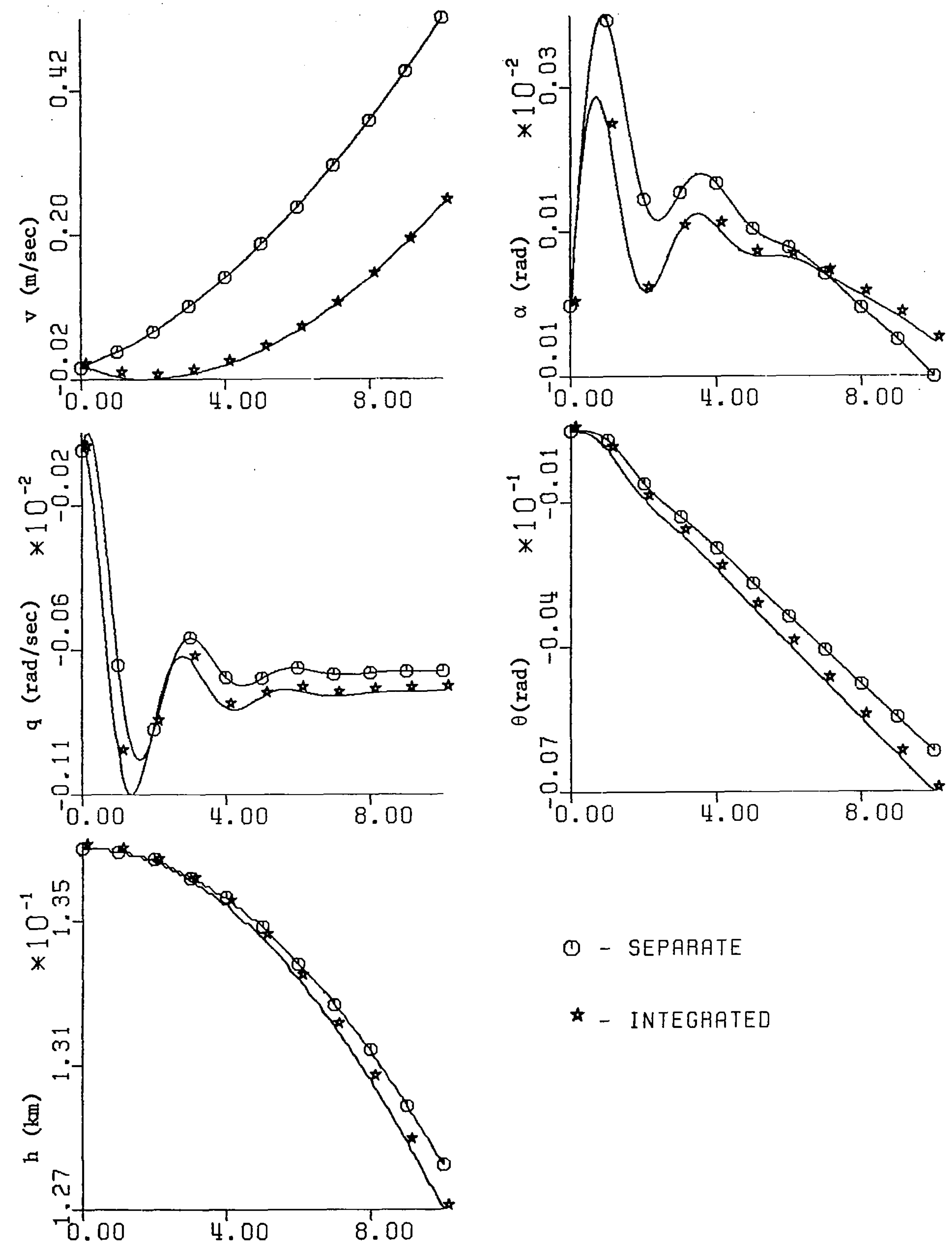

FIGURE 3. Separate and integrated system transient response. Offset in altitude of 0.137 km.

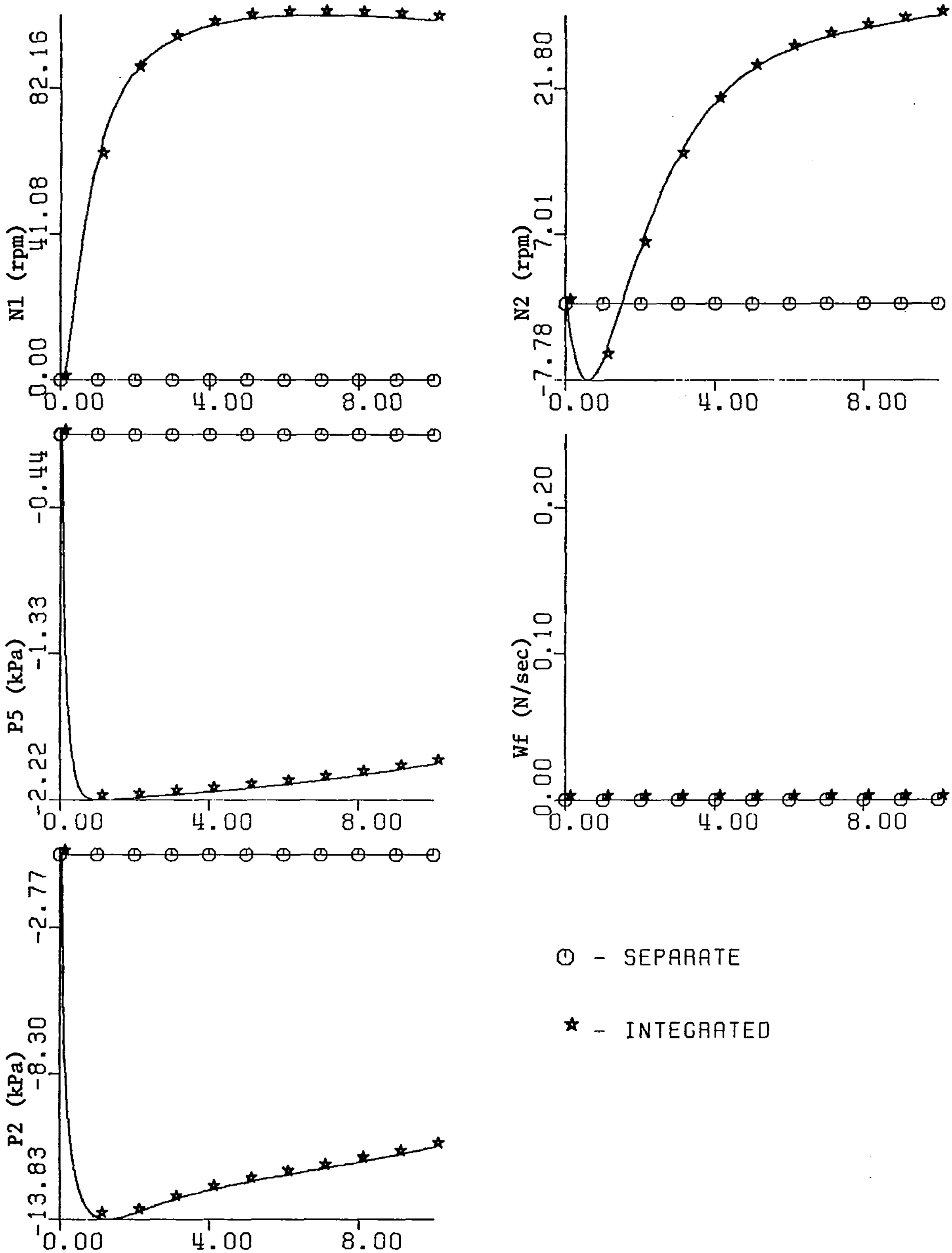

FIGURE 3. continued

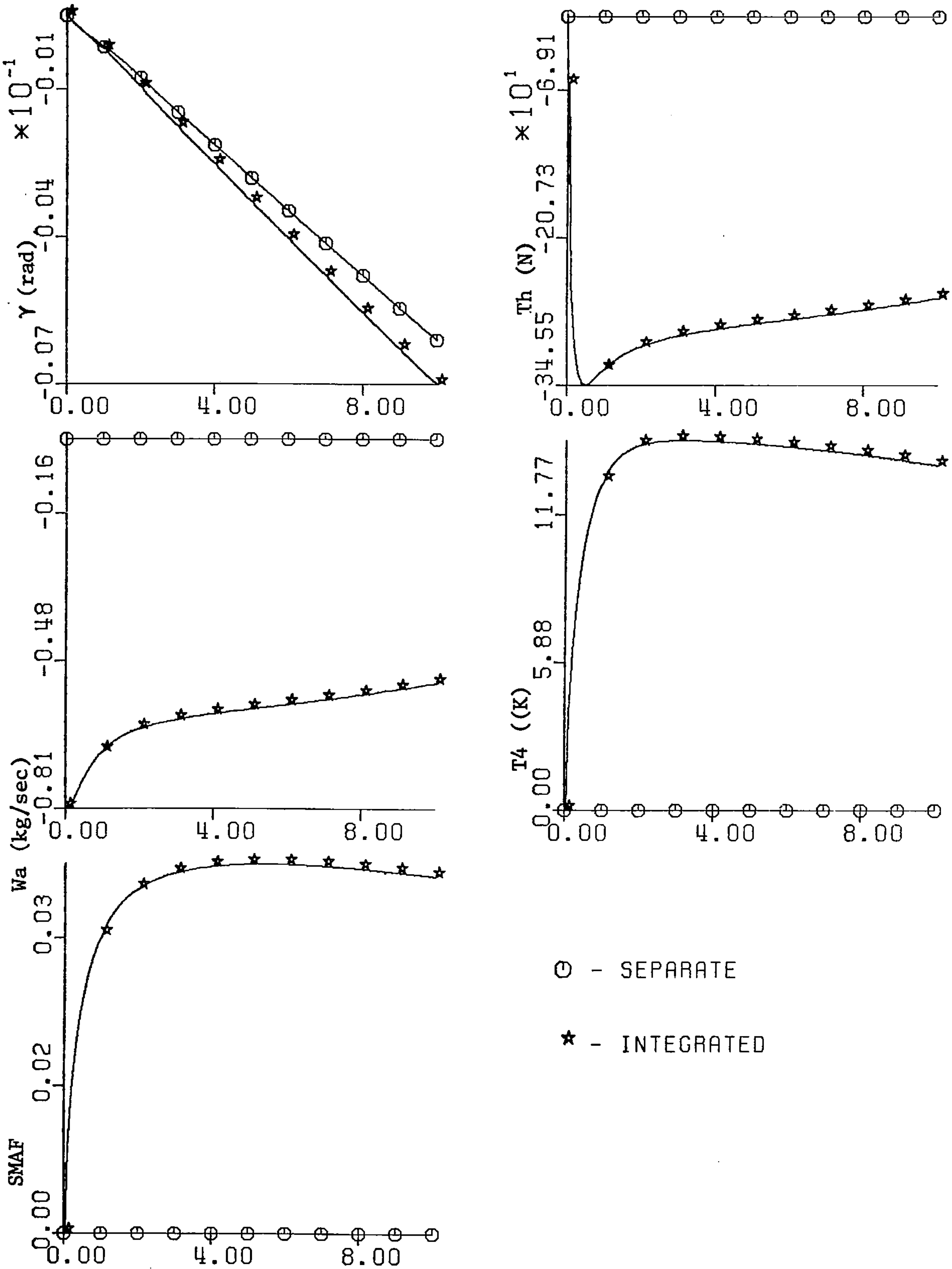

FIGURE 3. continued

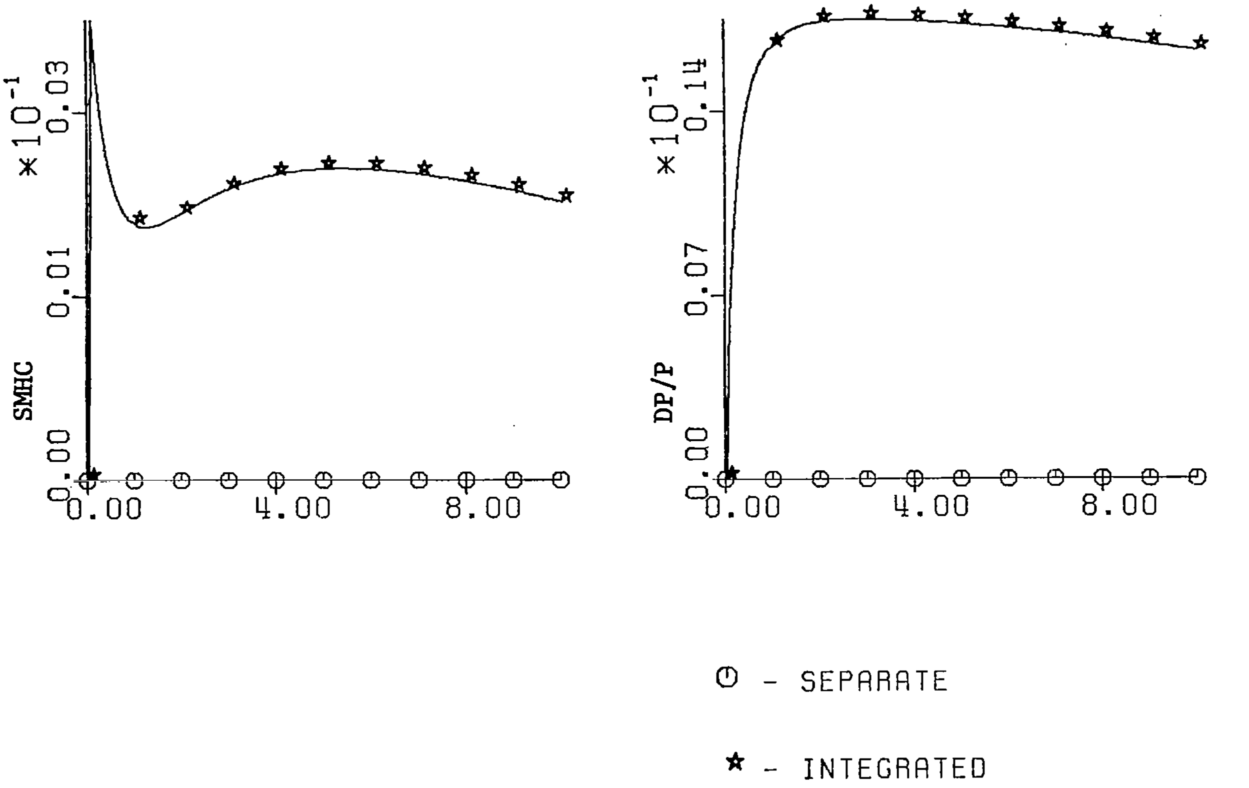

FIGURE 3. concluded.

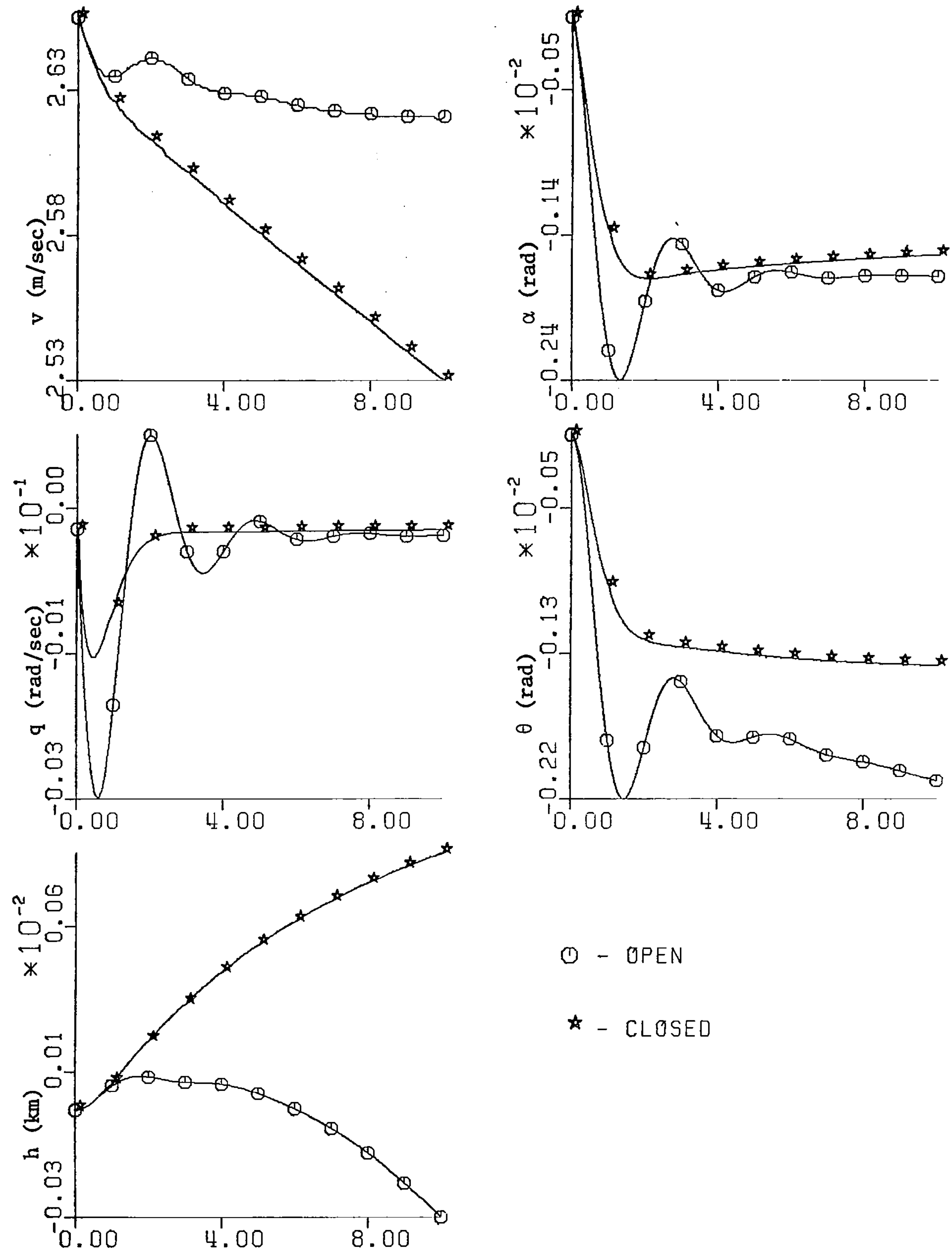

FIGURE 4. Aircraft open and closed loop transient response. Offset in velocity of 2.65 m/sec.

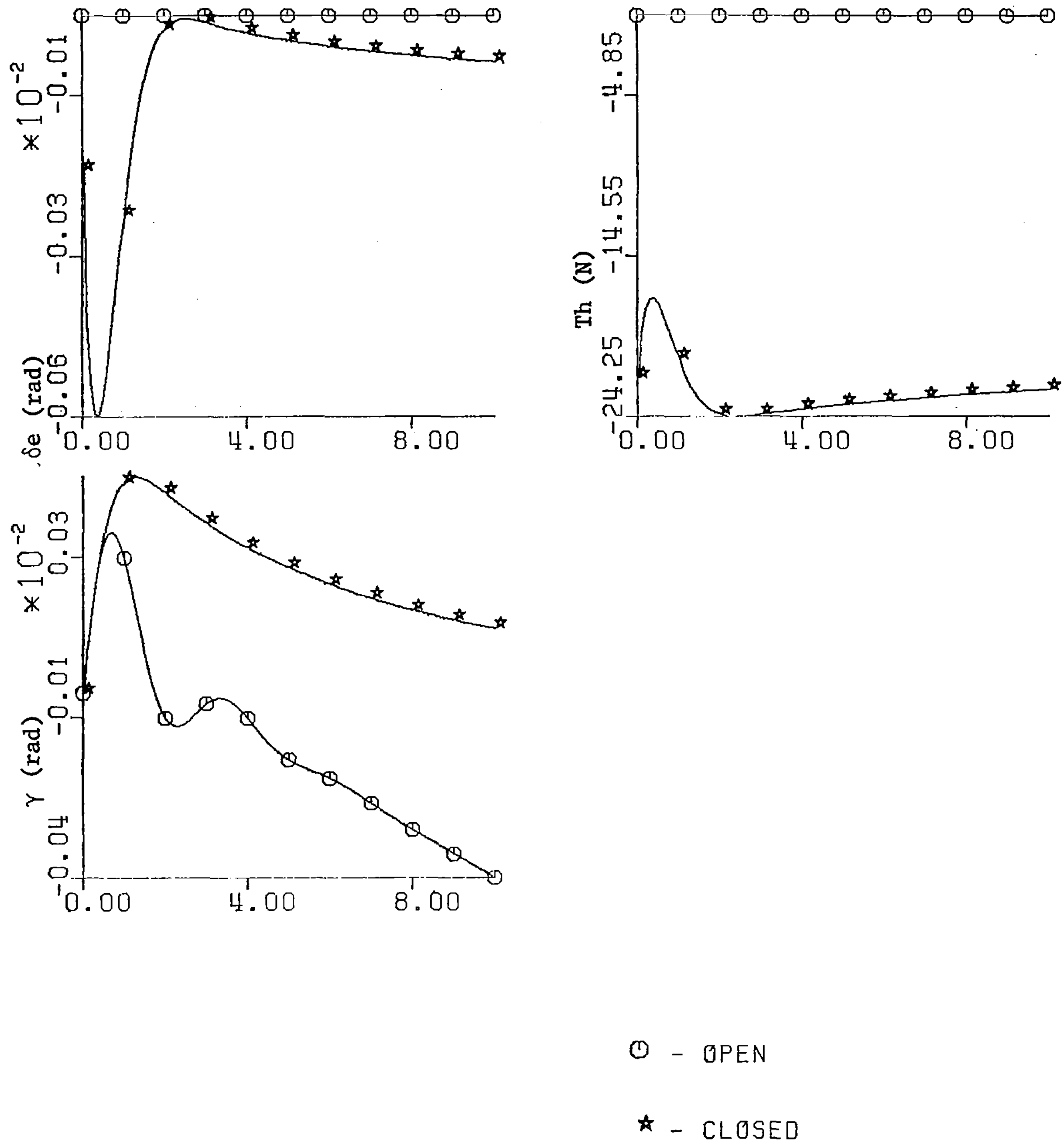

FIGURE 4. concluded.

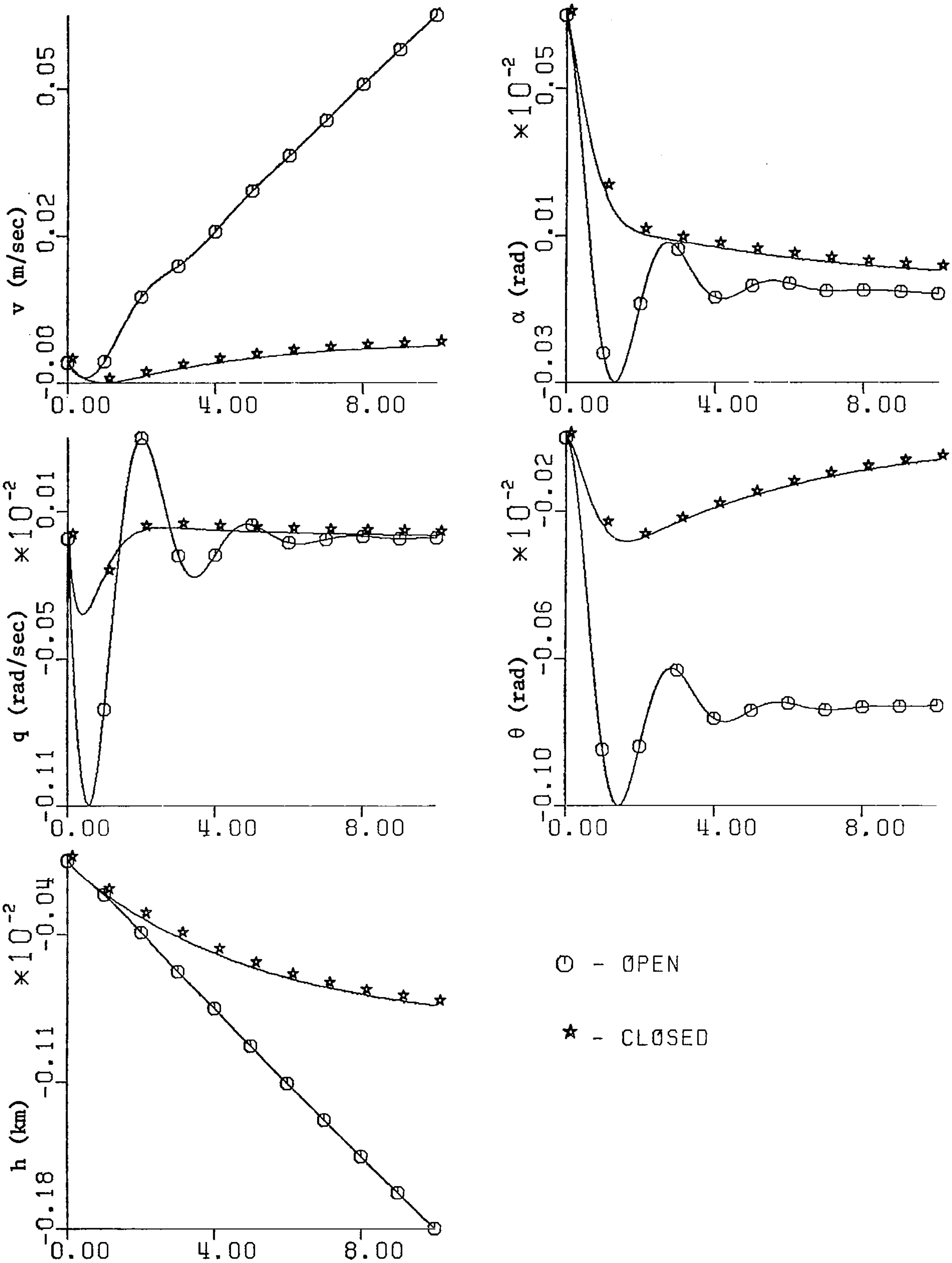

FIGURE 5. Aircraft open and closed loop transient response. Offset in angle of attack of 0.0008 rad.

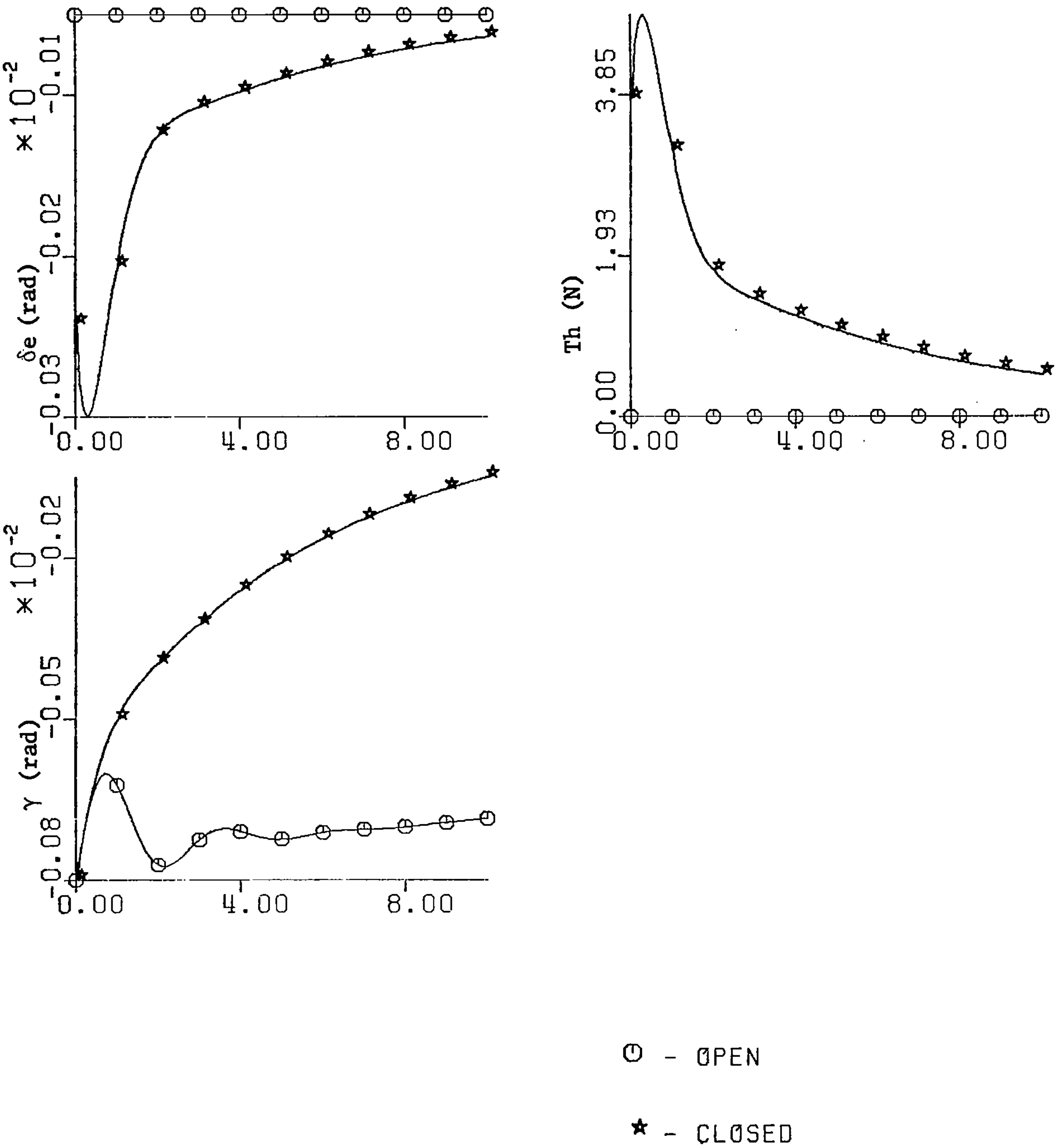

FIGURE 5. concluded.

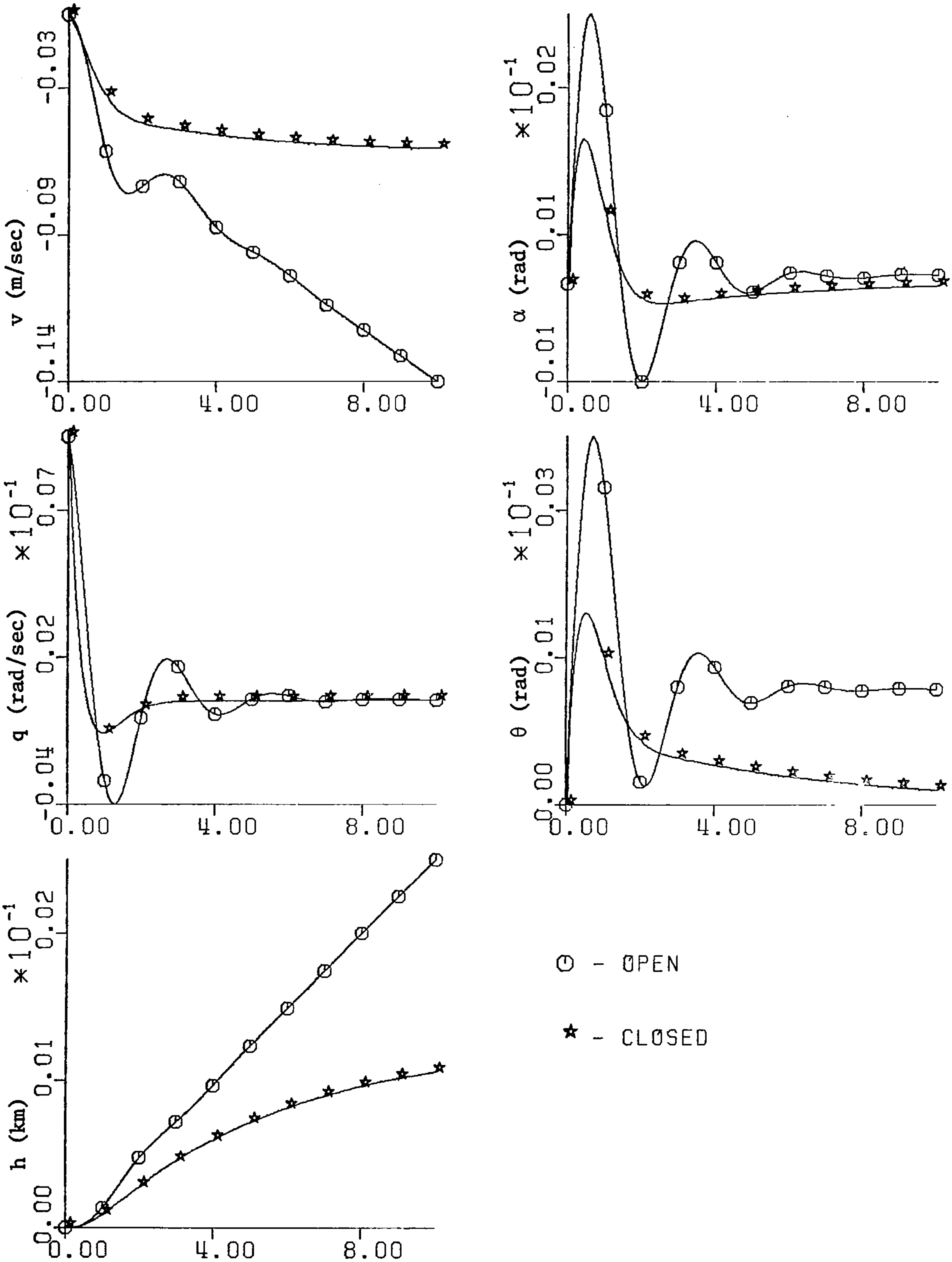

FIGURE 6. Aircraft open and closed loop transient response. Offset in pitch rate of 0.01 rad/sec.

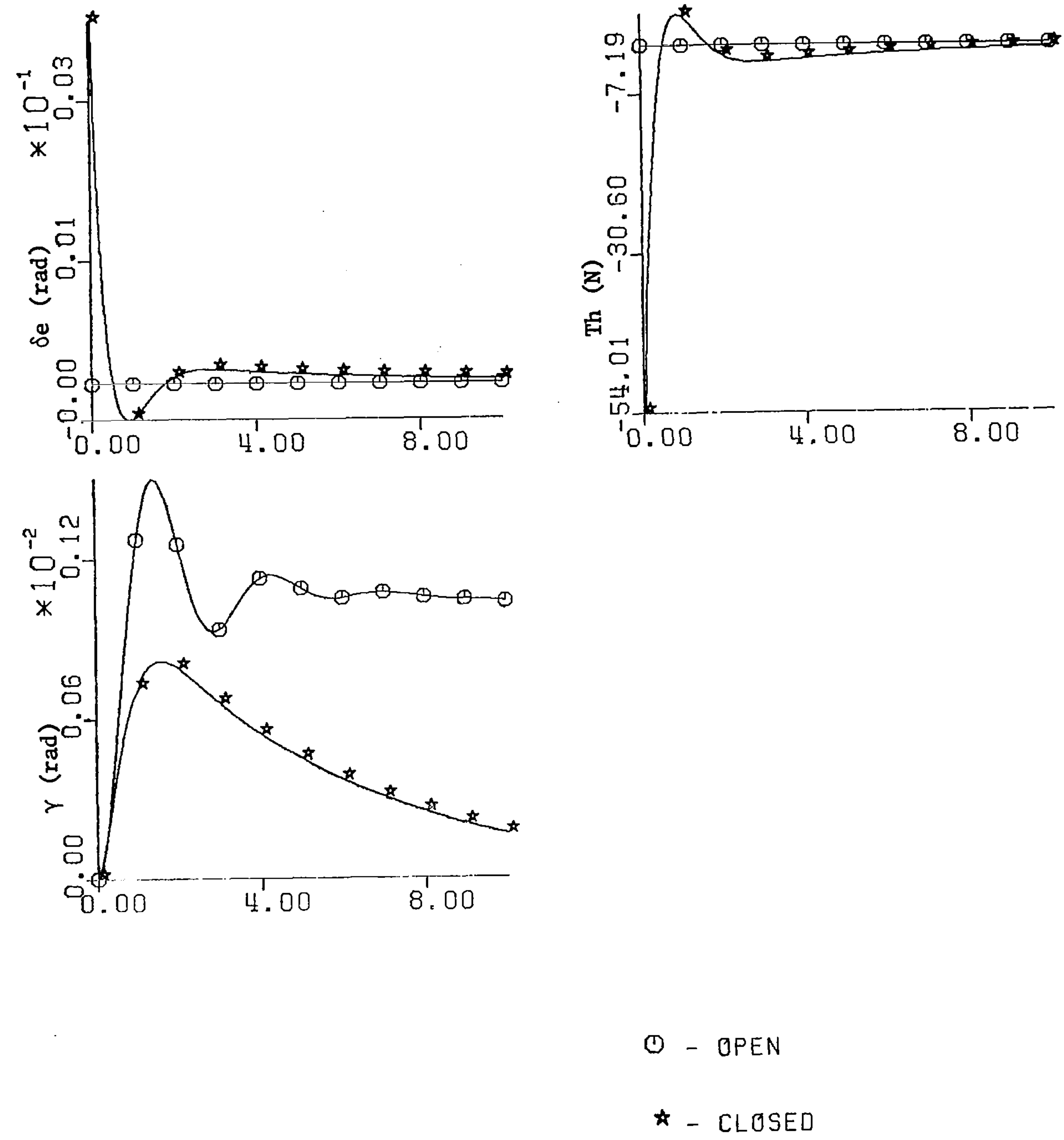

FIGURE 6. concluded.

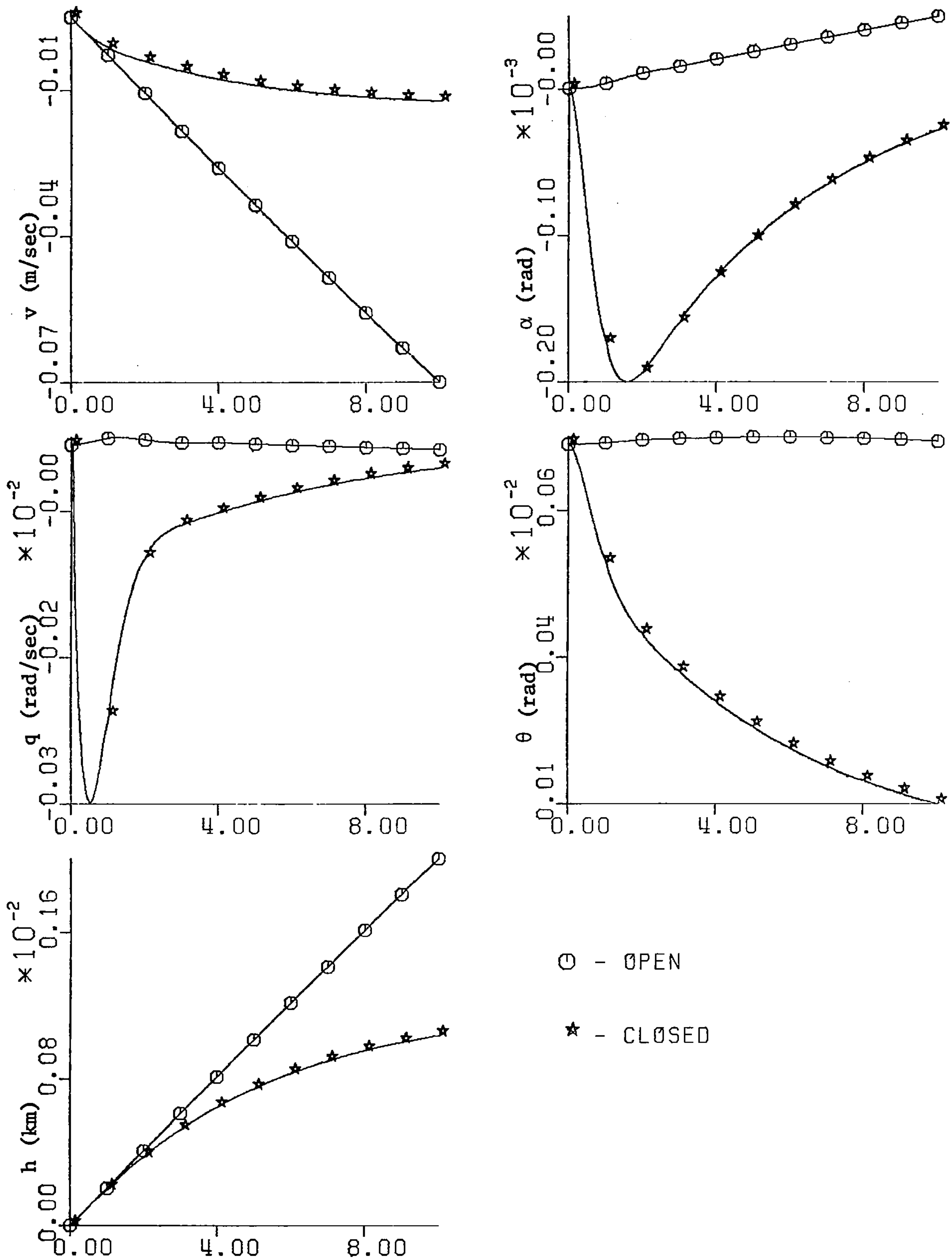

FIGURE 7. Aircraft open and closed loop transient response. Offset in pitch attitude of 0.0008 rad.

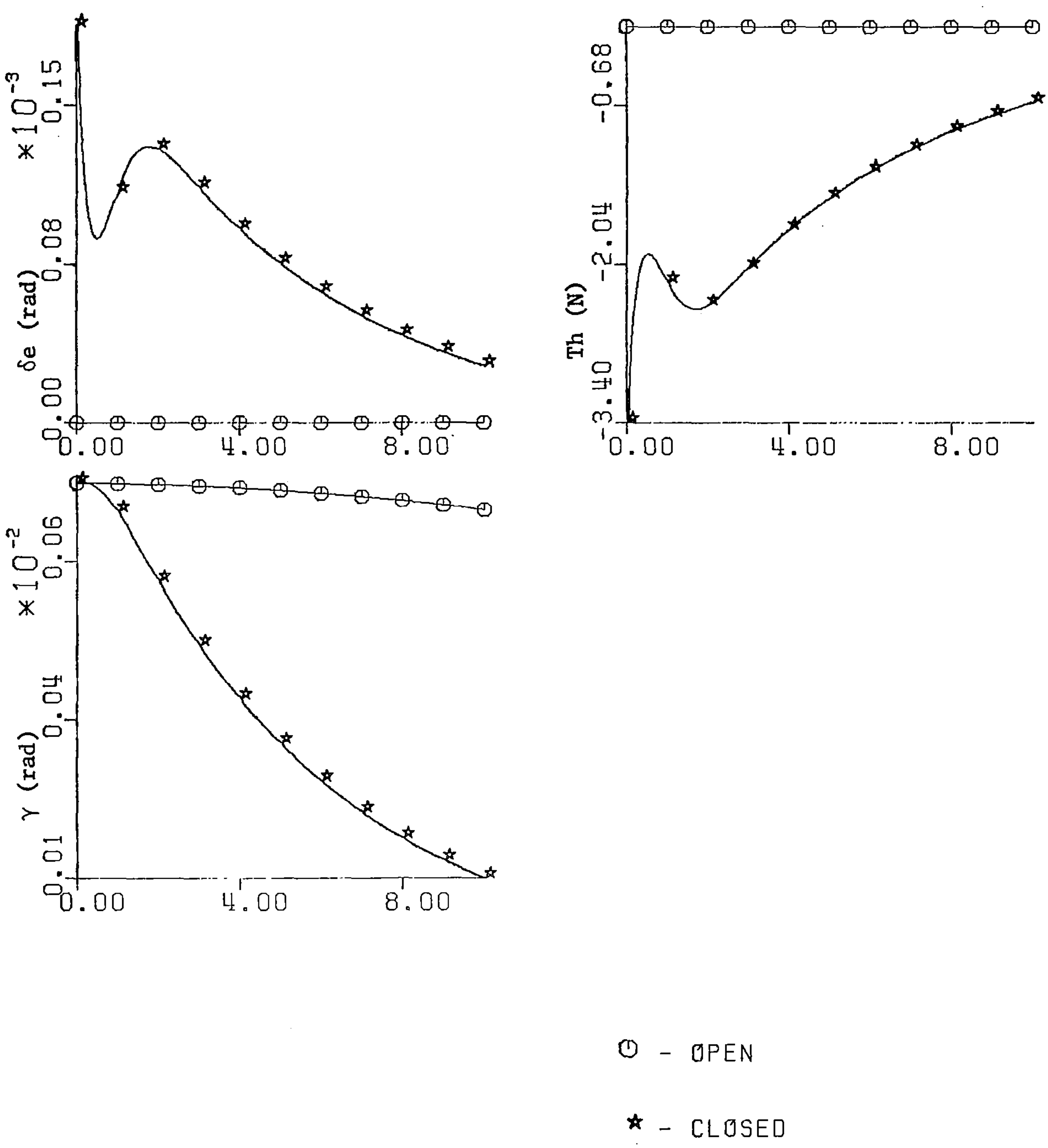

FIGURE 7. concluded.

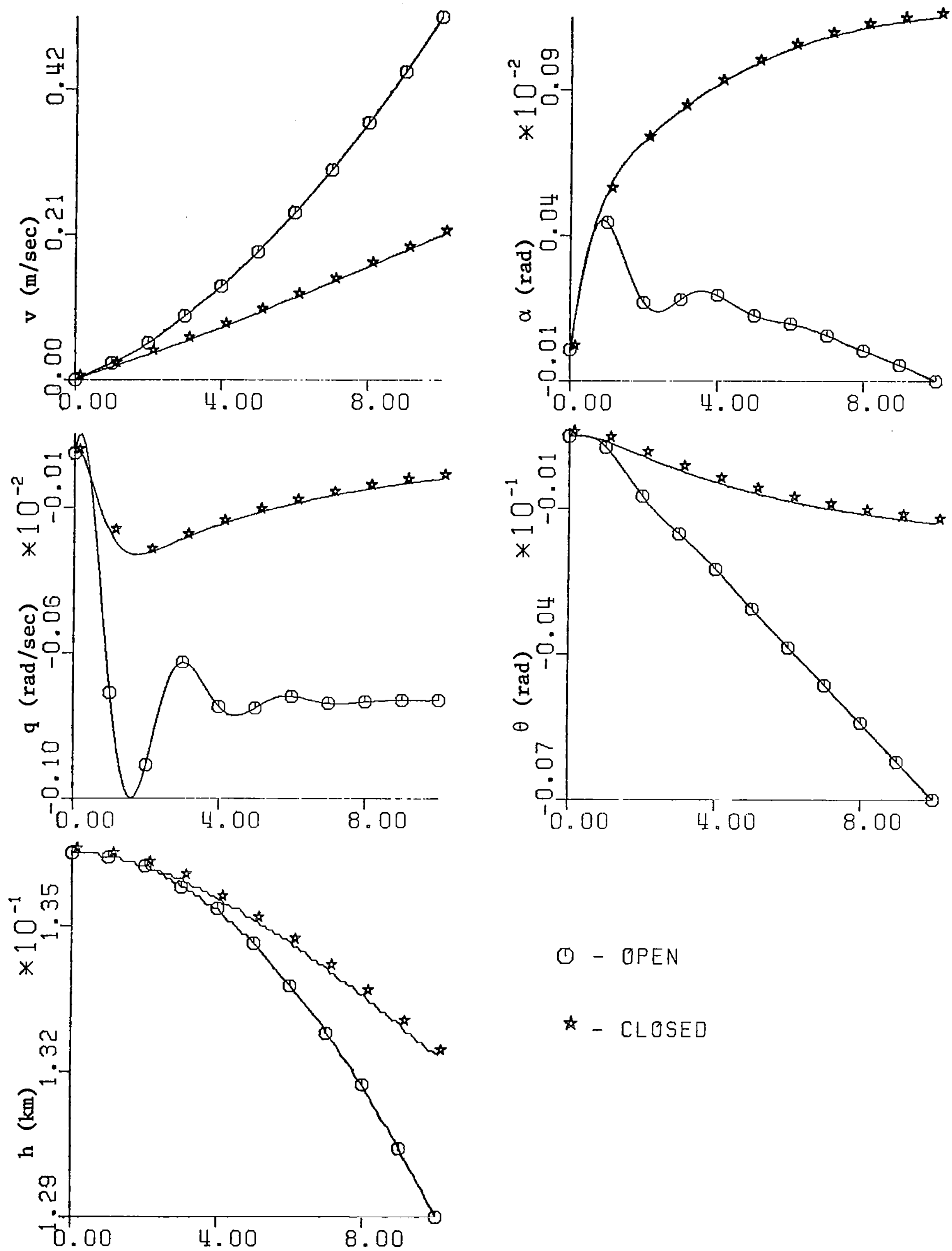

FIGURE 8. Aircraft open and closed loop transient response.
Offset in altitude of 0.137 km.

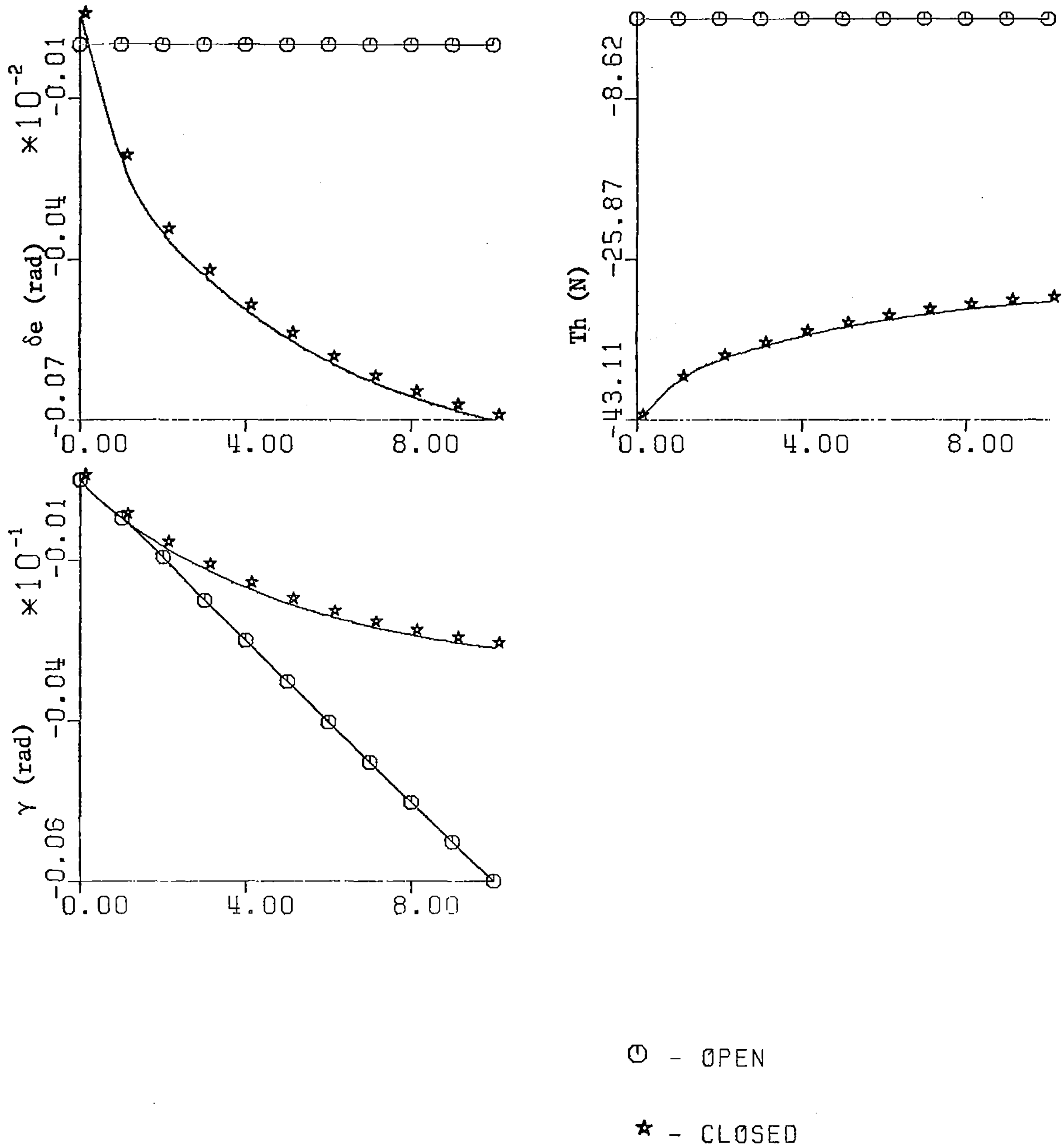

FIGURE 8. concluded.

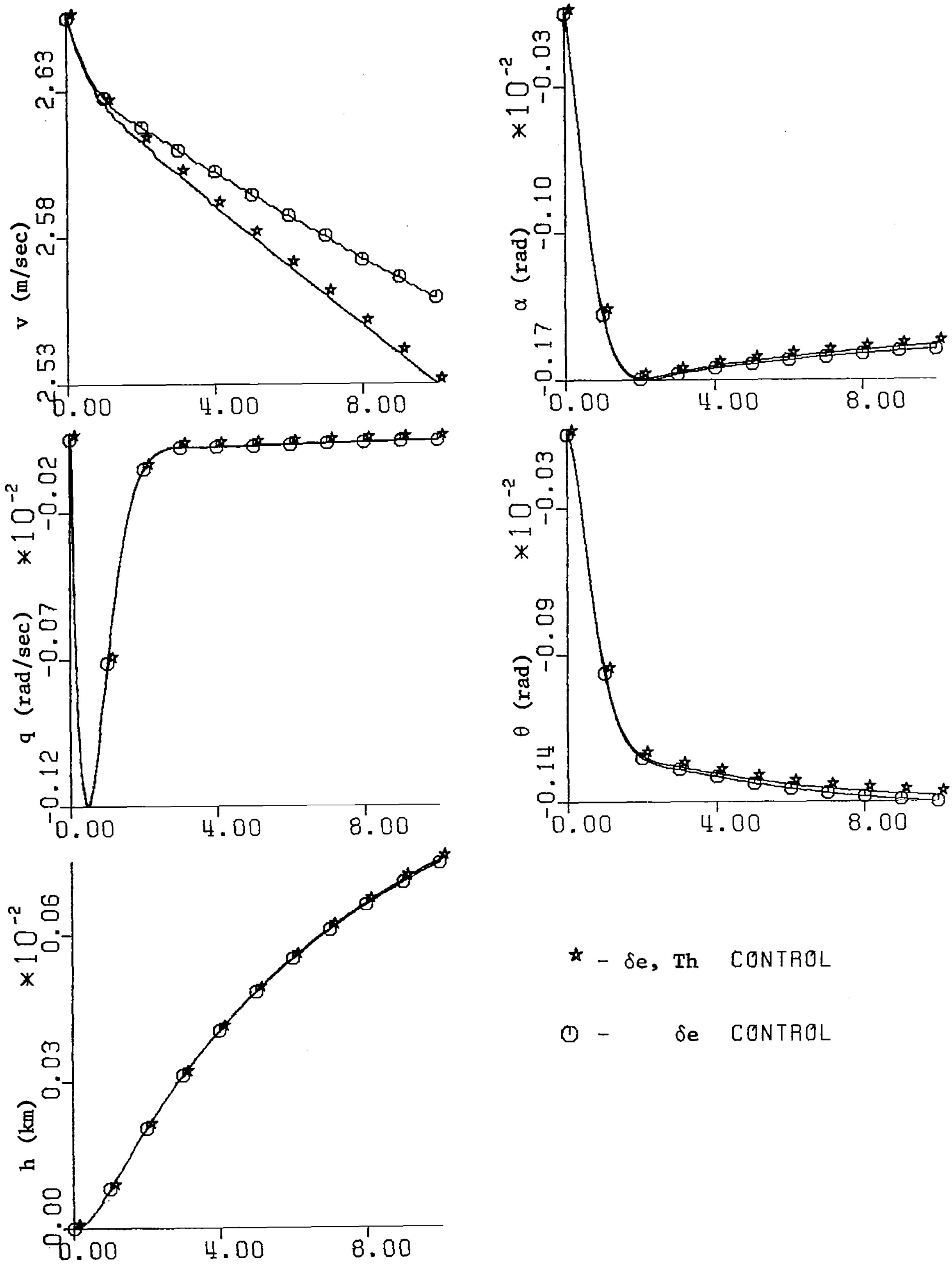

FIGURE 9. Comparison of aircraft closed loop transient response. Offset in velocity of 2.65 m/sec.

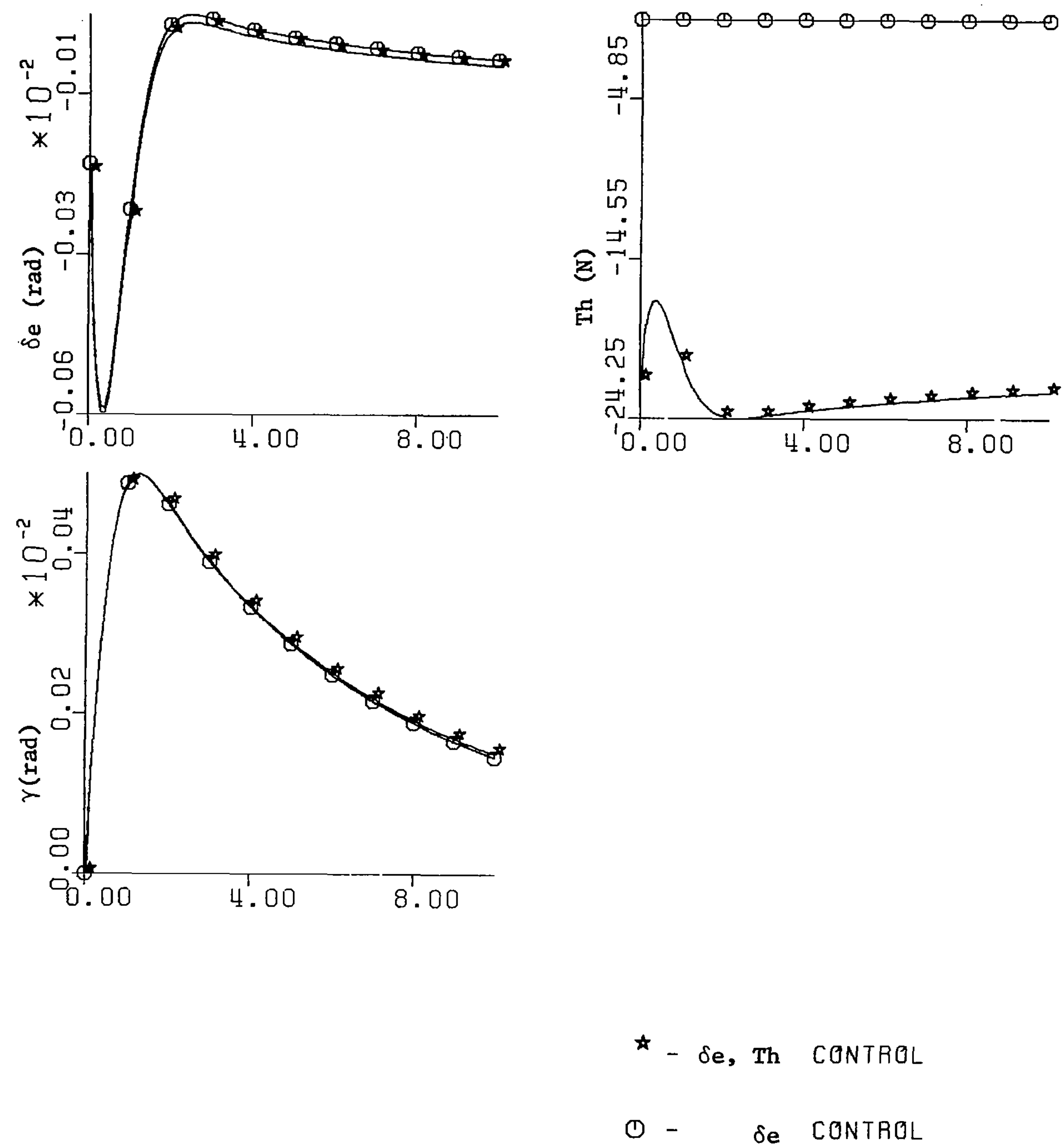

FIGURE 9. concluded.

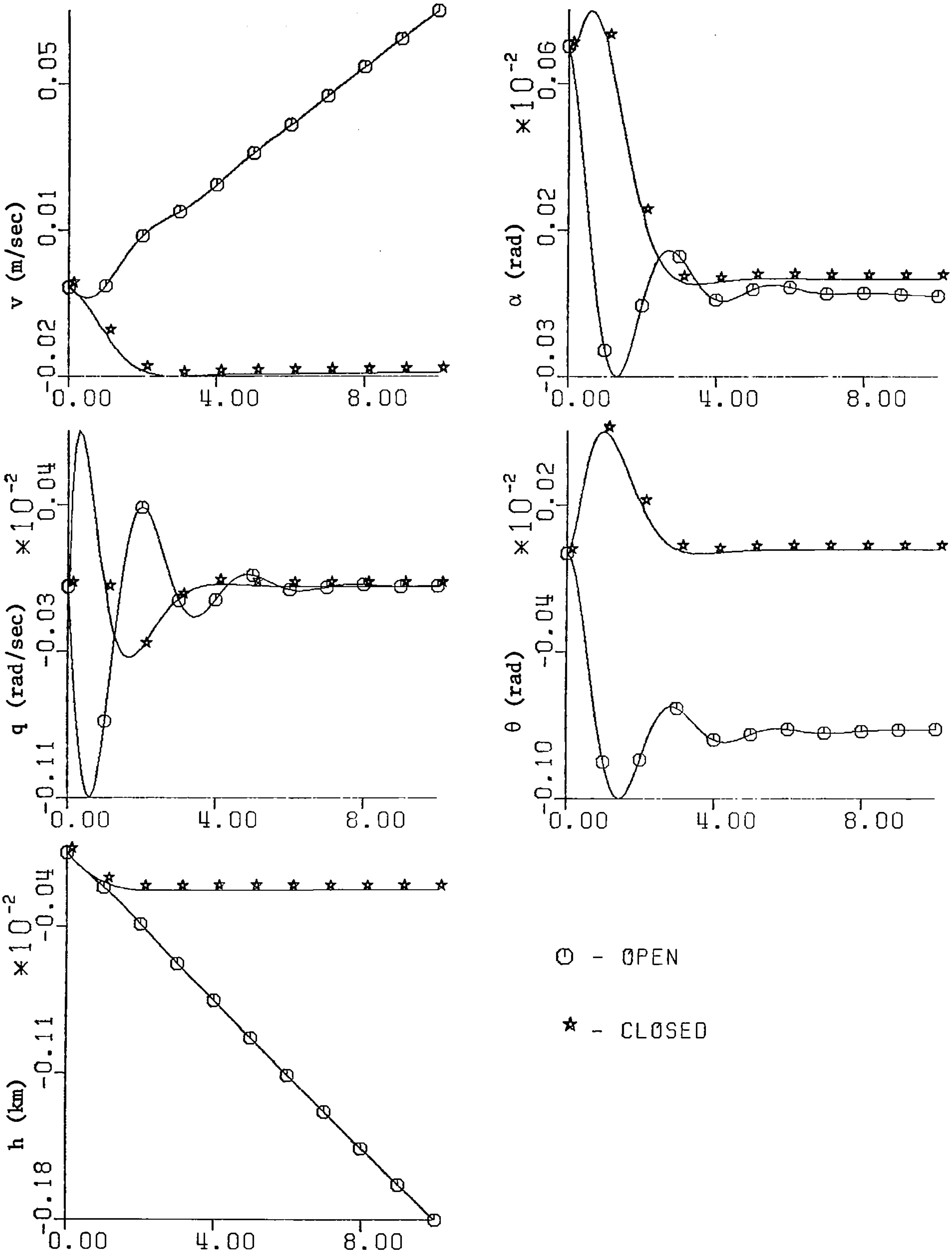

FIGURE 10. Integrated system open and closed loop transient response. Offset in angle of attack of 0.0008 rad.

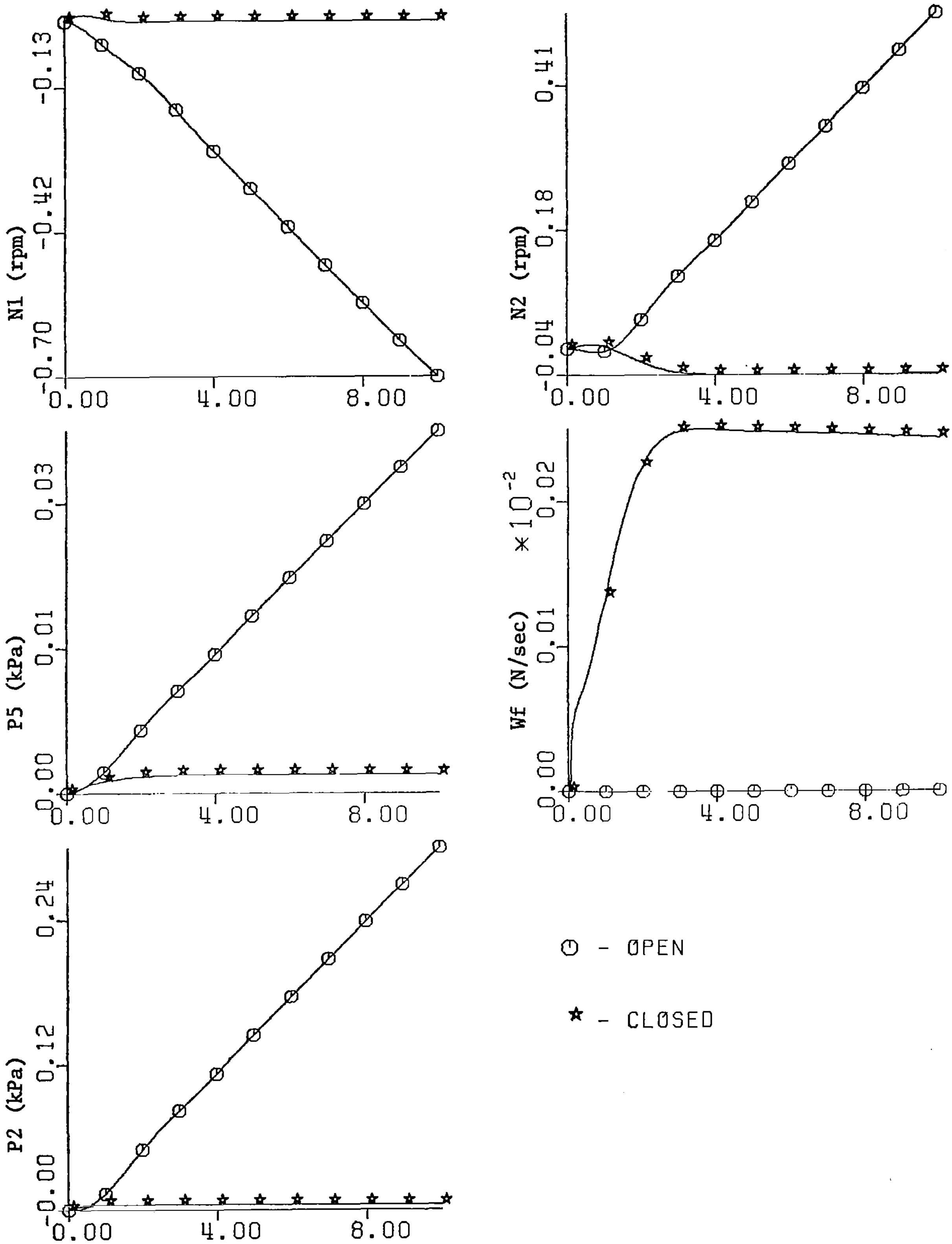

FIGURE 10. continued

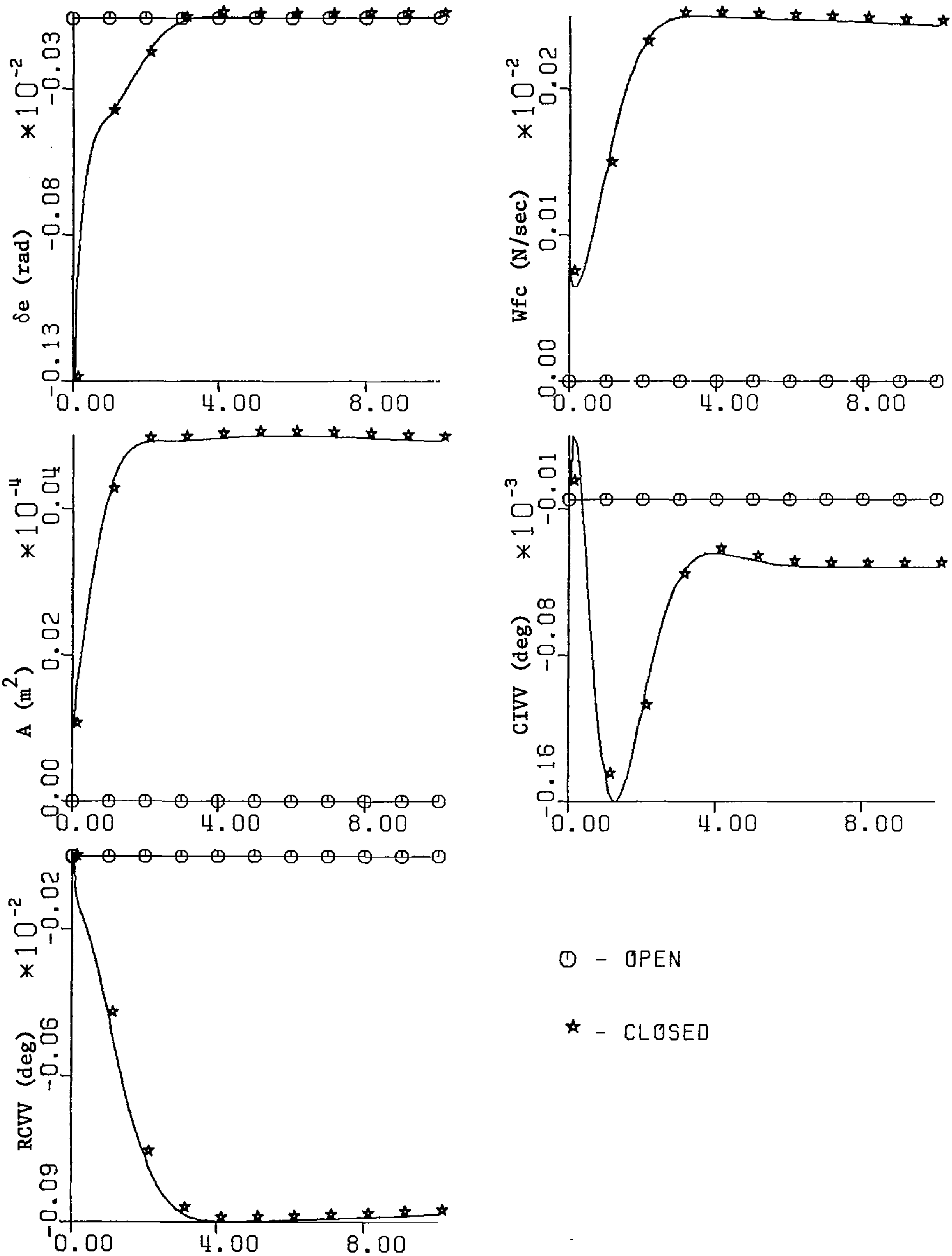

FIGURE 10. continued

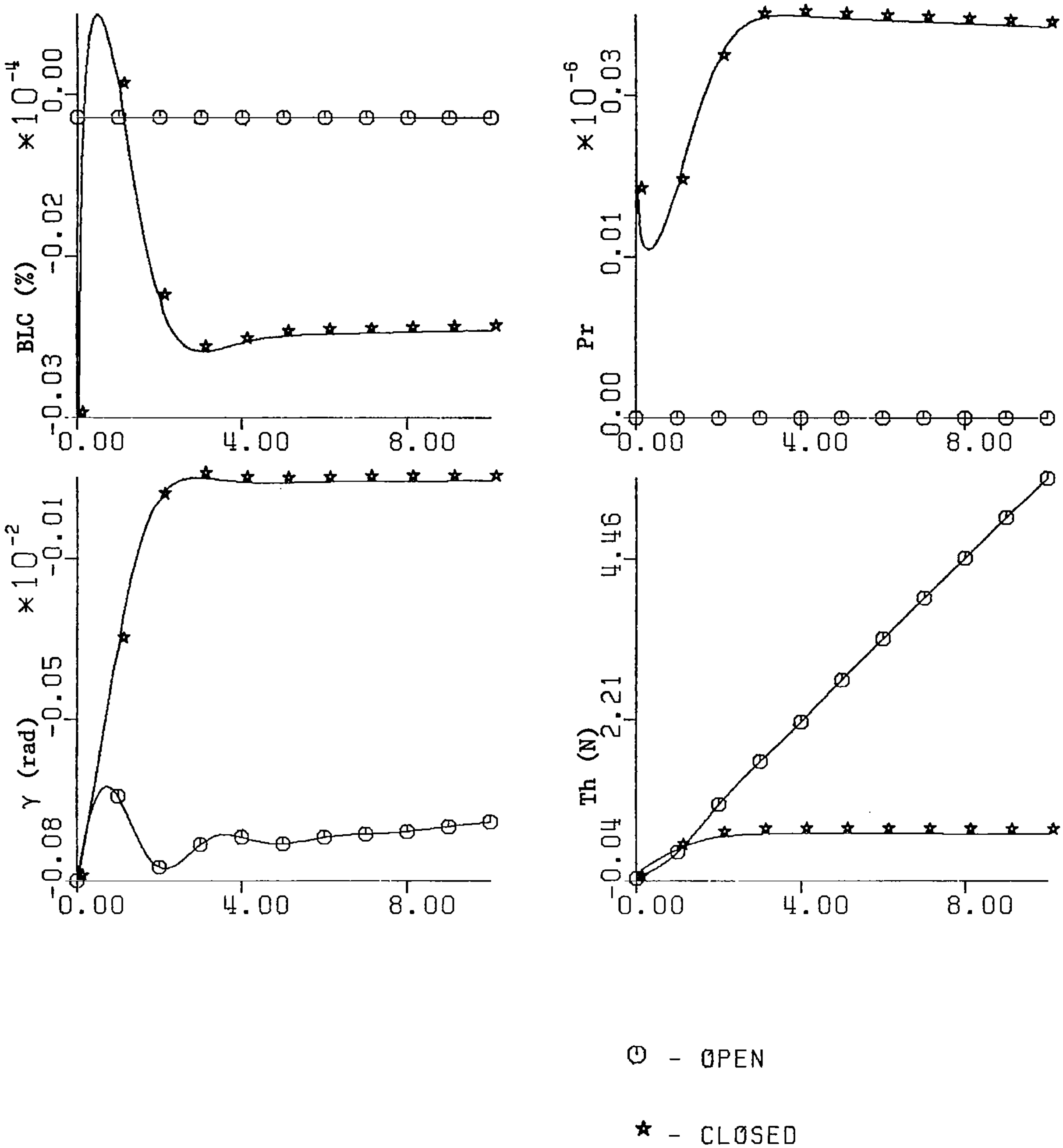

FIGURE 10. concluded.

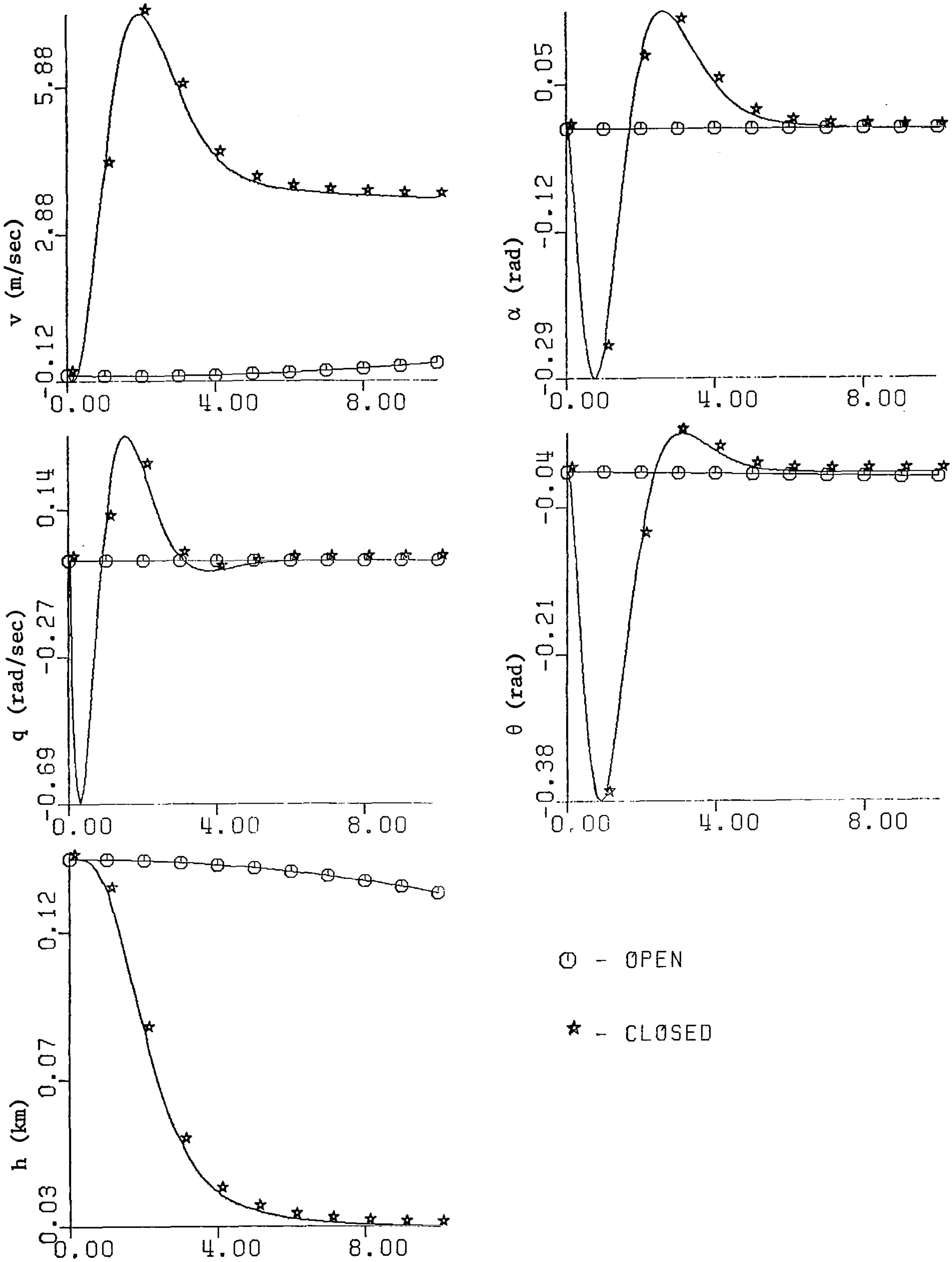

FIGURE 11. Integrated system open and closed loop transient response. Offset in altitude of 0.137 km.

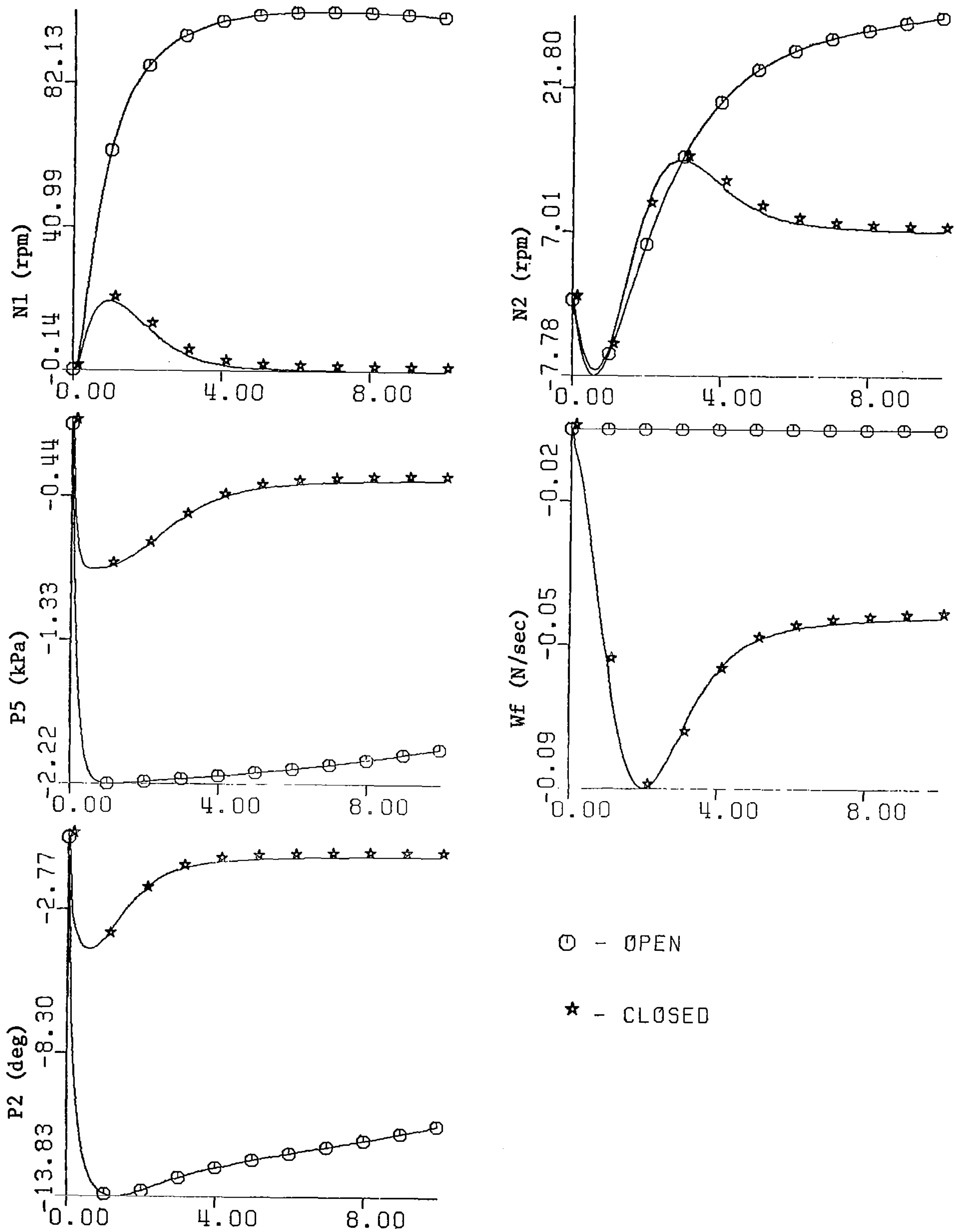

FIGURE 11. continued

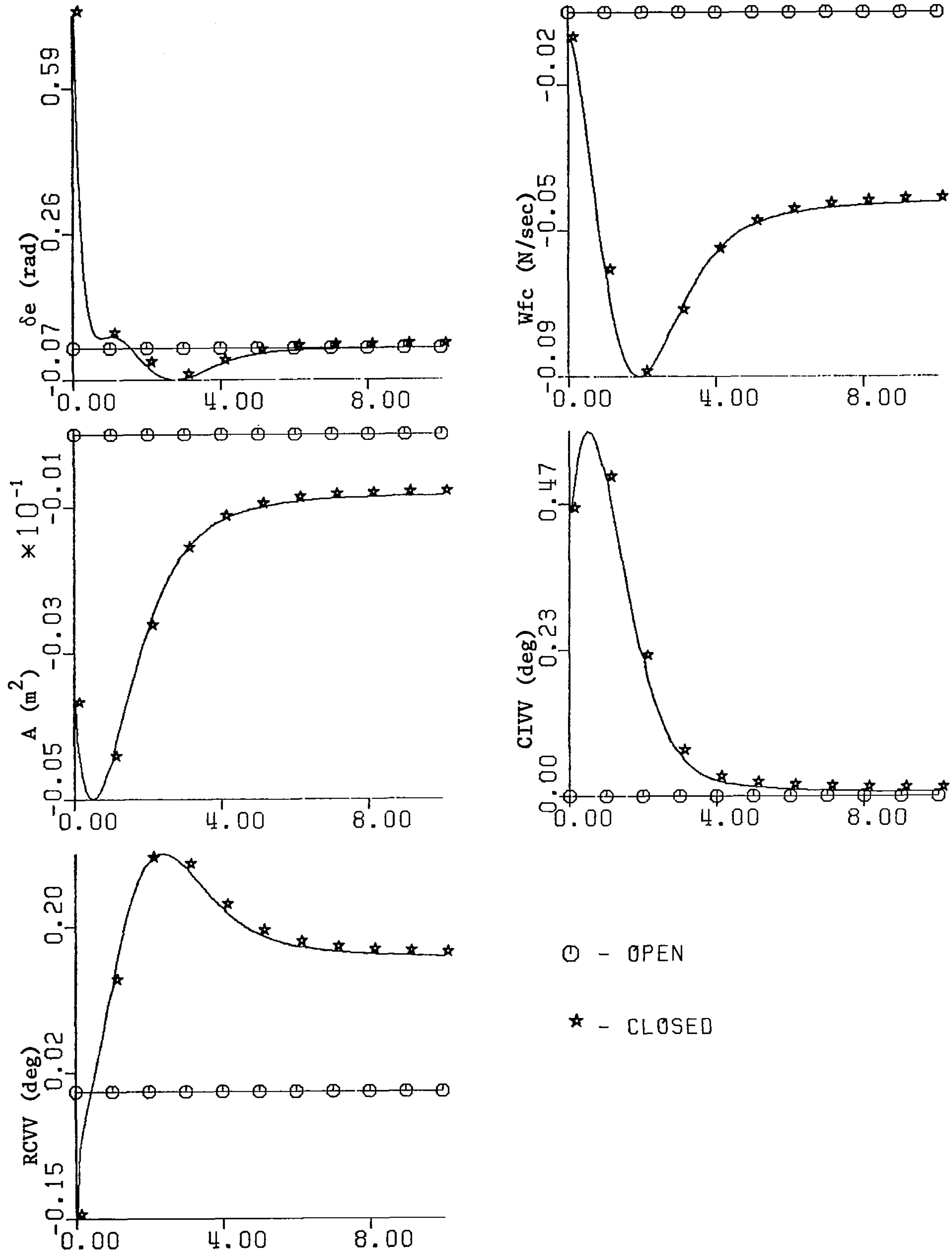

FIGURE 11. continued

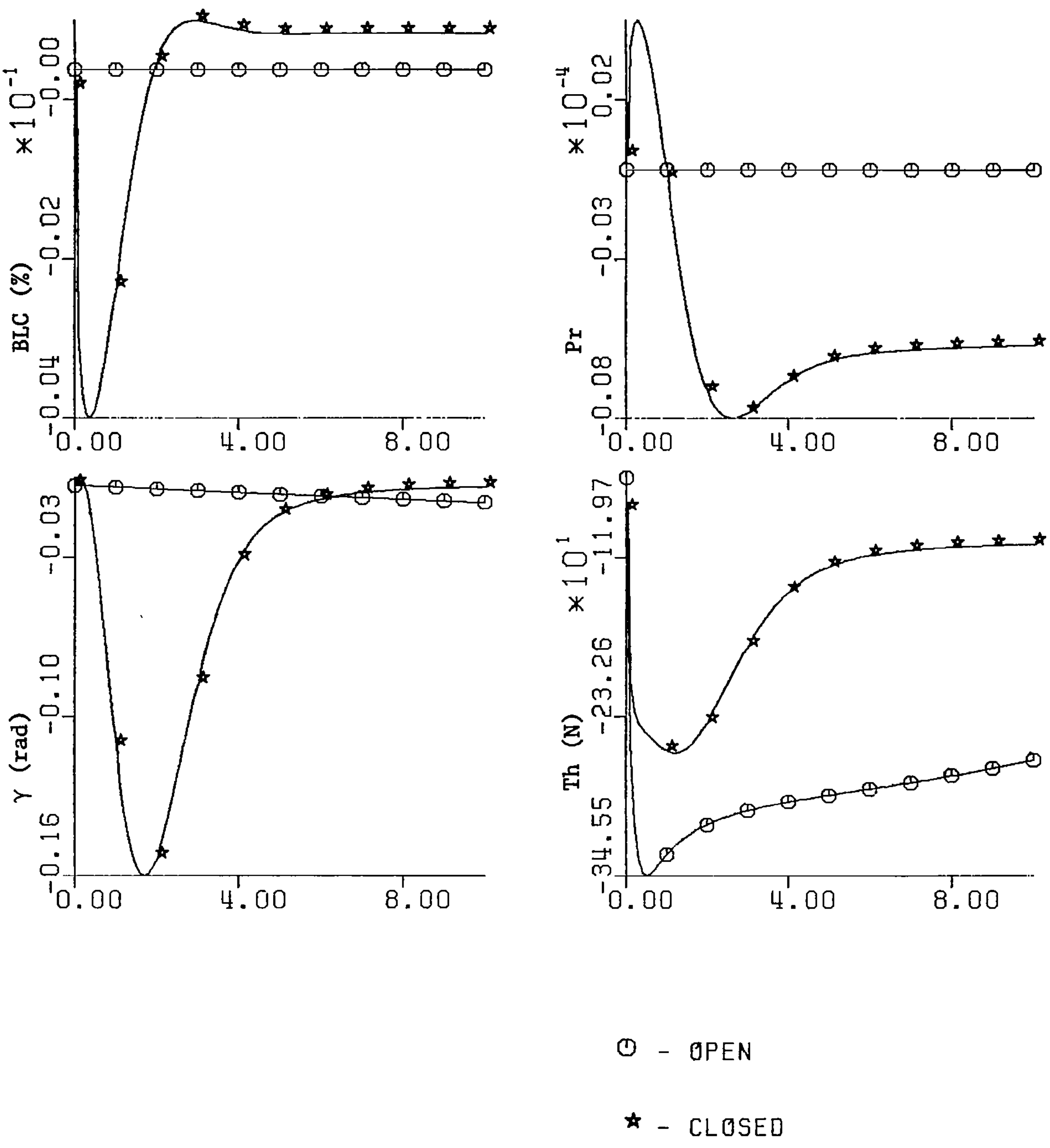

FIGURE 11. concluded.

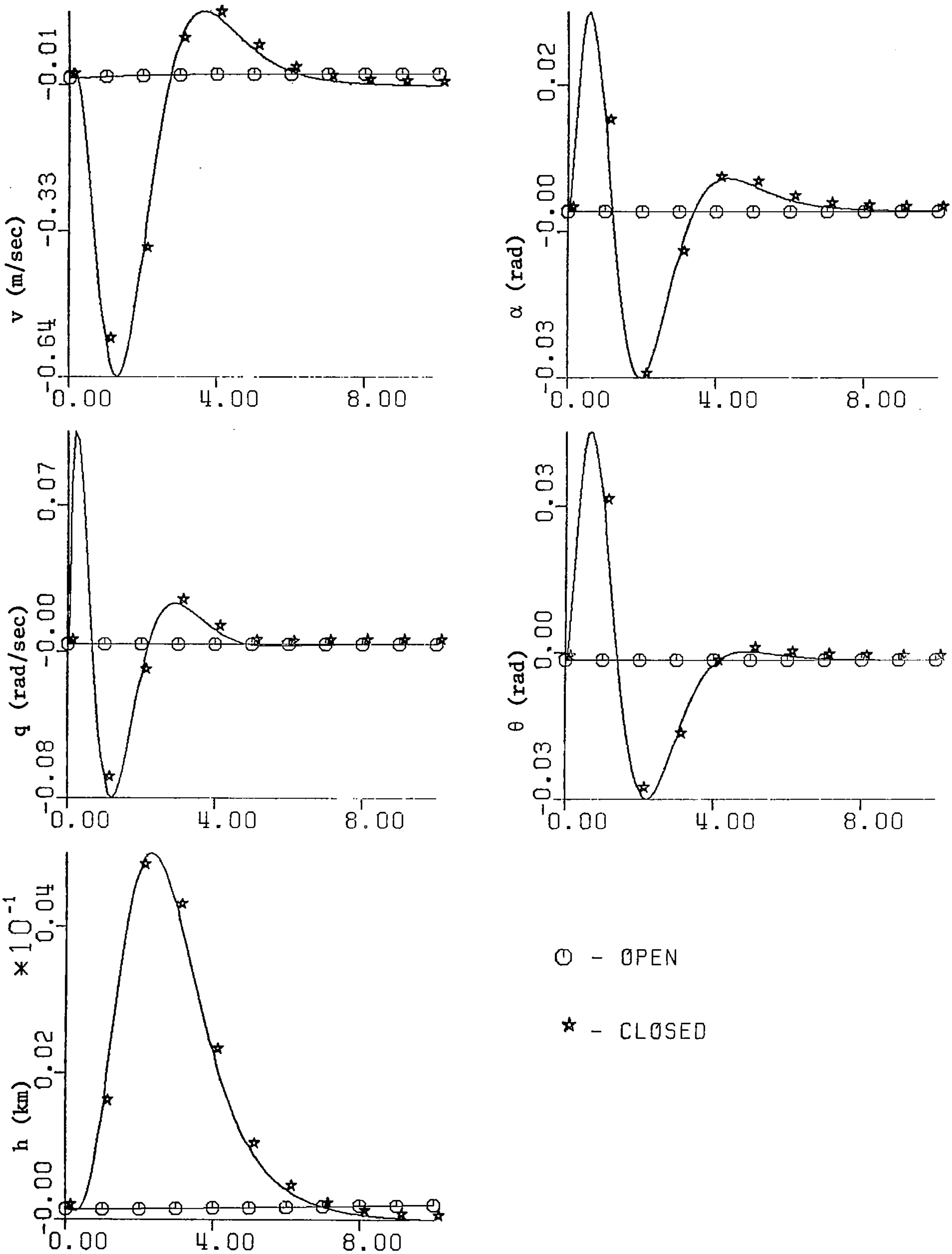

FIGURE 12. Integrated system open and closed loop transient response. Offset in compressor speed of 124. rpm.

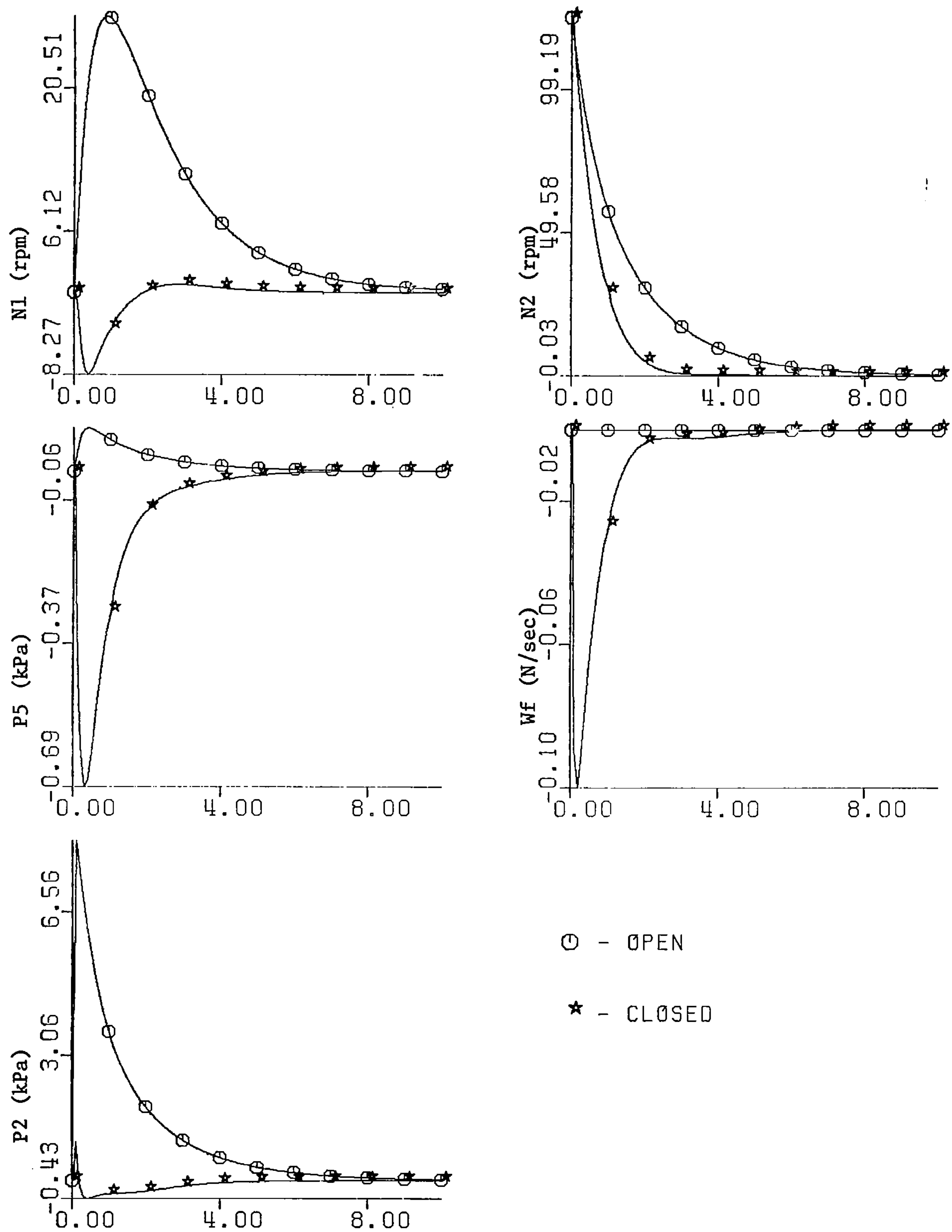

FIGURE 12. continued

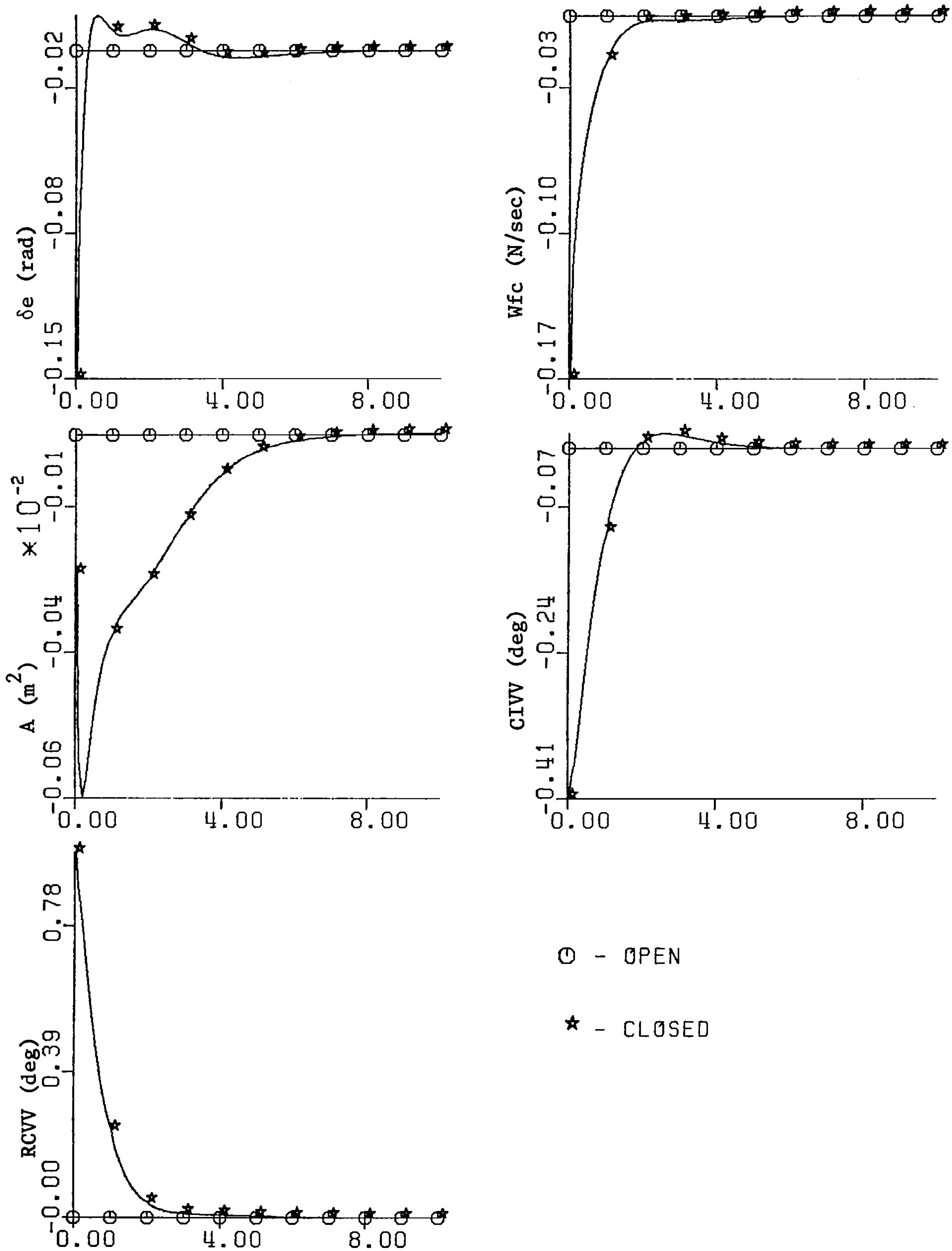

FIGURE 12. continued

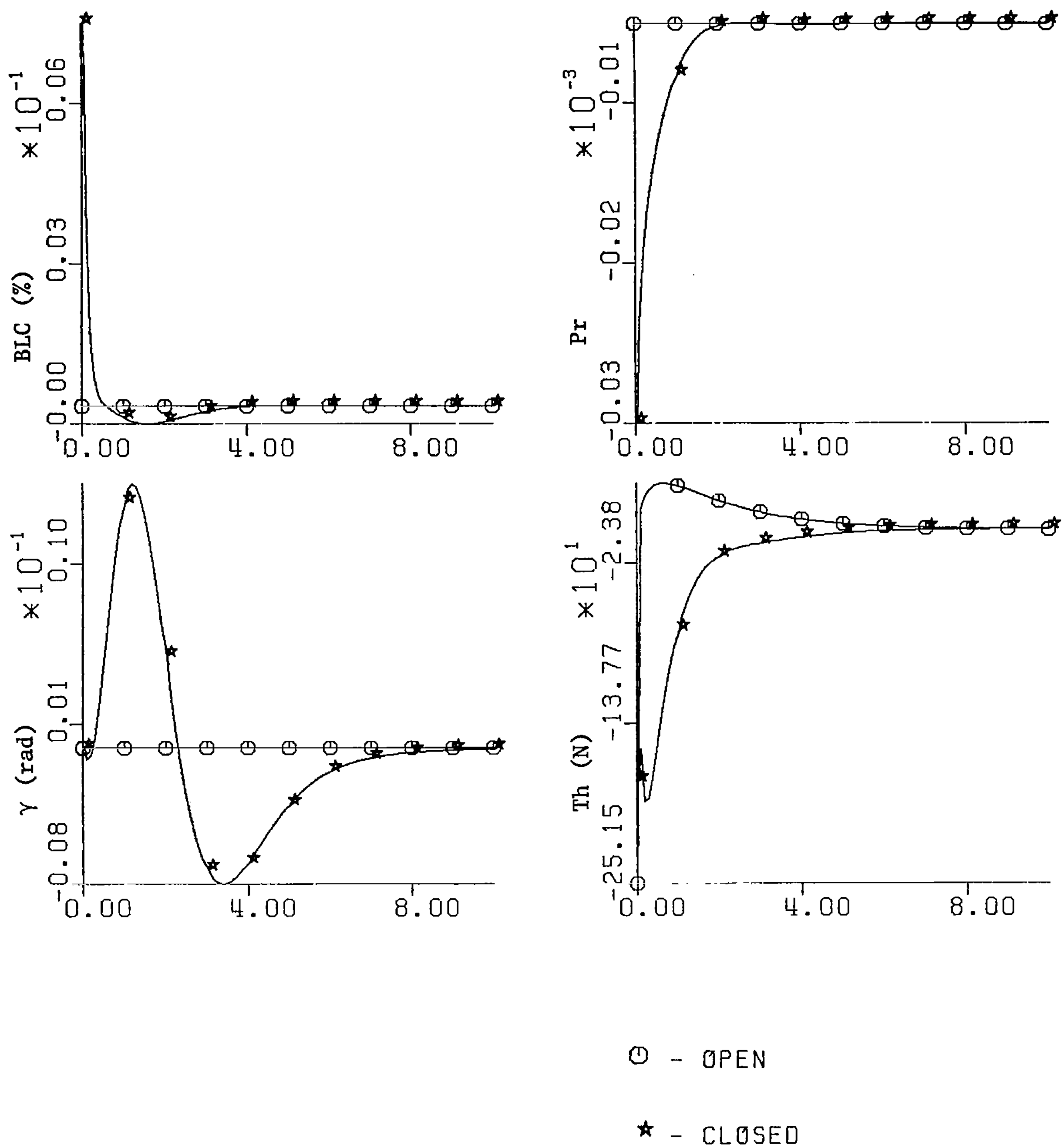

FIGURE 12. concluded.

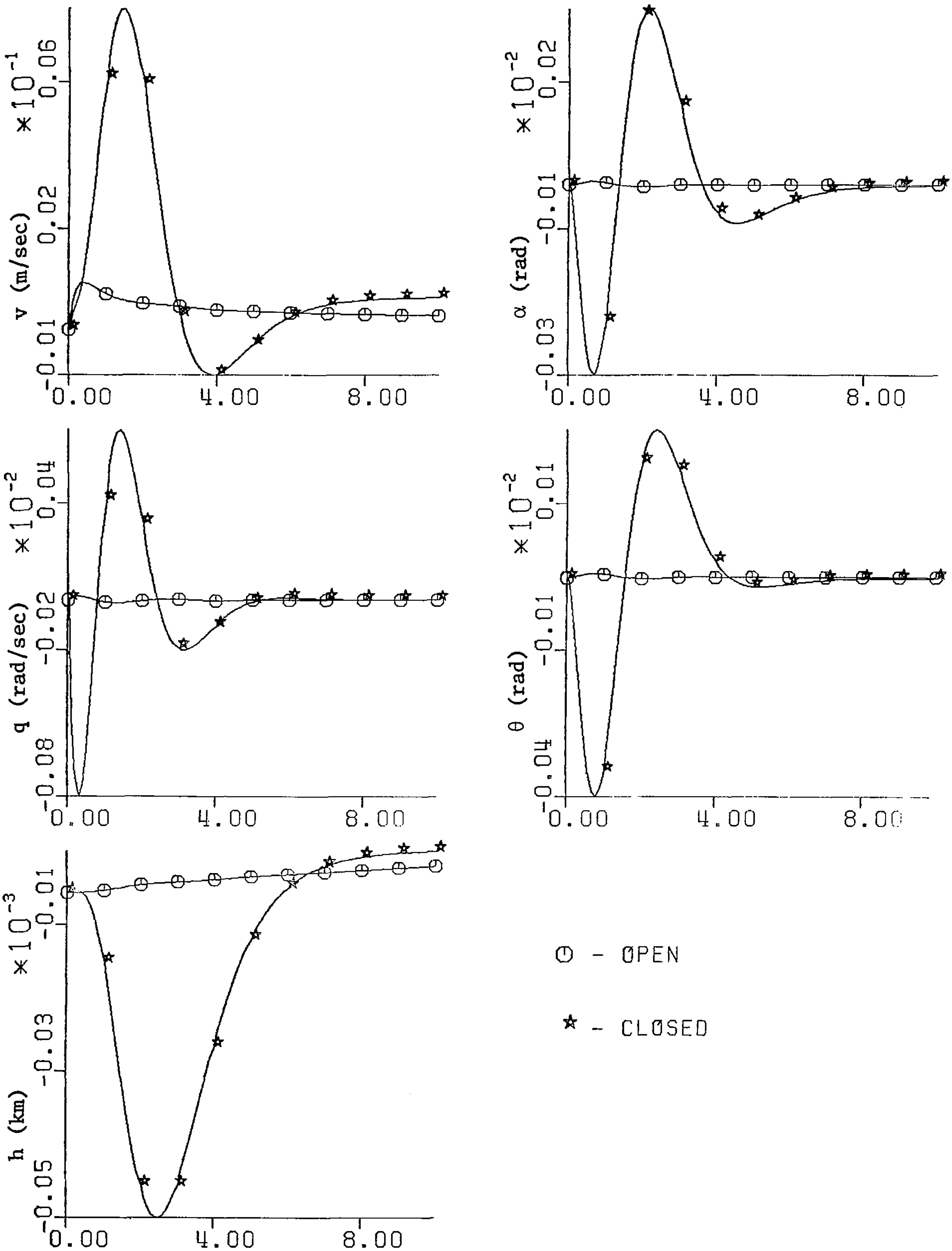

FIGURE 13. Integrated system open and closed loop transient response. Offset in augmentor pressure of 0.75 kPa.

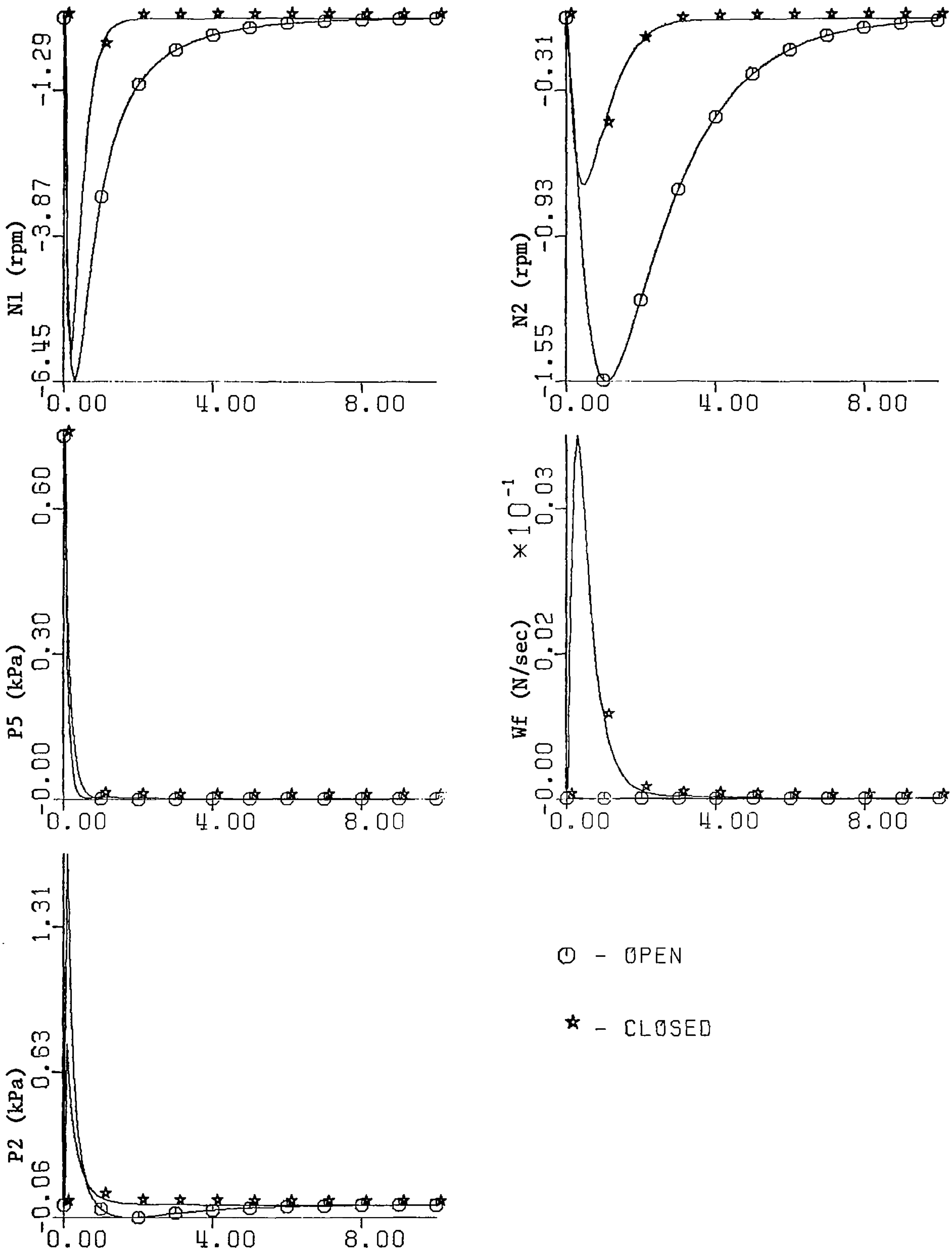

FIGURE 13. continued

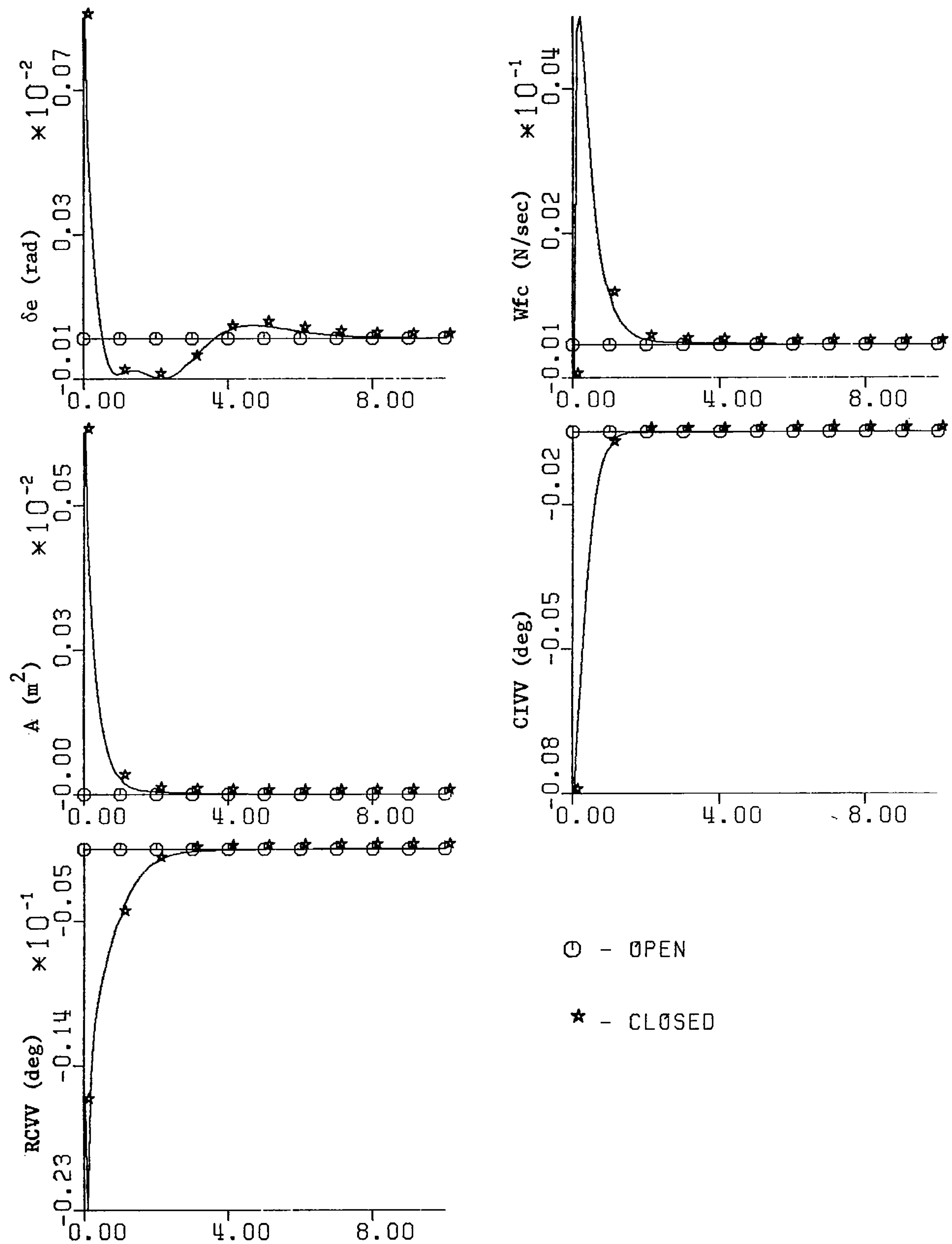

FIGURE 13. continued

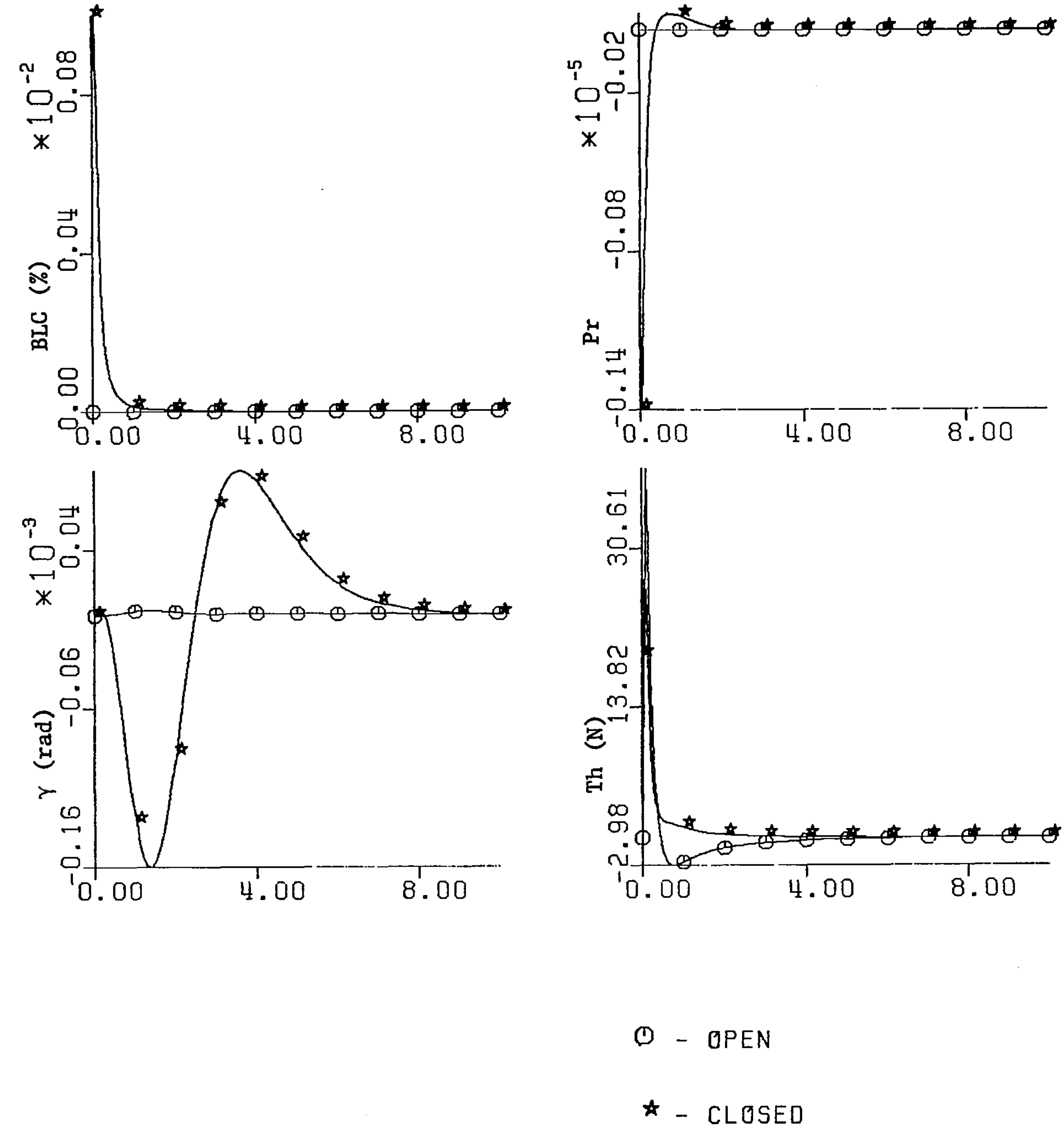

FIGURE 13. concluded.

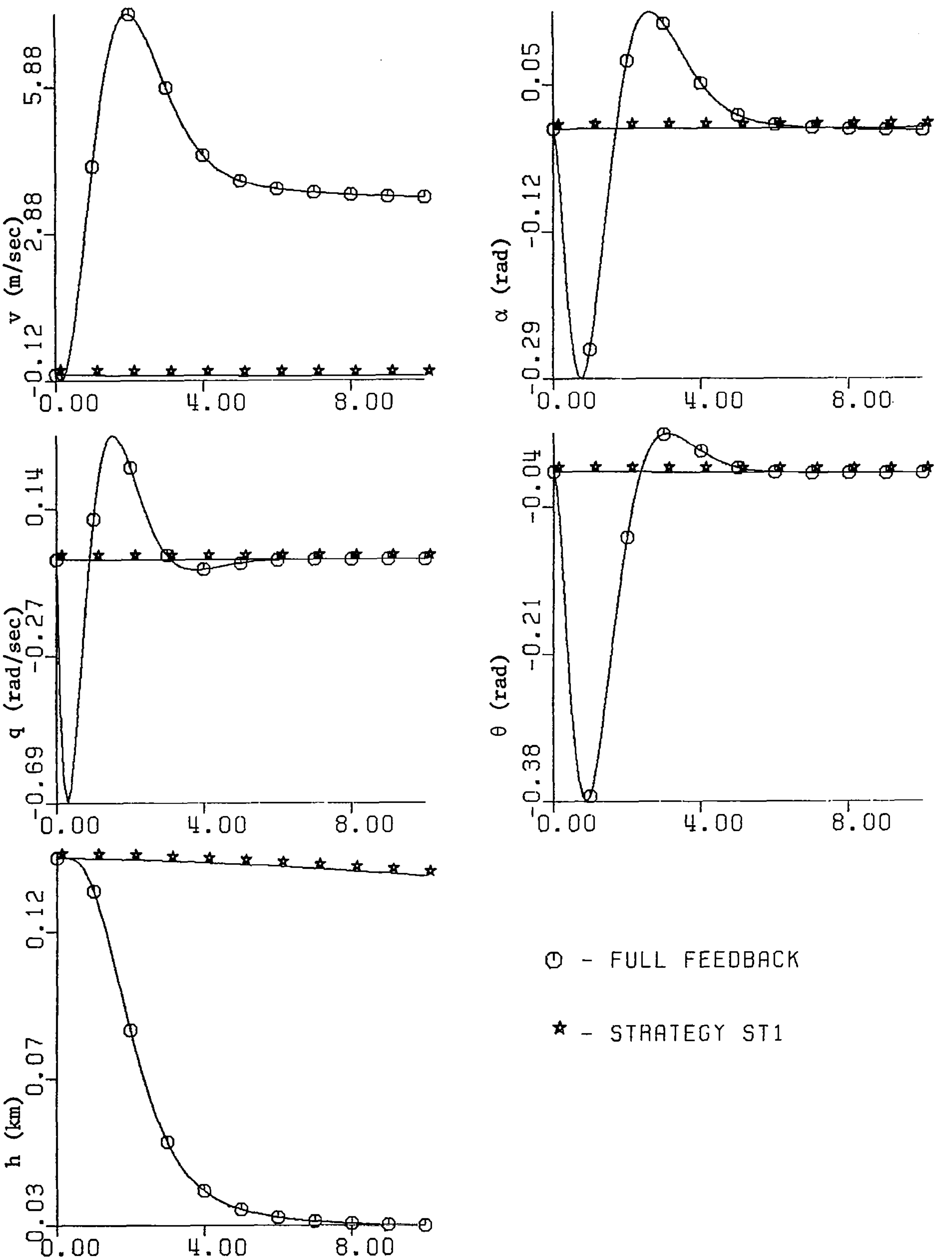

FIGURE 14. Comparison closed loop integrated system transient response. Offset in altitude of 0.137 km.

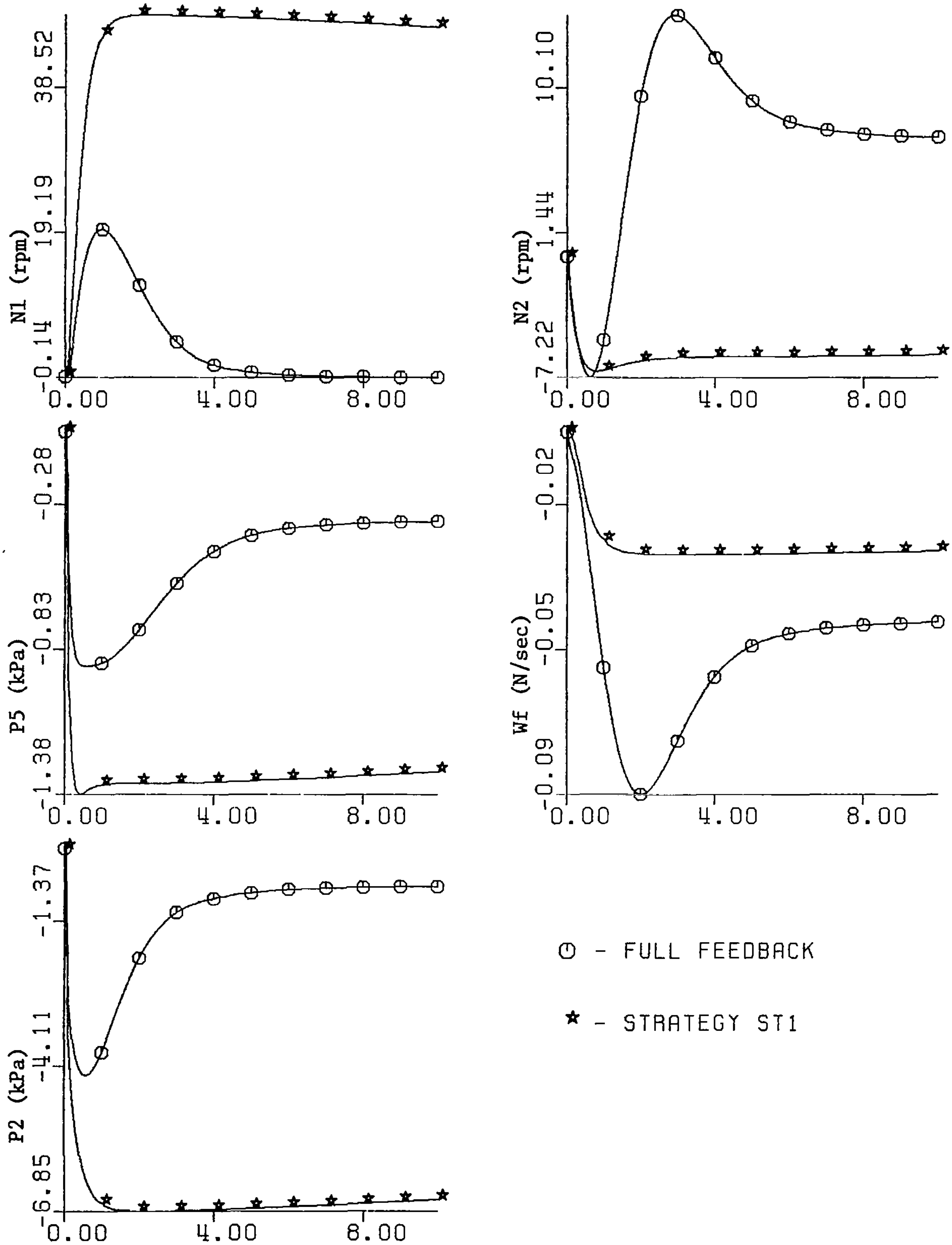

FIGURE 14. continued

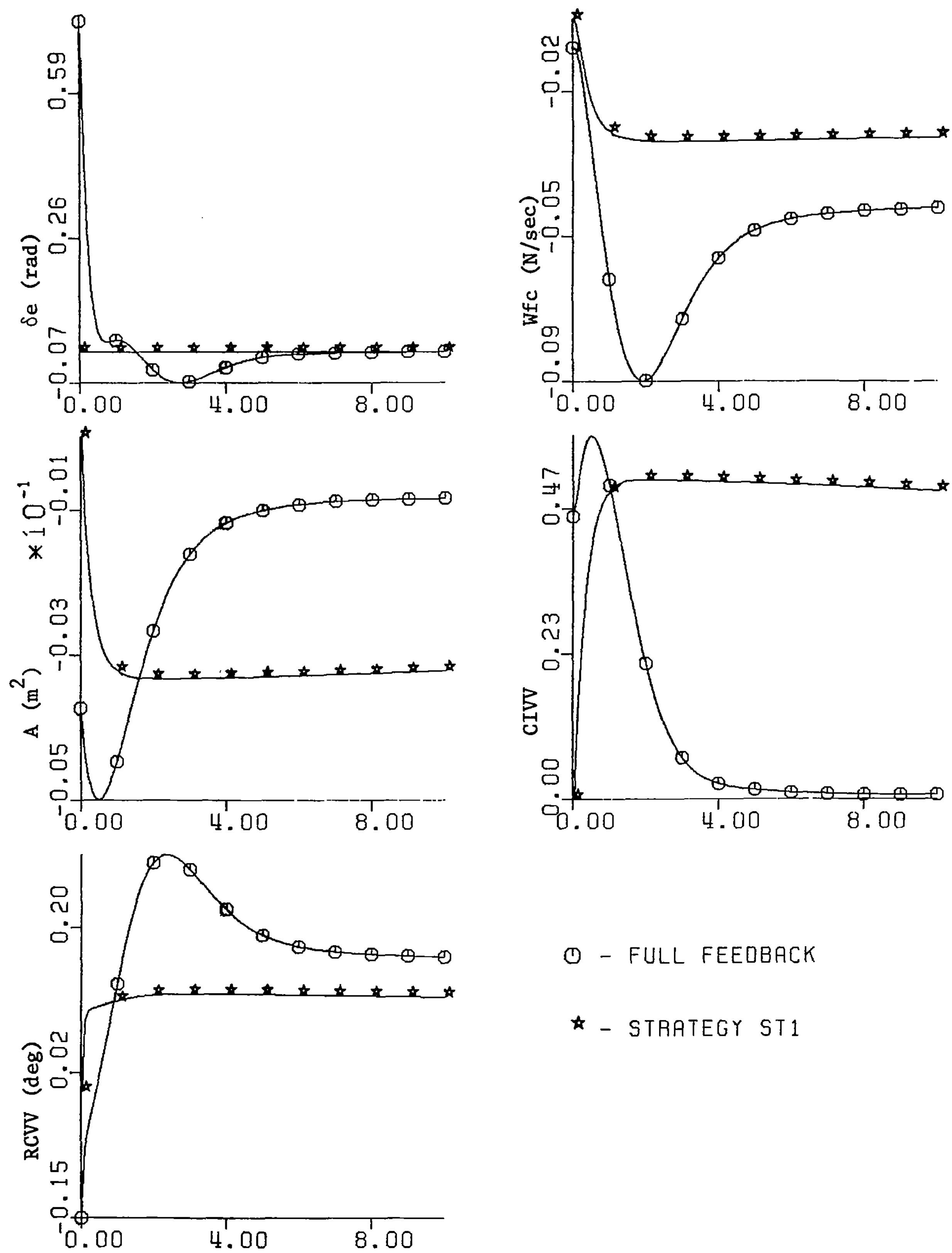

FIGURE 14. continued

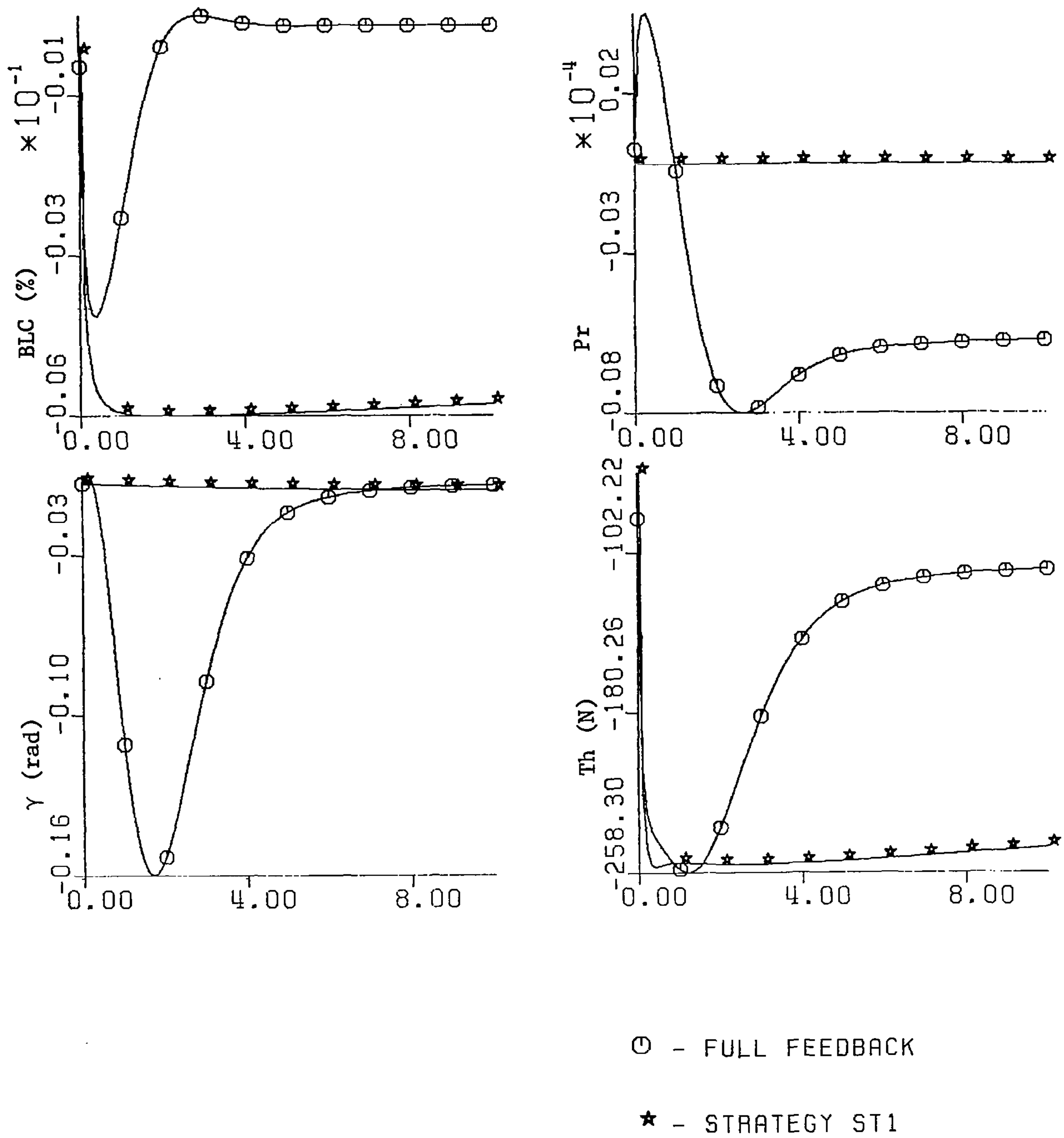

FIGURE 14. concluded.

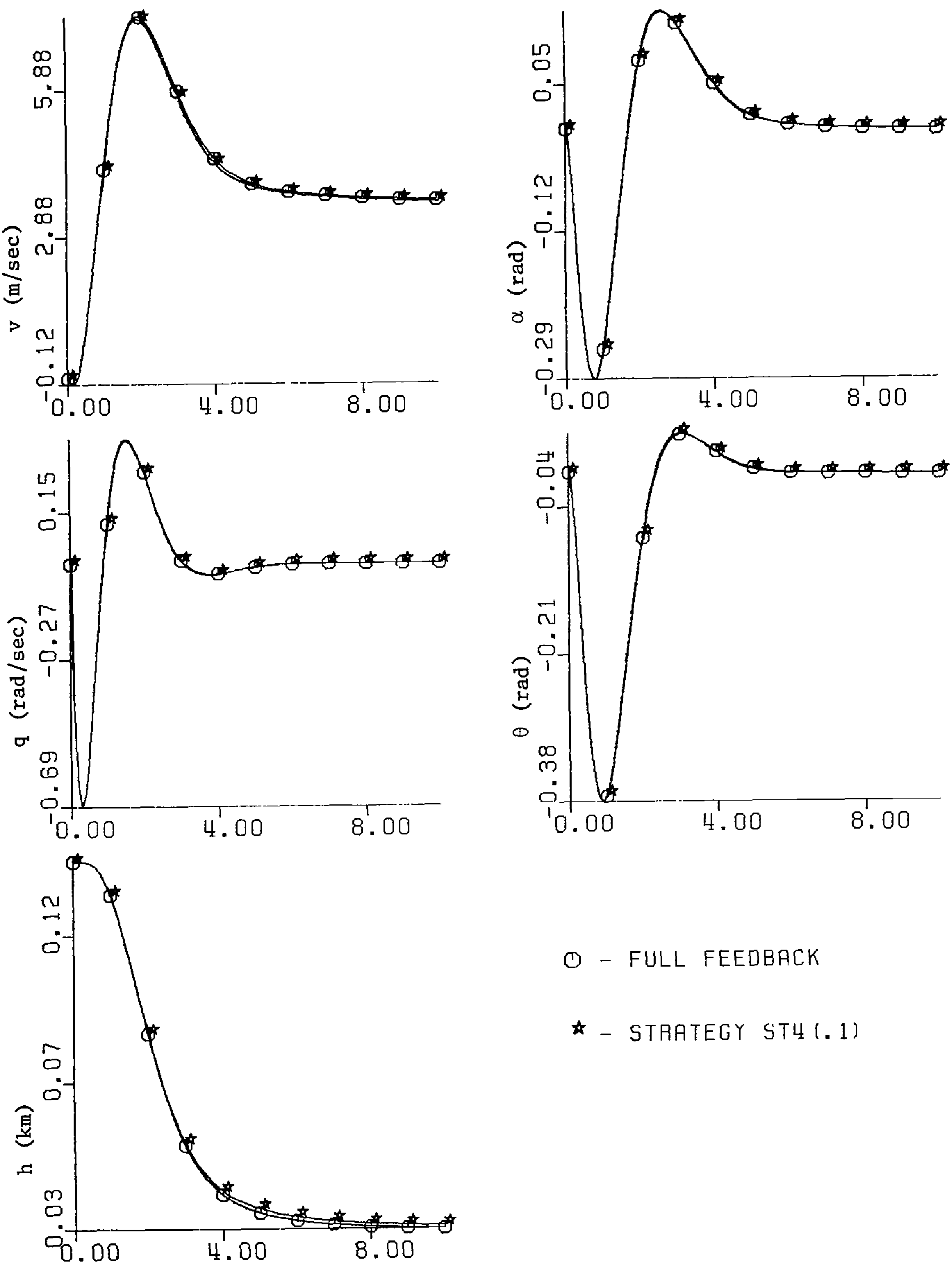

FIGURE 15. Comparison closed loop integrated system transient response.
Offset in altitude of 0.137 km.

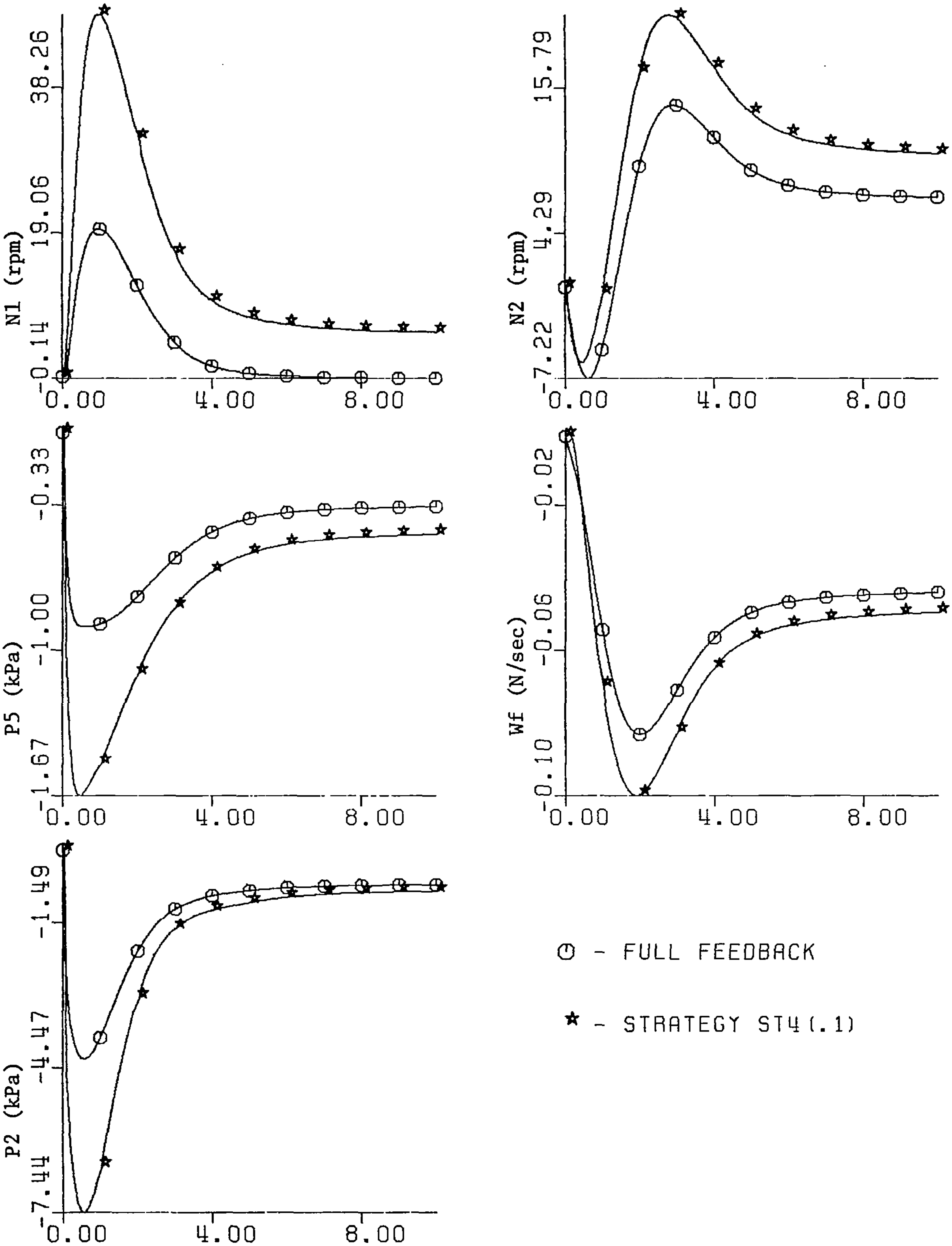

Ⓞ - FULL FEEDBACK

☆ - STRATEGY ST4(.1)

FIGURE 15. continued

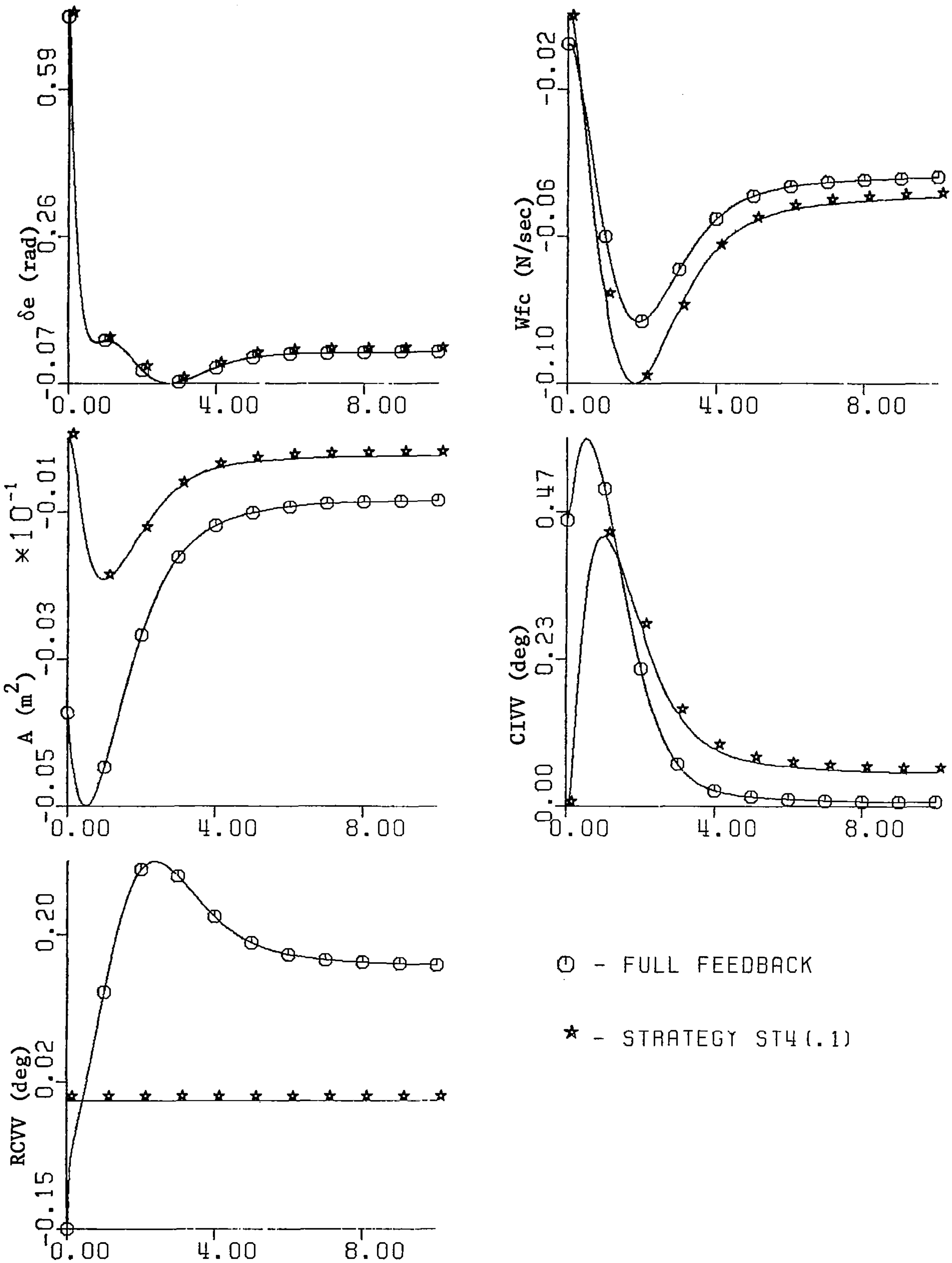

FIGURE 15. continued

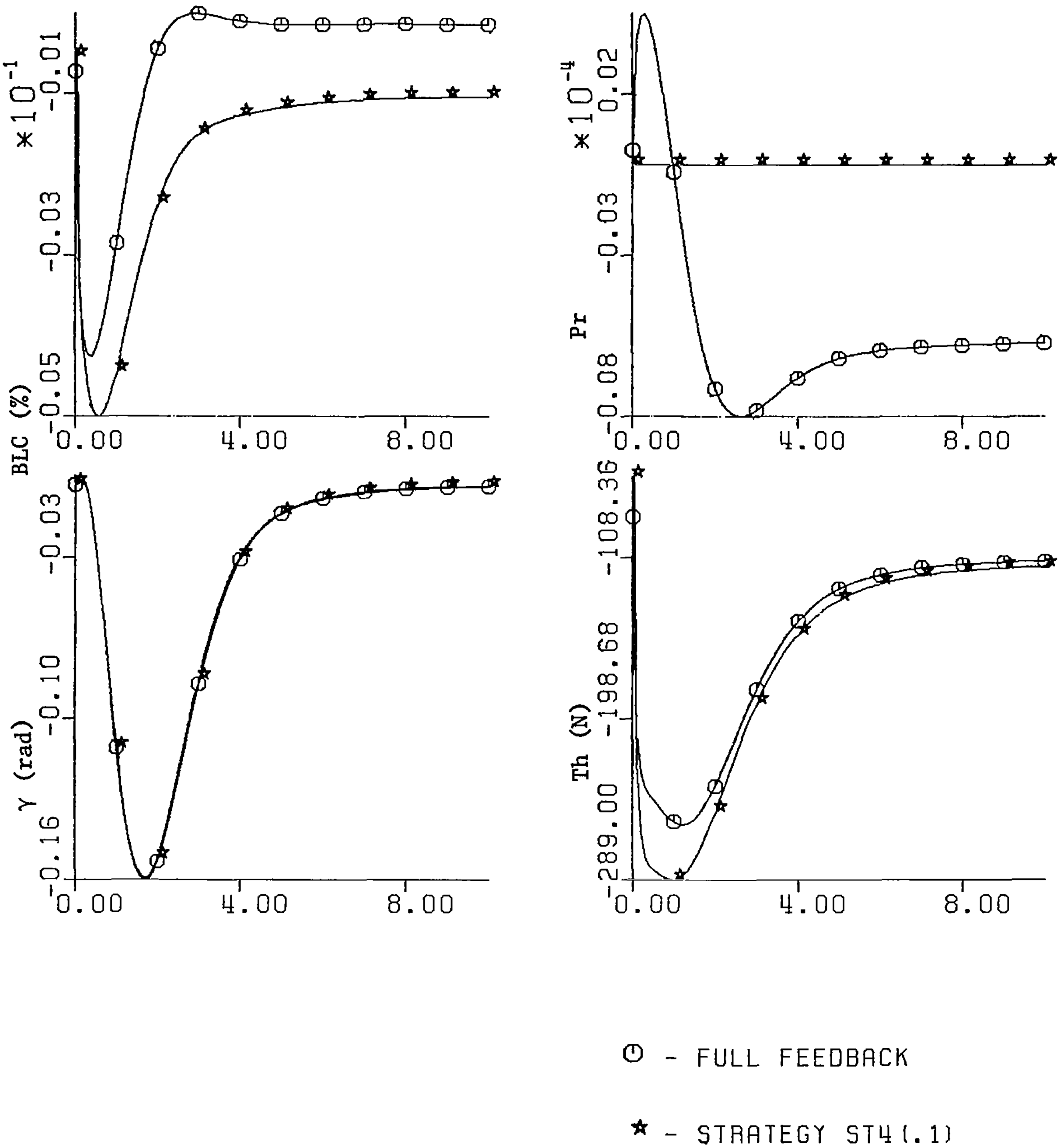

FIGURE 15. concluded.

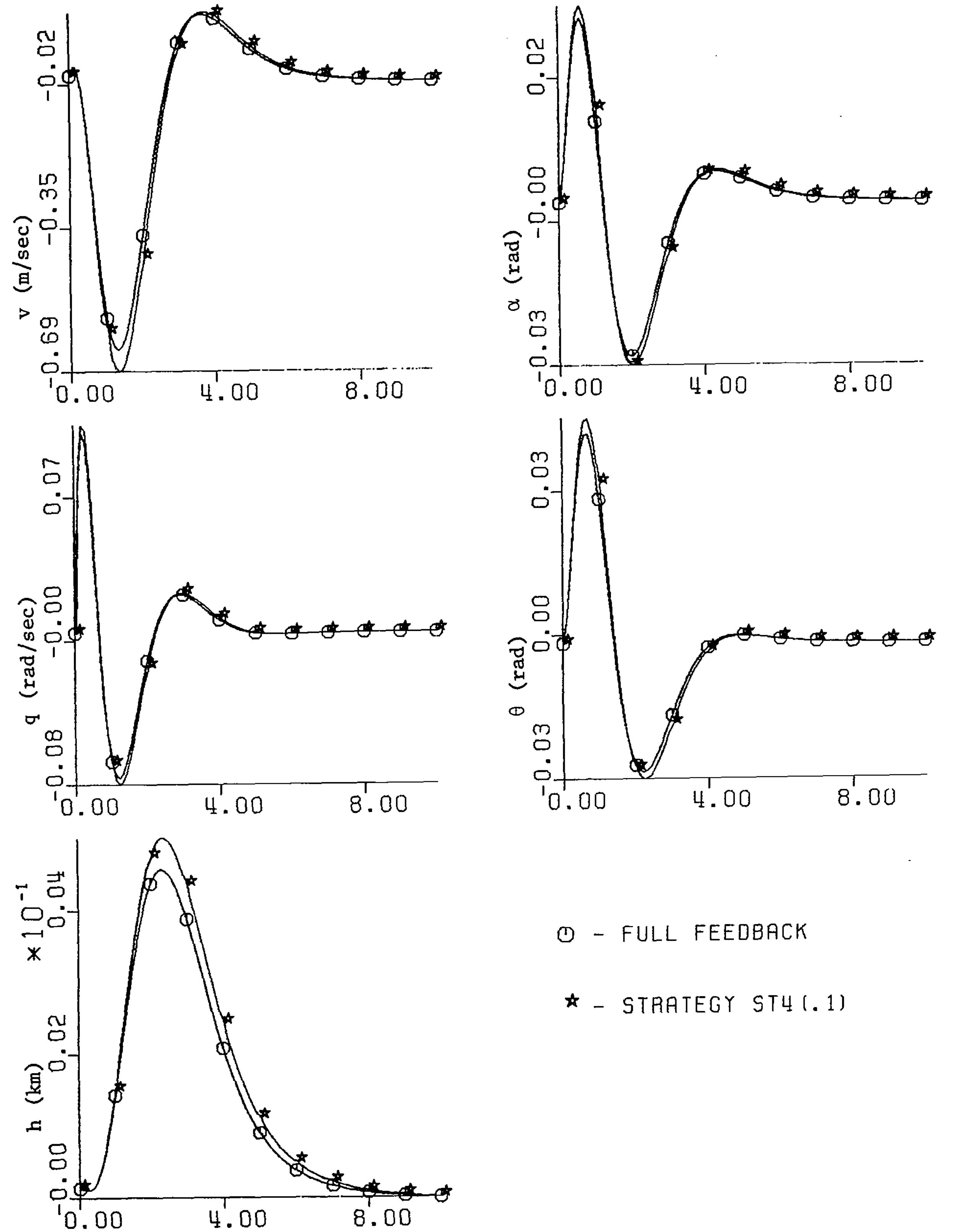

FIGURE 16. Comparison closed loop integrated system transient response.
Offset in compressor speed of 124. rpm.

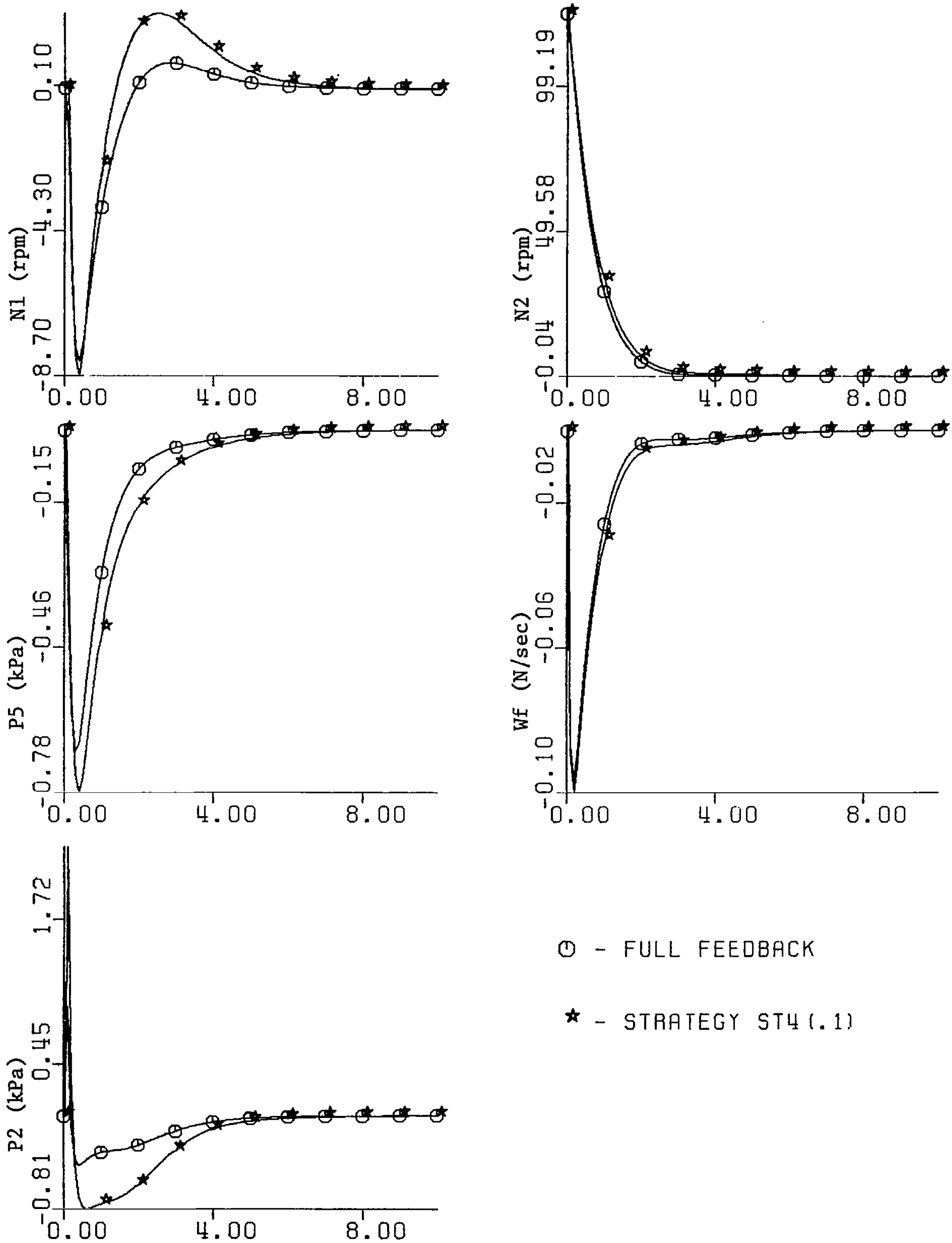

FIGURE 16. continued

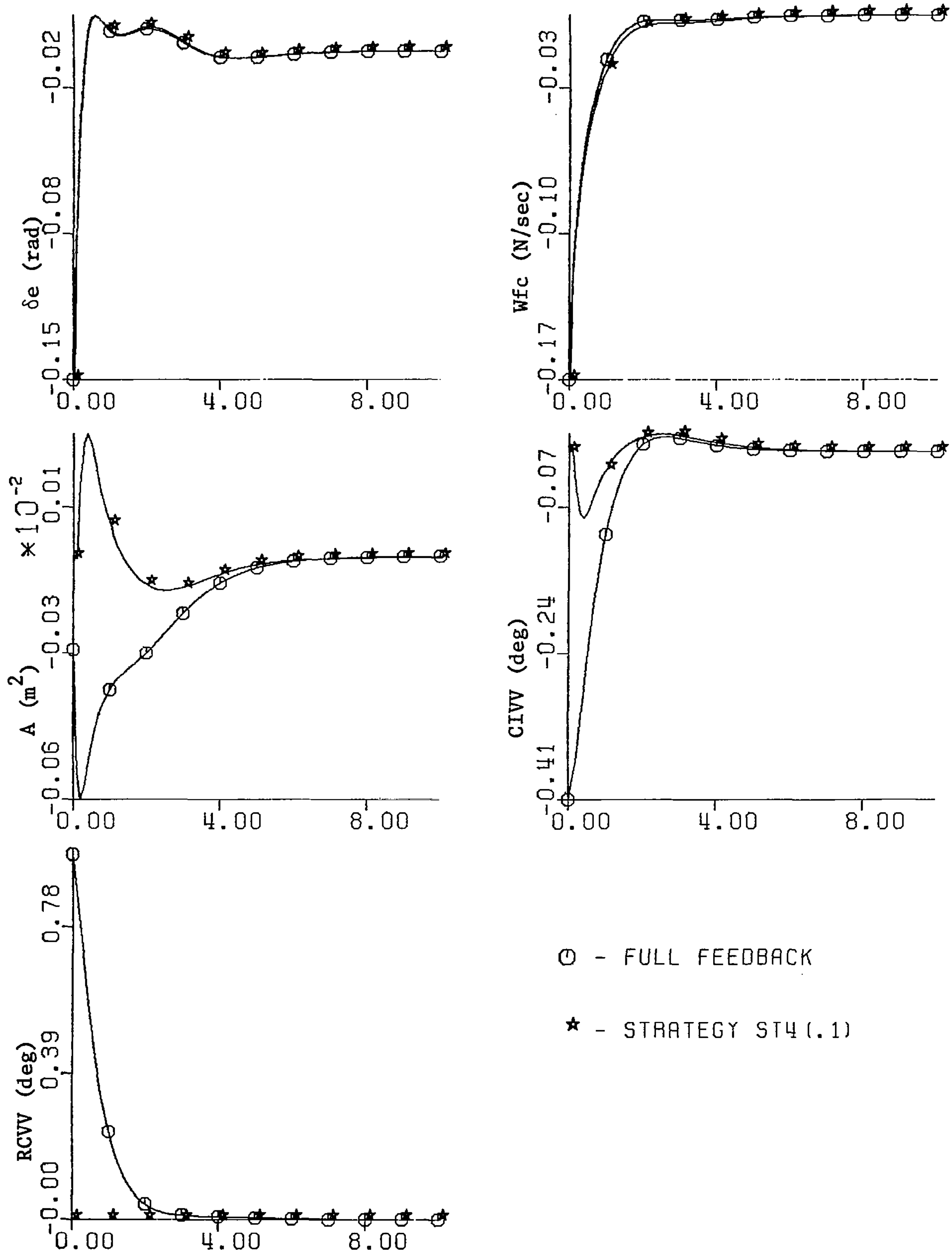

FIGURE 16. continued

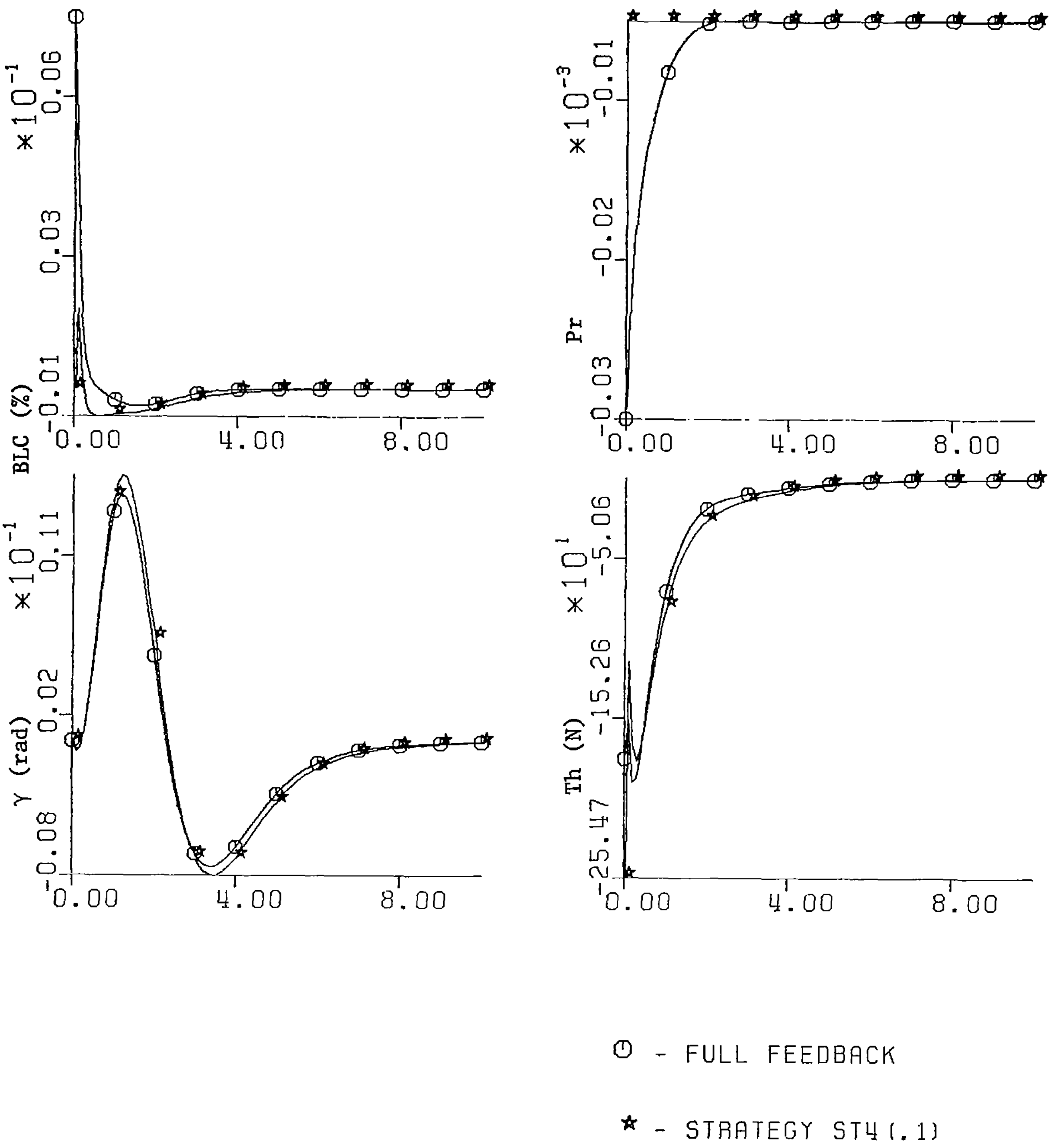

FIGURE 16. concluded.

1. Report No. NASA CR-3606	2. Government Accession No.	3. Recipient's Catalog No.
4. Title and Subtitle INTEGRATED AIRFRAME PROPULSION CONTROL		5. Report Date August 1982
		6. Performing Organization Code
7. Author(s) Robert E. Fennell and Stephen B. Black		8. Performing Organization Report No.
9. Performing Organization Name and Address Clemson University Department of Mathematical Sciences Clemson, SC 29631		10. Work Unit No.
		11. Contract or Grant No. NAG 1-81
12. Sponsoring Agency Name and Address National Aeronautics and Space Administration Washington, DC 20546		13. Type of Report and Period Covered Contractor Report (Oct. 80 - Apr. 82)
		14. Army Project No.

15. Supplementary Notes

Langley technical monitor: Frederick J. Lallman

16. Abstract

Perturbation equations which describe flight dynamics and engine operation about a given operating point are combined to form an integrated aircraft/propulsion system model. Included in the model are the dependence of aerodynamic coefficients upon atmospheric variables along with the dependence of engine variables upon flight condition and inlet performance. An off-design engine performance model is used to identify interaction parameters in the model. Inclusion of subsystem interaction effects introduces coupling between flight and propulsion variables.

To analyze interaction effects on control, consideration is first given to control requirements for separate flight and engine models. For the separate airframe model, feedback control provides substantial improvement in short period damping. For the integrated system, feedback control compensates for the coupling present in the model and provides good overall system stability. However, this feedback control law involves many non-zero gains. Analysis of suboptimal control strategies indicates that performance of the closed loop integrated system can be maintained with a feedback matrix in which the number of non-zero gains is small relative to the number of components in the feedback matrix.

17. Key Words (Suggested by Author(s))	18. Distribution Statement
Airframe/Engine Model, Optimal Control, Sensitivity Analysis, Suboptimal Control	Unclassified - Unlimited Subject Category 08

19. Security Classif. (of this report)	20. Security Classif. (of this page)	21. No. of Pages	22. Price*
Unclassified	Unclassified	98	A05

*For sale by the National Technical Information Service, Springfield, Virginia 22161

NASA-Langley, 1982